



Identification and functional characterisation of *Aedes albopictus* genes
against chikungunya virus

A thesis submitted in fulfilment of the requirements for the degree of Doctor of Philosophy

Ravi Kiran Vedururu

Master of Biotechnology, RMIT University

School of Science

College of Science, Engineering and Health

RMIT University

December 2019

Declaration

I certify that except where due acknowledgement has been made, the work is that of the author alone; the work has not been submitted previously, in whole or in part, to qualify for any other academic award; the content of the thesis is the result of work which has been carried out since the official commencement date of the approved research program; any editorial work, paid or unpaid, carried out by a third party is acknowledged; and, ethics procedures and guidelines have been followed.

I acknowledge the support I have received for my research through the provision of an Australian Government Research Training Program Scholarship.

I also acknowledge the support I have received for my research through the provision of a top-up scholarship by Health & Biosecurity, Commonwealth Scientific and Industrial Research Organisation.

Ravi Kiran Vedururu

Monday 16 December 2019

Acknowledgements

This work would not have been possible without the support of my family, friends and well-wishers. Your constant encouragement and support have helped me reach this stage.

Thank you Dr Prasad Paradkar for being my supervisor and giving me the opportunity to work in your lab and for your patient guidance. Thank you Dr Paul Gorry for being my supervisor and your guidance and help from the university side.

Thank you, Dr Matthew Neave, for teaching me bioinformatics. Thank you, Adam Foord, for your time, so many discussions and technical guidance. Thanks to all my fellow students and co-researchers for the company. Thank you Dr Victoria Beshay for your constant support. Your support and encouragement were really helpful for my successful and relatively stress-free completion of my PhD.

This acknowledgement would not be complete without thinking of late Dr Brian Meehan. Brian, thank you for being my teacher. You've taught me how to be a good person and a scientist. Without your mentorship I would not have reached the stage I have. I consider myself lucky to have had you as my teacher and mentor. I wish you were with us.

Last but not the least, thanks to my family, for supporting me and most importantly let me leave my job to go do a PhD. I am lucky to have you all. Special mention to my wife Prathusha and my little bundle of energy and joy, Tejas for putting up with me during this time.

Preface

This is a thesis with publications. While chapters 1 and 6 are the Introduction and Conclusion respectively, chapters 2-5 encompass the main body of work done. Chapters 2 and 3 have already been published. Chapters 4 and 5 are also presented in the form of manuscripts as we intend to publish them. At the time of submission of this thesis, chapter 4 is under peer review. The published chapters are reproduced here verbatim with only formatting changes done so they fit in with the larger body of work.

With the chapters being presented in the form of manuscripts, they have their own Abstracts, Introduction, Materials and methods, Results and Discussion sections. Although care was taken to not be repetitive in the Introduction and Discussion chapters of the thesis, some overlap was inevitable.

Table of Contents

Abstract -----	1
Chapter 1: Introduction -----	5
1.1 Chikungunya Virus -----	5
1.2 Virology & Chikungunya Disease-----	8
1.3 Vectors-----	12
1.4 Viral Transmission-----	14
1.5 Host-Pathogen Interactions -----	15
1.6 References-----	16
Chapter 2: RNA-Seq Analysis of <i>Aedes albopictus</i> Mosquito Midguts after Chikungunya Virus Infection -----	23
2.1 Abstract:-----	23
2.2 Introduction-----	24
2.3 Materials and Methods-----	26
2.3.1 Chikungunya Virus-----	26
2.3.2 <i>Aedes</i> Mosquito Rearing, Infection and RNA Extraction-----	26
2.3.3 qPCR-----	27
2.3.4 RNASeq and Viral Genome Sequencing -----	28
2.3.5 Differential Gene Expression and Gene Ontology Analysis -----	29
2.4 Results -----	30
2.4.1 Whole Genome Sequencing of CHIKV -----	30
2.4.2 RNA-Seq-----	31
2.4.3 Differential Expression and TopGO Analysis -----	32
2.4.4 RNASeq Data Validation on qRT-PCR -----	35
2.5 Discussion -----	37
2.6 References-----	41
Chapter 3: Whole Transcriptome Analysis of <i>Aedes albopictus</i> Mosquito Head and Thorax Post-Chikungunya Virus Infection -----	49
3.1 Abstract-----	49
3.2 Introduction-----	50
3.3 Results -----	51
3.3.1 RNA-Seq and DGE analysis -----	51
3.3.2 Ontology analysis -----	53
3.3.3 RT-qPCR based Validation of RNA-Seq data-----	55
3.3.4 Functional significance of BTKi in CHIKV infected RML12 cells-----	57
3.4 Discussion -----	61
3.5 Materials and Methods-----	64

3.6	References-----	69
Chapter 4:	Chikungunya virus undergoes genomic bottleneck during <i>Aedes albopictus</i> infection-----	74
4.1	Abstract-----	74
4.2	Introduction & Methods -----	75
4.3	Results & Discussion-----	76
4.4	Declarations -----	81
4.5	References-----	82
Chapter 5:	Evaluating Functional Significance of NPC2 Gene Homologue in <i>Aedes albopictus</i> during Chikungunya Virus Infection-----	85
5.1	Abstract-----	85
5.2	Introduction-----	86
5.3	Materials and Methods-----	87
5.4	Results-----	90
5.5	Discussion-----	93
5.6	References-----	95
Chapter 6:	Discussion-----	99
6.1	References-----	105
Appendices-----		110
	Appendix-I: List of Primers-----	110
	Appendix-II: List of differentially expressed genes D2_DESeq2-----	113
	Appendix-III: List of differentially expressed genes D2_edgeR-----	114
	Appendix-IV: List of differentially expressed genes D8_DESeq2-----	123
	Appendix-V: List of differentially expressed genes D8_edgeR-----	127

List of Tables

Table 1.1 Classification of Alphavirus -----	6
Table 2.1 RNASeq next-generation sequencing (NGS) data summary -----	31
Table 2.2 List of genes validated by qRT-PCR and comparison of expression fold changes -----	36
Table 3.1 RNASeq NGS data summary -----	51
Table 3.2 Differential Gene Expression analysis. -----	53
Table 3.3 List of genes validated by qRT-PCR -----	56
Table 3.4 Comparison of expression fold changes in chosen targets between qRT-PCR and RNASeq -----	57

List of Figures

Figure 1.1 Geographic distribution of Chikungunya-----	8
Figure 1.2: Alphaviral Virion Structure-----	9
Figure 1.3: Schematic representation of Chikungunya viral genome organization -----	10
Figure 2.1 Volcano plots from DESeq2 and edgeR for 2 dpi differential gene expression -----	33
Figure 2.2 topGo enrichment comparison in differentially expressed genes -----	34
Figure 3.1 Volcano plots from DESeq2 and edgeR -----	52
Figure 3.2 topGo enrichment comparison in differentially expressed genes -----	54
Figure 3.3 A: Comparison of BTKi expression between BTKi-KD and GFP-KD RML12 cells; B: Comparison of intracellular CHIKV RNA via RT-qPCR in BTKi and GFP knockdown RML12 cells; C: Comparison of % of apoptosis detected in BTKi-KD and GFP-KD RML12 cells; D: Comparison of TCID ₅₀ of extracellular CHIKV between BTKi and GFP knockdown RML12 cells -----	58
Figure 3.4 TUNEL staining of BTKi knocked down RML-12 cells post infection with CHIKV -----	60
Figure 4.1 Total number of unique variants (coding & non-Coding) from CHIKV from Vero cells (Vero), <i>Aedes albopictus</i> midguts (D2) and head & thoraces (D8) -----	78
Figure 4.2 Variants detected in Vero cell culture isolate, midgut and head/thorax independent libraries plotted as per their location on the CHIKV genome -----	79
Figure 5.1 Comparison of fold change NPC2 and CHIKV & CHIKV TCID ₅₀ between GFP/NPC2 overexpressing C6/36 cells -----	90
Figure 5.2 C6/36 cells over expressing NPC2 protein, infected with CHIKV -----	92

Publications during candidature

Vedururu RK, Neave MJ, Sundaramoorthy V, Green D, Harper JA, Gorry PR, Duchemin J-B, Paradkar PN. Whole Transcriptome Analysis of *Aedes albopictus* Mosquito Head and Thorax Post-Chikungunya Virus Infection. *Pathogens*. 2019;8(3):132. Published 2019 Aug 27. doi:10.3390/pathogens8030132

Vedururu RK, Neave MJ, Tachedjian M, Klein MJ, Gorry PR, Duchemin J-B, Paradkar PN. RNASeq Analysis of *Aedes albopictus* Mosquito Midguts after Chikungunya Virus Infection. *Viruses*. 2019;11(6):513. Published 2019 Jun 4. doi:10.3390/v11060513

Abstract

Chikungunya virus (CHIKV) of *Alphavirus* genus, has caused several outbreaks around the world in the last decade. Once a relatively unknown virus, it now causes seasonal infections in tropical and some temperate regions. This change in epidemiology is attributed to vector switch from *Aedes aegypti* to *Aedes albopictus*, an invasive pest leading to infections in temperate regions. Although recent research has identified mosquito factors influencing infections, our understanding of interaction between CHIKV and its new vector is limited.

Using whole transcriptome sequencing of CHIKV infected mosquitoes, we studied differential expression of genes in the midgut and head and thorax, the two critical barrier sites of the mosquito at two time points. We identified several up and down regulated transcripts in the mosquito host genome in response to the viral infection. Two days post-infection, in the midgut tissue of the mosquitoes, 250 differentially expressed transcripts (25 when the next-generation sequencing (NGS) reads were aligned to the published reference genome and 225 when the reads were aligned to a de novo custom transcriptome we generated) were identified. From the head and thorax tissue of the mosquitoes, 8 days post-infection, 159 differentially expressed transcripts (96 when the NGS reads were aligned to the published reference genome and 63 when the reads were aligned to the de novo custom transcriptome) were identified. Twenty-seven of the targets (13 from 2dpi/midgut and 14 from 8dpi/head & thorax) identified to be differentially expressed were validated separately via qRT-PCR. Seven transcripts found to be differentially expressed in midguts of *Ae. albopictus* two days post-infection were also assessed for changes in expression in midguts of *Ae. aegypti* two days post-infection. Apart from differential expression in genes, we also identified down regulation of long

non-coding RNAs that may also have functional relevance. The comparison between *Ae. albopictus* and *Ae. aegypti* also showed that the expression patterns of the same targets are different between the two species of mosquitoes after CHIKV infection.

From the targets we validated, two were selected for further functional studies. *Niemann-Pick 2* (NPC2) gene homologue was found to be significantly upregulated in the midguts of both *Ae. albopictus* and *Ae. aegypti* mosquitoes, two days post-infection with CHIKV. Known cytoplasmic lipid transporters, NPC family proteins had previously been implicated in pathogenesis of several viruses including dengue, Ebola and HIV. In fact, NPC2 protein was found to be essential for successful replication of CHIKV in human fibroblasts. To characterise the role of NPC2 during CHIKV in *Ae. albopictus* mosquito, the gene was over expressed in C6/36 mosquito cells 24 hours prior infection with the virus. The infectivity titres of extracellular mature virus and intracellular viral RNA levels were compared between wildtype cells and cells over expressing the protein. The expressed NPC2 protein and the virus were also labelled using antibodies and studied under confocal microscopy. While significant differences were not observed in the viral RNA levels or infectivity titres, confocal microscopy showed partial co-localisation of NPC2 protein and the virus.

Inhibitor of Bruton's tyrosine kinase (BTKi) was identified to be significantly upregulated 8 days post-infection in the head and thorax of *Ae. albopictus* mosquitoes. To assess its functional significance, BTKi was knocked-down using double-stranded RNA in RML12, a mosquito cell line. While no significant difference in viral RNA levels or infectivity titers was detected, BTKi gene knocked-down cells showed increased apoptosis 24 hours post-infection compared with control cells, suggesting involvement of BTKi in the mosquito response to viral infection. BTK is a pro-inflammatory cytoplasmic Tec kinase and is known to be involved in osteoclastogenesis, a hallmark of CHIKV pathogenesis. The

upregulation of BTKi a known anti-inflammatory protein post viral infection and increase in cellular apoptosis when the gene is knocked down may suggest a possible conserved mechanism at play between mosquitoes and mammals.

We also studied changes in the viral genome during mosquito infection. We detected changes in viral diversity, as shown by number of mutations in the viral genome, with increase in number of mutations in the midgut compared with mammalian host (Vero cell culture), followed by reduction in the number of mutations in head and thorax at 8 dpi, indicating a possible genomic bottleneck.

Taken together, these results will help in understanding *Ae. albopictus* interactions with CHIKV and can lead to development of novel disease control strategies.

Chapter-1

Introduction

Chapter 1: Introduction

1.1 Chikungunya Virus

Chikungunya virus (CHIKV) was first identified and described as an independent virus in 1955, in a report on an outbreak at the border of Tanzania and Mozambique in 1952. While the virus was partially isolated, complete isolation and characterisation was completed after an outbreak in Vellore, Southern India in 1964. The name chikungunya is believed to have been derived from the word “Kungunyala” of the local “Makonde” language roughly translating into “to bend”. Prior to being named Chikungunya, the viral affliction was also called “Kidinga pepo”, meaning “a disease characterised by a sudden cramp-like seizure, caused by an evil spirit” in Swahili (1-3).

Chikungunya virus is an enveloped, positive sense RNA virus (Baltimore classification: Class-IV) belonging to the *Alphavirus* genus in *Togaviridae* family. The viruses in *Alphavirus* genus are classified based on their geographical distribution into old world (Sindbis and Semliki forest group) and new world viruses (VWE-EEV group) (Table 1.1). Most alphaviruses are arboviruses, with a life cycle that involves a vertebrate host and hematophagous arthropod vectors. Interestingly the clinical diseases caused by these viruses also follow this geographic stratification. Old world viral infections cause high febrile illness, cutaneous exanthema and debilitating and often prolonged arthralgia while the new world viral infections typically cause equine and human encephalitic disease (4, 5).

Table 1.1 Classification of Alphavirus

Alphavirus		
Old world		New world
Sindbis group	Semliki forest group	VWE-EEV group
Sindbis virus	Semliki forest virus	Venezuelan equine encephalitis virus
	Chikungunya virus	Eastern equine encephalitis virus
	Barmah Forest virus	Western equine encephalitis virus
	Ross River virus	
	O'nyong'nyong virus	
	Una virus	

It is also now accepted that what is now called chikungunya was the original classical dengue and what is now called dengue is what was originally called the “Breakbone fever”. Lack of serological and molecular diagnostic methods and similarity in clinical symptoms of chikungunya and dengue led to this confusion. It is now clear that while the onset and early symptoms of both the diseases are similar, arthralgia and arthritis associated with chikungunya tend to endure for much longer periods, sometimes months (6).

Historically, David Bylon, a Dutch municipal surgeon, working in Jakarta, Indonesia was credited with recording the first outbreak in 1779 (7). Epidemiological observations and studying of recordings of various disease outbreaks show that periodic outbreaks of chikungunya have been occurring approximately every 40 years, in 1770s, 1824, 1871, 1902, 1923, and 1963. These outbreaks started in eastern Africa and spread across towards South-East Asia crossing over the Indian Ocean regions including India, Sri Lanka, Burma and islands of the region like Madagascar, Mauritius, except for the one recorded outbreak in 1827-28 in the Caribbean islands (8). This outbreak is believed to be an

extension of the 1824 outbreak in Zanzibar, Africa, which spread in both east and west directions. In this outbreak, considered to be the last one in the Americas before 2005, about 12000 cases were recorded. The most recent outbreak (2005-ongoing), occurring after ~40 years after the last outbreak in 1963, has also spread around the world (8).

The current and ongoing chikungunya outbreak is the biggest yet, both in terms of the duration of the outbreak and the number of people infected. Starting in the French La Reunion Islands in 2005 where over 244,000 (about 50% of the population) cases were recorded with 203 deaths (mortality: 0.08%) (9, 10). The outbreak then spread to other regions including the Indian subcontinent. During the 2005-2006 outbreak in India, over a million cases were diagnosed (11). Since then chikungunya disease has become seasonal and endemic with regular outbreaks in multiple Asian, African and American regions. While the Reunion Islands were where the first large scale infections was recorded, this outbreak is also believed to have started in East Africa. Chikungunya infections have also been recorded in Europe with cases in Italy, France and Spain (12-14). Current geographic distribution of CHIKV is presented in Figure 1.1.

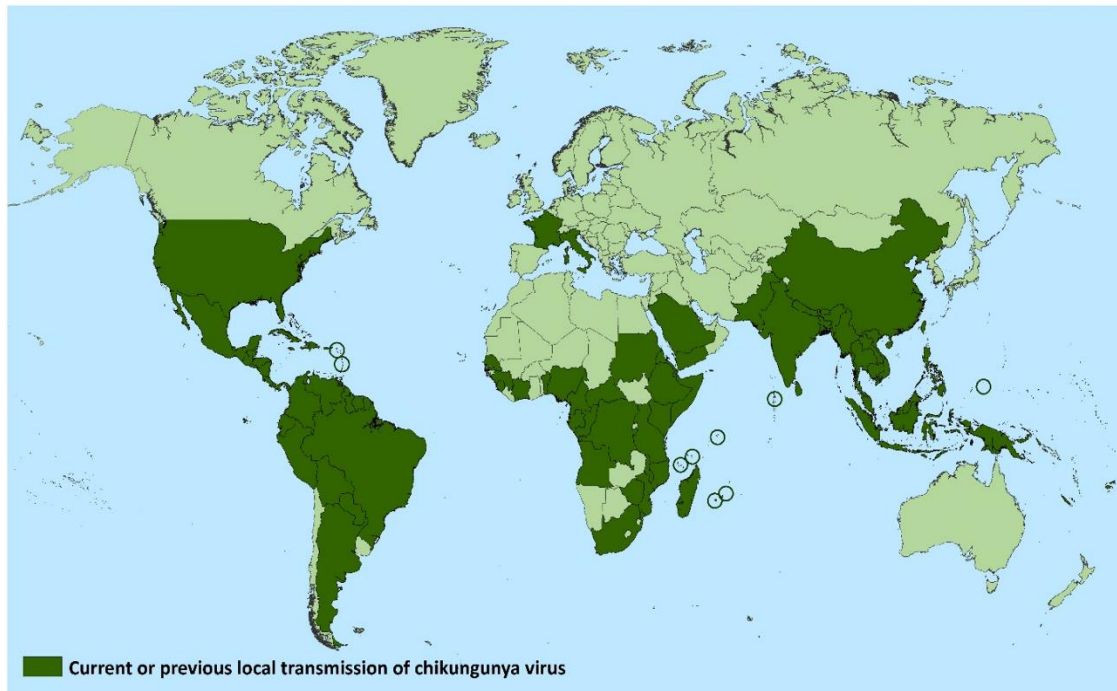


Figure 1.1 Geographic distribution of Chikungunya (as of 17th September 2019, local transmissions only)(15)

1.2 Virology & Chikungunya Disease

The chikungunya virion is ~70nm in diameter. The viral genome is surrounded by a capsid protein shell surrounded by a host derived lipid envelope with glycoprotein spikes. Both the capsid shell and the protein spikes (heterodimers of E1 and E2 proteins) are arranged in T=4 lattice. 80 spikes are arranged as trimers of heterodimers per virion particle while 240 individual proteins form a single capsid unit (16-19)(Figure 1.2).

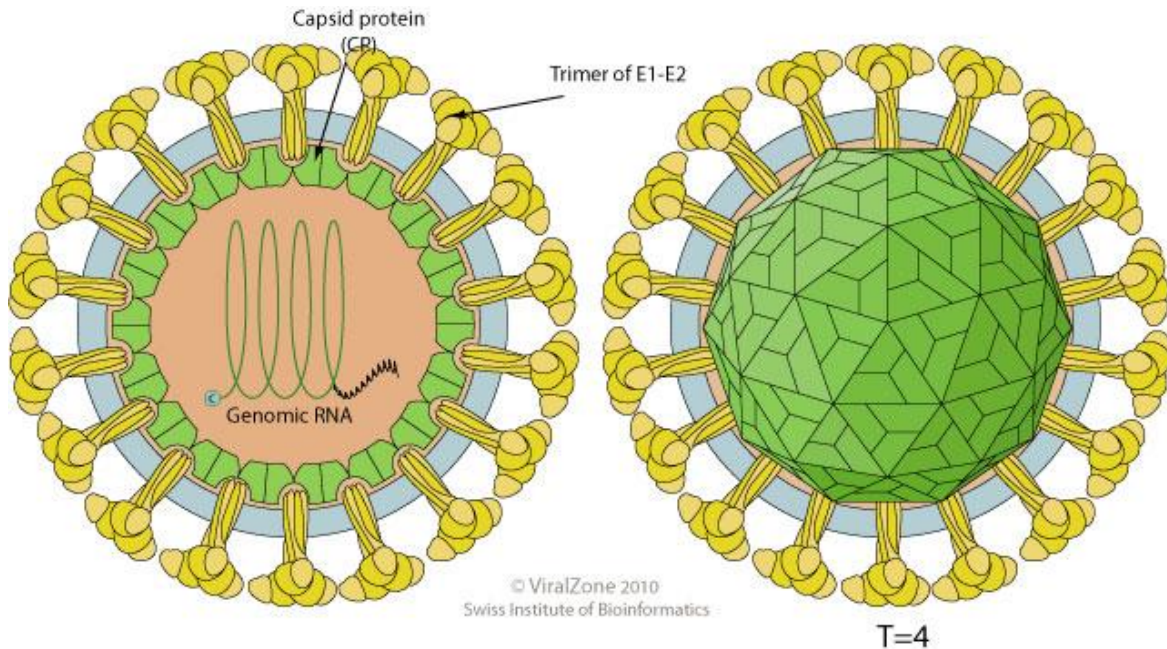


Figure 1.2: Alphaviral Virion Structure (18, 19)

The single stranded, positive sense RNA genome is about 11-12 kb in length with two open reading frames (ORFs) that code for two polyproteins, one structural and one non-structural. The viral genome is capped (5') and polyadenylated (3'). Virion RNA is infectious and acts as both genomic and mRNA. During early stages of infection, the genome is translated into a non-structural polyprotein (P123) which is processed and cleaved by a combination of both viral and host proteases. P123 is cleaved into NSP1, NSP2 (Viral protease) and NSP3. NSP4 or RNA dependent RNA polymerase (RdRp) is expressed by suppression of termination at the 3' end of the nonstructural polyproteins. These nonstructural proteins help further establish the infection through viral genome replication. In later stages of infection, structural polyproteins are expressed through sub-genomic mRNA transcription (16-19).

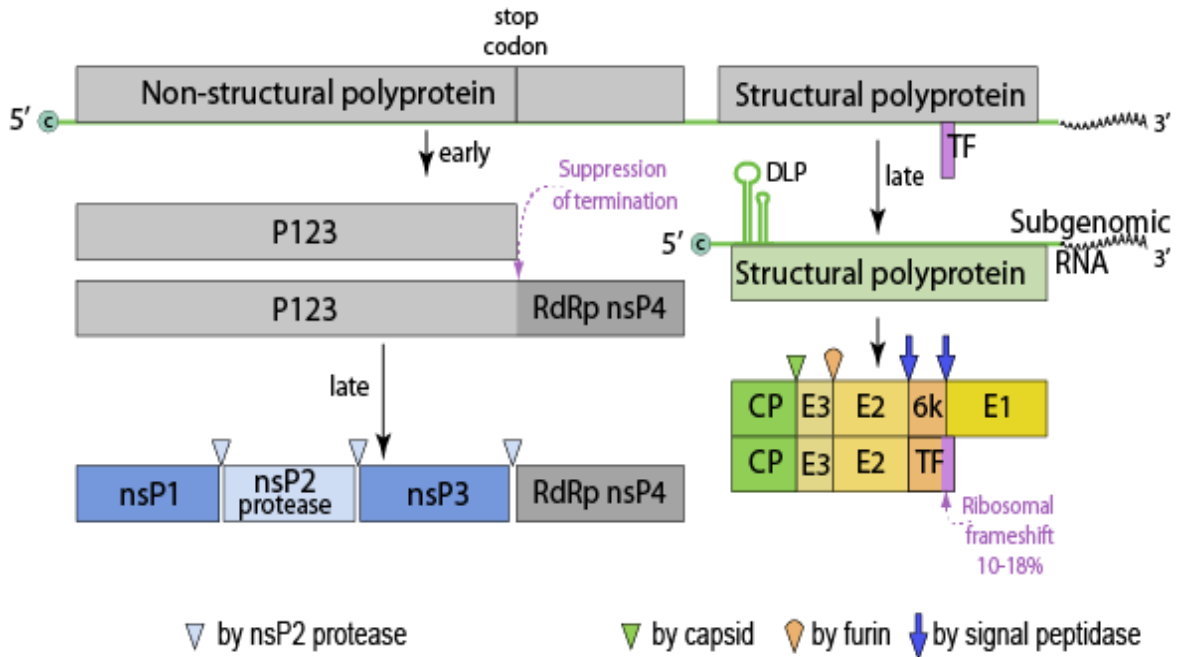


Figure 1.3: Schematic representation of *Chikungunya* viral genome organization (18, 19)

A Downstream Hairpin Loop (DLP) close to the 5' region of the sub-genomic structural protein coding ORF aids in inhibition of translation shut off via host Protein Kinase R pathways. The structural polyprotein is expressed in late stages of infection through promotion of sub-genomic mRNA translation. As with non-structural proteins, the polyprotein is cleaved into functional individual proteins by a combination of viral and host proteolytic activity. Ribosomal frameshifting at the 6K region results in the translation of the TF protein (Figure 1.3) (16-19).

Chikungunya viral fever is characterised with sudden onset febrile illness lasting for about a week often with poor response to antipyretic treatments, musculoskeletal joint pains and headache. Fatigue, anorexia and nausea are common. Peripheral joints including knees and elbows are heavily inflamed with effusions. Different cutaneous changes are also observed in over 50% of patients. While the symptoms become tolerable after the first week, there are high chances of relapse (20).

While not commonly fatal, critical complications of central nervous system following CHIKV infections have been observed. The symptoms are interesting in that they are similar to the symptoms of diseases caused by the “New world” alphaviruses (21).

Chikungunya viral disease in humans is a two-stage condition. The first ten days of CHIKV infection is defined as the acute state of infection followed by a chronic phase. A small proportion of infections remain asymptomatic, usually less than 10%. Mother to child vertical transmission has been noted in near term viremic mothers. About 50% of the children born in this condition were infected, often with central nervous system complications and poor prognosis. Unlike Zika infection, malformations or developmental deformities including megaloccephaly are not observed in CHIKV infections of pregnant women. The risk of miscarriage was higher before the 22nd week of pregnancy (22-25).

Chronic stage of infection is observed as rebound symptoms post the initial improvement, signified by prolonged rheumatism and reduced quality of life. The symptoms were worse in patients with pre-existing complications including cardiac and arthritic issues, progressive age and obesity (26). CHIKV-induced rheumatism is the most frequent manifestation of the chronic stage. It consists of three clinical components, singly or in combination: 1) distal polyarthritis or monoarthritis mildly improved with non-steroid anti-inflammatory drugs, 2) frequent tenosynovitides in the hands, wrists, or ankles, highly sensitive to short-term systemic cortico-therapy, and 3) exacerbation of pain in previously injured joints and bones requiring painkillers. Rebound symptoms have been observed years after original infection and significantly affect lifestyle of patients. No effective vaccines are available, and treatment is mostly symptomatic with painkillers and NSAIDs for relief from pain (27-29).

1.3 Vectors

Mosquitoes belonging to the *Aedes* genus of the Culicine family have been known to be competent vectors for several arboviruses (30). *Ae. aegypti* had been the traditional classical vector for CHIKV. While other species of the *Aedes* genus have also been competent vectors of the virus, their utility in the wild has not been clearly studied (31, 32). Since the Reunion Island outbreak, *Ae. albopictus* has been observed to be more involved in viral transmission. Research showed that a single mutation in codon 226 of the E1 gene of the viral genome, improved fitness of CHIKV in *Ae. albopictus*. This genetic shift has been implicated for most of the recent outbreaks where despite absence of the traditional vector *Ae. aegypti*, CHIKV has successfully established infections through *Ae. albopictus* (33).

Ae. aegypti, also called Yellow Fever mosquito, is a known vector for transmitting a wide variety of arboviruses including yellow fever, chikungunya, dengue and Zika. Originating in Africa, they have now spread to most tropical and subtropical regions of the world on all continents (34-36). The males feed on sugars from flower nectar while the females need both sugar for growth and protein from blood for egg laying. While capable of feeding at all times, preference is observed to be between dawn and dusk. The average life span is two to four weeks and eggs can stay viable for a long time (up to a year) thus allowing repopulation of an area after particularly long adverse seasons. *Ae. aegypti* has evolved into an urban dweller, preferring to live in close proximity to human settlements. Egg laying happens in stagnant but clean (non-muddy) waters around human habitats such as rain water trapped in waste bottles and barrels (37).

Ae. albopictus, also called Asian tiger mosquito, is an invasive pest (38). It is capable of acting as a vector to most arboviruses transmitted by *Ae. aegypti* including some parasitic

nematodes. True to its nature of being an invasive species, *Ae. albopictus* has been expanding its traditional habitat of tropical and sub-tropical regions to much cooler temperate regions (39). While they stay active yearlong in the warm tropical regions, they have been observed to undergo hibernation during winter. Adult *Ae. albopictus* mosquitoes have also been noted to survive in favourable microhabitats even in winter and freezing temperatures (40).

It is now believed that the mosquitoes reached North America through used auto tire trade from Asia and spread rapidly, establishing themselves and thrived (41). In Australia, while *Ae. aegypti* is well entrenched in Australian mainland, *Ae. albopictus* mosquitoes are only endemic to Torres strait island (42, 43). While CHIKV is not endemic to Australia, Barmah Forest virus (BFV) and Ross River virus (RRV) are endemic alphaviruses and cause routine infections. The symptoms caused are similar to other old world alphaviral diseases (44). Multiple vertebrates in Australia show antibodies to both BFV and RRV (45).

While several human chikungunya cases have been diagnosed in mainland Australia, these are all in travellers returning from CHIKV endemic areas and infected overseas (46). CHIKV is not endemic to Australia as of now, but it is clear that it is only a matter of time before the virus spreads in Australia. Competent vectors (in particular *Ae. albopictus*), a known pest is slowly but surely spreading their footprint. With ever increasing global travelling, global warming and explosion of population, an effective multipronged approach to tackle this fast approaching problem is needed to control the mosquito numbers and thus diminish the chances of not just CHIKV becoming endemic but prevent/eradicate RRV and BFV infections.

1.4 Viral Transmission

Female mosquitoes require protein for oogenesis. This protein need is met through blood feeding from warm blooded animals, which exposes them to a variety of blood borne pathogens. While not every pathogen is adapted to survive the digestive system of mosquitoes, infect the cells, replicate and establish infections, several arboviruses have (47, 48). The virus enters and replicates in the midgut epithelium and disseminates further into the haemocoel and then makes its way to the salivary glands of the mosquito, which are present in the top 1/3rd thorax region (49). Once the salivary glands of the mosquitoes are infected, virus is usually found in the saliva of the mosquito (50-53). At this stage the mosquito is considered infective. When a female mosquito bites an organism for blood feeding, saliva is injected at the site, so the anti-inflammatory and pain suppressing proteins in the saliva ensure the host is not irritated and thus the virus in the saliva enters the blood stream of a new host. The midgut and salivary gland of the mosquito, thus, are considered the two critical barrier sites (50). A single mosquito can infect multiple hosts in the process of blood feeding from each round of egg laying. Previous reports also indicate vertical transmission of various arboviruses including CHIKV occurs in the wild from mother to egg (54, 55). Vertical transmission in humans has also been reported but the period of gestation during infection has a significant effect on the viability of pregnancy and survival of progeny (51, 56).

Considering the invasive nature of *Ae. albopictus*, it is considered only a matter of time before it establishes itself on the Australian mainland. Once a competent vector is established, autochthonous infections of CHIKV are inevitable. The current project aims to increase our understanding of the interaction between CHIKV and its new preferred vector *Ae. albopictus* at the two critical barrier sites through transcriptome studies.

1.5 Host-Pathogen Interactions

With the objective of better understanding host-pathogen interactions, multiple studies have been published that report significant changes in transcriptional activity in the host during viral infections. Previous studies have used transcriptome-based approaches to identify mosquito-virus interactions, tissue-specific responses during the course of infection have not been characterised (57-62). Here, using next-generation sequencing, we characterised the whole transcriptome response at the midgut (the first barrier site) and head and thorax (containing the salivary glands and viral dissemination sites), in *Ae. albopictus* in response to CHIKV infection.

Briefly, we infected lab reared *Ae. albopictus* mosquitoes with CHIKV by oral challenge. Two days post-infection, the midguts and eight days post-infection, heads and thoraxes of the mosquitoes were collected. Total RNA was isolated and RNA-Seq was performed to detect differentially expressed genes.

We also analysed the viral genome reads obtained from the midgut and head and thorax of the mosquitoes and compared the sequence to the original mammalian host origin viral sequence.

The objective of this project is to gain a clearer understanding of the host-pathogen interactions between CHIKV and *Ae. albopictus* mosquito at the two critical barrier sites to a transcriptome level through an un-biased RNA-Seq approach. The study also helps in understanding the modifications the viral genome undergoes as it transfers from a mammalian host to a mosquito vector.

1.6 References

1. Robinson MC. An epidemic of virus disease in Southern Province, Tanganyika Territory, in 1952-53. I. Clinical features. *Transactions of the Royal Society of Tropical Medicine and Hygiene*. 1955;49(1):28-32.
2. Mason PJ, Haddow AJ. An epidemic of virus disease in Southern Province, Tanganyika Territory, in 1952-1953. *Transactions of the Royal Society of Tropical Medicine and Hygiene*. 1957;51(3):238-40.
3. Carey DE, Myers RM, Reuben R, Rodrigues FM. Studies on dengue in Vellore, South India. *Bulletin of the World Health Organization*. 1966;35(1):61-.
4. Kamath S, Das AK, Parikh FS. Chikungunya. *Journal of Association of Physicians India*. 2006;54.
5. Kucharz EJ, Cebula-Byrska I. Chikungunya fever. *European Journal of Internal Medicine*. 2012;23(4):325-9.
6. Kuno G. A Re-Examination of the History of Etiologic Confusion between Dengue and Chikungunya. *PLoS Neglected Tropical Diseases*. 2015;9(11):e0004101.
7. Carey DE. Chikungunya and dengue: A Case of Mistaken Identity? *Journal of the History of Medicine and Allied Sciences*. 1971;XXVI(3):243-62.
8. Halstead SB. Reappearance of Chikungunya, Formerly Called Dengue, in the Americas. *Emerging Infectious Diseases*. 2015;21(4):557-61.
9. Josseran L, Paquet C, Zehgnoun A, Caillere N, Le Tertre A, Solet J-L, *et al*. Chikungunya disease outbreak, Reunion Island. *Emerging Infectious Diseases*. 2006;12(12):1994-5.
10. Soumahoro M-K, Boelle P-Y, Gaüzere B-A, Atsou K, Pelat C, Lambert B, *et al*. The Chikungunya Epidemic on La Réunion Island in 2005-2006: A Cost-of-Illness Study. *PLoS neglected tropical diseases*. 2011;5(6):e1197.
11. Lahariya C, Pradhan SK. Emergence of chikungunya virus in Indian subcontinent after 32 years: A review. *Journal of vector borne diseases*. 2006;43(4):151-60.
12. Amraoui F, Failloux AB. Chikungunya: an unexpected emergence in Europe. *Current Opinions in Virology*. 2016;21:146-50.
13. Rezza G, Nicoletti L, Angelini R, Romi R, Finarelli AC, Panning M, *et al*. Infection with chikungunya virus in Italy: an outbreak in a temperate region. *Lancet*. 2007;370(9602):1840-6.

14. Venturi G, Di Luca M, Fortuna C, Remoli ME, Riccardo F, Severini F, *et al.* Detection of a chikungunya outbreak in Central Italy, August to September 2017. *Euro Surveill.* 2017;22(39):17-00646.
15. Prevention CfDCa. Countries and territories where chikungunya cases have been reported* (as of September 17, 2019). [Image on internet]. 2019.
16. Strauss JH, Strauss EG. The alphaviruses: gene expression, replication, and evolution. *Microbiological Reviews.* 1994;58(3):491-562.
17. Jose J, Snyder JE, Kuhn RJ. A structural and functional perspective of alphavirus replication and assembly. *Future Microbiology.* 2009;4:837-56.
18. Masson P, Hulo C, De Castro E, Bitter H, Gruenbaum L, Essioux L, *et al.* ViralZone: recent updates to the virus knowledge resource. *Nucleic Acids Research.* 2013;41(Database issue):D579-D83.
19. Hulo C, de Castro E, Masson P, Bougueleret L, Bairoch A, Xenarios I, *et al.* ViralZone: a knowledge resource to understand virus diversity. *Nucleic Acids Research.* 2011;39(Database issue):D576-82.
20. Duvignaud A, Fianu A, Bertolotti A, Jaubert J, Michault A, Poubeau P, *et al.* Rheumatism and chronic fatigue, the two facets of post-chikungunya disease: the TELECHIK cohort study on Reunion island. *Epidemiology and infection.* 2018;146(5):633-41.
21. Mehta R, Soares CN, Medialdea-Carrera R, Ellul M, da Silva MTT, Rosala-Hallas A, *et al.* The spectrum of neurological disease associated with Zika and chikungunya viruses in adults in Rio de Janeiro, Brazil: A case series. *PLoS Neglected Tropical Diseases.* 2018;12(2):e0006212.
22. Nakkhara P, Chongsuvivatwong V, Thammapalo S. Risk factors for symptomatic and asymptomatic chikungunya infection. *Transactions of the Royal Society of Tropical Medicine and Hygiene.* 2013;107(12):789-96.
23. Contopoulos-Ioannidis D, Newman-Lindsay S, Chow C, LaBeaud AD. Mother-to-child transmission of Chikungunya virus: A systematic review and meta-analysis. *PLoS Neglected Tropical Diseases.* 2018;12(6):e0006510.
24. Cardona-Correa SE, Castano-Jaramillo LM, Quevedo-Velez A. [Vertical transmission of chikungunya virus infection. Case Report]. *Revista chilena de pediatria.* 2017;88(2):285-8.

25. Oliveira RdMAB, Barreto FKdA, Maia AMPC, Gomes IP, Simião AR, Barbosa RB, *et al.* Maternal and infant death after probable vertical transmission of chikungunya virus in Brazil – case report. *BMC Infectious Diseases*. 2018;18(1):333.
26. Krutikov M, Manson J. Chikungunya Virus Infection: An Update on Joint Manifestations and Management. *Rambam Maimonides Med J*. 2016;7(4):e0033.
27. Simon F, Javelle E, Oliver M, Leparç-Goffart I, Marimoutou C. Chikungunya Virus Infection. *Current Infectious Disease Reports*. 2011;13(3):218-28.
28. Bonifay T, Prince C, Neyra C, Demar M, Rousset D, Kallel H, *et al.* Atypical and severe manifestations of chikungunya virus infection in French Guiana: A hospital-based study. *PLoS One*. 2018;13(12):e0207406.
29. Cunha RVd, Trinta KS. Chikungunya virus: clinical aspects and treatment - A Review. *Mem Inst Oswaldo Cruz*. 2017;112(8):523-31.
30. Huang Y-JS, Higgs S, Vanlandingham DL. Arbovirus-Mosquito Vector-Host Interactions and the Impact on Transmission and Disease Pathogenesis of Arboviruses. *Frontiers in Microbiology*. 2019;10(22).
31. Lwande OW, Obanda V, Lindström A, Ahlm C, Evander M, Näslund J, *et al.* Globe-Trotting *Aedes aegypti* and *Aedes albopictus*: Risk Factors for Arbovirus Pandemics. *Vector-Borne and Zoonotic Diseases*. 2019.
32. Wong HV, Chan YF, Sam IC, Sulaiman WY, Vythilingam I. Chikungunya Virus Infection of *Aedes* Mosquitoes. *Methods in molecular biology (Clifton, NJ)*. 2016; 1426:119-28. DOI: 10.1007/978-1-4939-3618-2_11
33. Tsetsarkin KA, Chen R, Weaver SC. Interspecies transmission and chikungunya virus emergence. *Current Opinion in Virology*. 2016;16:143-50.
34. Tedjou AN, Kamgang B, Yougang AP, Njiokou F, Wondji CS. Update on the geographical distribution and prevalence of *Aedes aegypti* and *Aedes albopictus* (Diptera: Culicidae), two major arbovirus vectors in Cameroon. *PLoS Neglected Tropical Diseases*. 2019;13(3):e0007137.
35. Kamal M, Kenawy MA, Rady MH, Khaled AS, Samy AM. Mapping the global potential distributions of two arboviral vectors *Ae. aegypti* and *Ae. albopictus* under changing climate. *PLoS One*. 2019;13(12):e0210122.
36. Dickens BL, Sun H, Jit M, Cook AR, Carrasco LR. Determining environmental and anthropogenic factors which explain the global distribution of *Ae. aegypti* and *Ae. albopictus* *BMJ Global Health*. 2018;3(4):e000801.

37. Catherine Zettel PK. Yellow fever mosquito *Aedes aegypti* (Linnaeus) (Insecta: Diptera: Culicidae) University of Florida, Institute of Food and Agricultural Sciences 2009
38. Shragai T, Harrington LC. *Aedes albopictus* (Diptera: Culicidae) on an Invasive Edge: Abundance, Spatial Distribution, and Habitat Usage of Larvae and Pupae Across Urban and Socioeconomic Environmental Gradients. *Journal of Medical Entomology*. 2019;56(2):472-82.
39. Bonizzoni M, Gasperi G, Chen X, James AA. The invasive mosquito species *Aedes albopictus*: current knowledge and future perspectives. *Trends in parasitology*. 2013;29(9):460-8.
40. Leslie Rios JEM. Asian tiger mosquito 2004 [cited 2016. Available from: http://entomology.ifas.ufl.edu/creatures/aquatic/asian_tiger.htm.
41. Yee DA. Tires as habitats for mosquitoes: a review of studies within the eastern United States. *Journal of Medical Entomology*. 2008;45(4):581-93.
42. Nicholson J, Ritchie SA, Van Den Hurk AF. *Aedes albopictus* (Diptera: Culicidae) as a Potential Vector of Endemic and Exotic Arboviruses in Australia. *Journal of Medical Entomology*. 2014;51(3):661-9.
43. van den Hurk AF, Nicholson J, Beebe NW, Davis J, Muzari OM, Russell RC, *et al*. Ten years of the Tiger: *Aedes albopictus* presence in Australia since its discovery in the Torres Strait in 2005. *One Health*. 2016;2:19-24.
44. Harley D, Sleigh A, Ritchie S. Ross River virus transmission, infection, and disease: a cross-disciplinary review. *Clinical microbiology reviews*. 2001;14(4):909-32.
45. Kay BH, Boyd AM, Ryan PA, Hall RA. Mosquito feeding patterns and natural infection of vertebrates with Ross River and Barmah Forest viruses in Brisbane, Australia. *American Journal of Tropical Medicine and Hygiene*. 2007;76(3):417-23.
46. Suhrbier A, Devine G. Chikungunya virus, risks and responses for Australia. *Australian and New Zealand journal of public health*. 2016;40(3):207-9.
47. Braack L, Gouveia de Almeida AP, Cornel AJ, Swanepoel R, de Jager C. Mosquito-borne arboviruses of African origin: review of key viruses and vectors. *Parasites & Vectors*. 2018;11(1):29.
48. Huang Y-JS, Higgs S, Vanlandingham DL. Arbovirus-Mosquito Vector-Host Interactions and the Impact on Transmission and Disease Pathogenesis of Arboviruses. *Frontiers in Microbiology*. 2019;10:22-.

49. Arias-Goeta C, Mousson L, Rougeon F, Failloux A-B. Dissemination and Transmission of the E1-226V Variant of Chikungunya Virus in *Aedes albopictus* Are Controlled at the Midgut Barrier Level. *PLoS One*. 2013;8(2):e57548.
50. Franz AWE, Kantor AM, Passarelli AL, Clem RJ. Tissue Barriers to Arbovirus Infection in Mosquitoes. *Viruses*. 2015;7(7):3741-67.
51. Kuno G, Chang G-JJ. Biological Transmission of Arboviruses: Re-examination of and New Insights into Components, Mechanisms, and Unique Traits as Well as Their Evolutionary Trends. *Clinical Microbiology Reviews*. 2005;18(4):608-37.
52. Dong S, Kantor AM, Lin J, Passarelli AL, Clem RJ, Franz AWE. Infection pattern and transmission potential of chikungunya virus in two New World laboratory-adapted *Aedes aegypti* strains. *Scientific Reports*. 2016;6:24729.
53. Dubrulle M, Mousson L, Moutailler S, Vazeille M, Failloux A-B. Chikungunya Virus and *Aedes* Mosquitoes: Saliva Is Infectious as soon as Two Days after Oral Infection. *PLoS One*. 2009;4(6):e5895.
54. Lequime S, Paul RE, Lambrechts L. Determinants of Arbovirus Vertical Transmission in Mosquitoes. *PLoS Pathogens*. 2016;12(5):e1005548.
55. Honório NA, Wiggins K, Eastmond B, Câmara DCP, Alto BW. Experimental Vertical Transmission of Chikungunya Virus by Brazilian and Florida *Aedes Albopictus* Populations. *Viruses*. 2019;11(4):353.
56. Chompoonsri J, Thavara U, Tawatsin A, Boonserm R, Phumee A, Sangkitporn S, et al. Vertical transmission of Indian Ocean Lineage of chikungunya virus in *Aedes aegypti* and *Aedes albopictus* mosquitoes. *Parasite Vectors*. 2016 Apr 23;9:227..
57. Dong S, Behura SK, Franz AWE. The midgut transcriptome of *Aedes aegypti* fed with saline or protein meals containing chikungunya virus reveals genes potentially involved in viral midgut escape. *BMC Genomics*. 2017;18(1):382.
58. Etebari K, Hegde S, Saldaña MA, Widen SG, Wood TG, Asgari S, et al. Global Transcriptome Analysis of *Aedes aegypti* Mosquitoes in Response to Zika Virus Infection. *mSphere*. 2017;2(6):e00456-17.
59. Shrinet J, Srivastava P, Sunil S. Transcriptome analysis of *Aedes aegypti* in response to mono-infections and co-infections of dengue virus-2 and chikungunya virus. *Biochemical and Biophysical Research Communications*. 2017;492(4):617-23.

60. Bonizzoni M, Dunn WA, Campbell CL, Olson KE, Marinotti O, James AA. Complex Modulation of the *Aedes aegypti* Transcriptome in Response to Dengue Virus Infection. PLoS One. 2012;7(11):e50512.
61. Fragkoudis R, Chi Y, Siu RW, Barry G, Attarzadeh-Yazdi G, Merits A, *et al.* Semliki Forest virus strongly reduces mosquito host defence signaling. Insect Molecular Biology. 2008;17(6):647-56.
62. Liu Y, Zhou Y, Wu J, Zheng P, Li Y, Zheng X, *et al.* The expression profile of *Aedes albopictus* miRNAs is altered by dengue virus serotype-2 infection. Cell & bioscience. 2015;5:16.

Chapter-2

RNASeq Analysis of *Aedes albopictus* Mosquito Midguts after Chikungunya Virus Infection

Vedururu RK, Neave MJ, Tachedjian M, Klein MJ, Gorry PR, Duchemin J-B, Paradkar PN. RNASeq Analysis of *Aedes albopictus* Mosquito Midguts after Chikungunya Virus Infection. *Viruses*. 2019;11(6):513. Published 2019 Jun 4. doi:10.3390/v11060513

Chapter 2: RNASeq Analysis of *Aedes albopictus* Mosquito Midguts after Chikungunya Virus Infection

Ravi kiran Vedururu 1,2, Matthew J. Neave 1, Mary Tachedjian 1, Melissa J. Klein 1, Paul R. Gorry 3, Jean-Bernard Duchemin 1,† and Prasad N. Paradkar 1,*

1CSIRO Health & Biosecurity, Australian Animal Health Laboratory, Geelong, 3220, Australia;

2School of Applied Sciences, RMIT University, Bundoora, 3083, Australia

3School of Health and Biomedical Science, RMIT University, Bundoora, 3083, Australia; Paul.Gorry@rmit.edu.au

†Current Address: Mosquitoes and Emerging Arboviruses, Institut Pasteur de la Guyane, Cayenne, French Guiana 97306.

*Correspondence: Prasad.Paradkar@csiro.au; Tel.: +61-3-52275462

Received: 4 May 2019; Accepted: 2 June 2019; Published: 4 June 2019

2.1 Abstract:

Chikungunya virus (CHIKV) is an emerging pathogen around the world and causes significant morbidity in patients. A single amino acid mutation in the envelope protein of CHIKV has led to a shift in vector preference towards *Aedes albopictus*. While mosquitoes are known to mount an antiviral immune response post-infection, molecular interactions during the course of infection at the tissue level remain largely uncharacterised. We performed whole transcriptome analysis on dissected midguts of *Aedes albopictus* infected with CHIKV to identify differentially expressed genes. For this, RNA was extracted at two days post-infection (2-dpi) from pooled midguts. We initially identified 25 differentially expressed genes (p-value <0.05) when mapped to a reference transcriptome. Further, multiple differentially expressed genes were identified from a

custom de novo transcriptome, which was assembled using the reads that did not align with the reference genome. Thirteen of the identified transcripts, possibly involved in immunity, were validated by qRT-PCR. Homologues of seven of these genes were also found to be significantly upregulated in *Aedes aegypti* midguts 2 dpi, indicating a conserved mechanism at play. These results will help us to characterise the molecular interaction between *Aedes albopictus* and CHIKV and can be utilised to reduce the impact of this viral infection.

Keywords: Chikungunya; *Aedes albopictus*; RNASeq; Host–pathogen interactions

2.2 Introduction

Arboviruses, such as the dengue, chikungunya, and Zika viruses, are a significant burden on public health systems worldwide. These viruses are transmitted by mosquitoes and can cause high morbidity and mortality, with dengue alone causing more than 300 million infections per year [1]. First identified and described in 1955 in a report on an outbreak at the border of Tanzania and Mozambique in 1952, chikungunya virus (CHIKV) is an enveloped, positive sense RNA virus belonging to the alphavirus genus in the *Togaviridae* family [2,3]. CHIKV infection in humans causes high febrile illness, cutaneous exanthema and debilitating and often prolonged arthralgia [4–6].

While *Aedes aegypti* is the traditional vector for CHIKV, *Aedes albopictus* has been observed to be implicated in viral transmission ever since the Reunion Island outbreak in 2005–2006 [7]. A single amino acid change in codon 226 of the E1 gene, which encodes for the envelope protein of the virus, has improved the fitness of the Indian Ocean lineage CHIKV in *Aedes albopictus* [8]. As an invasive species, *Aedes albopictus* has been expanding its traditional habitat of tropical and sub-tropical regions to much cooler temperate regions. *Aedes albopictus* also survives in favourable microhabitats, even in winter and

freezing temperatures [9]. These factors have further increased the risk of CHIKV to cause outbreaks in areas where mosquito-borne viral diseases are uncommon, such as Northern America and temperate Europe [10,11].

For a mosquito to become infective, the virus needs to cross two critical barrier tissues: the midgut and salivary glands. These infection barriers can be influenced by multiple factors, including viral factors, such as viral glycoproteins, or vector factors, such as the presence of a viral receptor, host replication factors and the microbiome composition of the midgut [12]. When an adult female *Aedes albopictus* mosquito is exposed to CHIKV in the process of blood feeding, the virus infects the midgut usually in a matter of hours [13–15]. Inside mosquitoes, after feeding, the blood meal moves down to the midgut where the virus must contact epithelial cells before digestion of the blood meal and formation of the peritrophic matrix takes place. Following the successful infection of the midgut, the virus must then overcome midgut escape barriers to disseminate to other tissues, such as the haemocoel [16]. From the haemocoel, the virus makes its way to the salivary glands of the mosquito. Once the virus is detected in the saliva, the mosquito is considered to be infective and a competent vector [17,18].

Since vector competence of the mosquito is initially dependent on infection of the midgut (Virus crossing the first critical barrier), understanding the molecular interactions between virus and mosquito midgut becomes essential. Although previous studies have used transcriptome-based approaches to identify mosquito–virus interactions, tissue-specific responses during the course of infection are not well-understood [19–24]. Here, using next-generation sequencing, we characterised the whole transcriptome response at the midgut in *Aedes albopictus* in response to CHIKV infection.

2.3 Materials and Methods

2.3.1 Chikungunya Virus

Chikungunya virus isolate 06113879 (Mauritius strain), isolated from a viraemic traveller who returned to Australia in 2006, was obtained from the Victorian Infectious Diseases Reference Laboratory (VIDRL), Melbourne [25]. The isolate was passaged in Vero cells (ATCC, Virginia, USA) four times, followed by once in C6/36 (*Aedes albopictus* larval cell line) followed again by Vero cells, and was then used for the experiments. A TCID₅₀ assay was performed on Vero cells to determine viral titer.

2.3.2 Aedes Mosquito Rearing, Infection and RNA Extraction

All experiments were performed under biosafety level 3 (BSL-3) conditions in the insectary at the Australian Animal Health Laboratory, CSIRO. Insectary conditions were maintained at 27.5 °C and 70% in relative humidity with a 12 h light and dark cycle. Female mosquitoes (5–8 days old) were challenged with a chicken blood meal spiked with CHIKV (1 in 100 dilution of stock virus, TCID₅₀ 1.5 × 10⁹/mL) through chicken skin membrane feeding. After one hour, the mosquitoes were anaesthetised with CO₂, and the blood-fed females sorted and kept in 200 mL cardboard cup containers at 27.5 °C, 70% humidity and a 14:10 day:night photoperiod for 2 days with 10% sugar solution ad libitum. For controls, females were fed with blood mixed with media supernatant from an uninfected Vero cell culture. Midguts were dissected at 2 dpi and were stored in 50 µL of Qiagen RLTplus buffer with 5–10 silica beads (1 mm) at –80°C.

Bead beating was performed on MP Biomedicals FastPrep -24™ homogeniser, 3 cycles, speed: 6.5 m/s, 45 s each cycle. RNA was extracted using the RNeasy™ kit (Qiagen Australia), and cDNA was generated by using random hexamers and Superscript-III

reverse transcriptase (Thermo Fisher Scientific Inc. Scoresby, Victoria, Australia) following the manufacturer's protocols.

Complementary DNA (cDNA) generated from the RNA extracted from the midguts pools was tested for CHIKV viral RNA using an in-house-designed qRT-PCR, using primers specific for the E1 gene (S1 Table). For RNASeq data validation, adult *Aedes albopictus* female mosquitoes were infected with CHIKV as described above. RNA was extracted from the midguts of 5 infected mosquitoes 2 dpi, and cDNA was generated individually by previously described protocols. cDNA from the midguts of 5 uninfected mosquitoes was used as controls. Mosquitoes from multiple generations but approximately of the same age were used for the experiments.

For comparison of differential gene expression in *Aedes aegypti*, RNA was collected from the midguts of 6 mosquitoes and infected with CHIKV through blood feeding at 2 dpi. RNA that was extracted from the midguts of 5 uninfected mosquitoes was used as a control. cDNA was generated as described above and qPCR was performed with *Aedes aegypti* gene-specific primers.

2.3.3 qPCR

Quantitative PCR (qPCR) was performed using gene-specific primers and 18s rRNA specific primers as internal controls were used to validate the expression changes of 8 targets. Midgut tissue from three infected and control mosquitoes was used for validation of 5 long non-coding RNAs (lncRNAs) by the above-mentioned method.

qPCR was performed on an Applied Biosystems QuantStudio™ 6 using the SYBR Green Master Mix: SYBR Premix Ex Taq II (Tli RNase H Plus) (Takara- Scientifix Pty Ltd., Clayton, Victoria, Australia). The following cycling conditions were used with a melt

curve at the end, 30 s at 95 °C, 40 cycles of 5 s at 95 °C and 30 s at 60 °C. The baseline and Ct values were calculated automatically using the supplied QuantStudio™ Software (Thermo Fisher Scientific Inc. Scoresby, Victoria, Australia), and the $\Delta\Delta\text{Ct}$ values were calculated using the average ΔCt value of controls and 18s rRNA as a reference.

2.3.4 RNASeq and Viral Genome Sequencing

To identify the genes involved in the initial infection stage, midguts from CHIKV-infected *Aedes albopictus* mosquitoes at 2 dpi from 6 mosquitoes were pooled together for RNA extraction to obtain sufficient material. This was also required to avoid using a low-RNA input RNAseq kit, which would likely introduce bias during the PCR amplification stage. The pool size was kept as low as possible to retain information on biological variations.

Libraries for RNASeq were prepared using Nugen's Ovation Universal RNASeq kit, following manufacturer's specification with a minor modification in the HL-dsDNase treatment. During first strand synthesis with DNase treatment, HL-dsDNase from Thermo Fisher Scientific was used in our library preparation, along with the 10x buffer supplied that their protocol used. The libraries were pooled and sequenced on a single lane of HiSeq-2500 (Macrogen Inc, Seoul, South Korea) to generate 2×100 bp reads. The fastq files were deposited in NCBI's (National Center for Biotechnology Information) Sequence Read Archive (SRA Accession ID: SRP140387).

The Qiagen QIAseq FX Single Cell RNA Library kit was used for Illumina library preparation from total RNA extracted from CHIKV-infected Vero cell culture supernatant using the RNeasy™ kit (Qiagen, Chadstone, Victoria, Australia). The library was sequenced on a Miniseq (Illumina, Scoresby, Victoria, Australia), with the mid-output kit (300 cycles) generating 2×150 bp paired-end reads. The resultant fastq files

were quality-trimmed and assembled to a consensus sequence on the CLC Genomics workbench v9.5.2. The sequence was annotated and submitted to GenBank (MH229986).

2.3.5 Differential Gene Expression and Gene Ontology Analysis

Quality trimming of the raw sequences was performed using Trimmomatic v0.36. The reads were aligned to the CHIKV reference sequence (GenBank ID: MH229986) to assess the infection status using Hisat2 v2.0.5 [26].

Following removal of *Gallus gallus* (GenBank assembly accession: GCA_000002315.3) reads (due to chicken blood feeding) using SAMtools v1.3.1, the remaining reads were aligned to the *Aedes albopictus* Foshan strain genome sequence (AaloF1) from Vectorbase using Hisat2, and the resultant SAM file was sorted and converted into a BAM file using SAMtools [27,28].

On Galaxy virtual lab v1.4.6.p5, featureCounts v1.4.6-p5 was used to quantify aligned transcripts from the sorted BAM files with default parameters for paired-end reads, and DESeq2 v2.11.38 was used to obtain differentially expressed genes between the controls and infected samples by using default parameters [29,30].

Using Trinity v2.3.2, a custom de novo transcriptome was built by combining the unaligned reads from midguts (D2) [31,32]. This transcriptome was used as a reference genome. edgeR was used to align the reads, measure the transcript counts and quantify the differentially expressed genes. The differentially expressed genes were annotated using BlastX [33,34].

The gene ontology (GO) IDs of the differentially expressed genes were obtained using the Biomart tool, and topGO analysis was performed to identify the Molecular Functions (MF), Biological Processes (BP) and Cellular Components (CC) that were either enriched

or depleted in the differentially expressed genes [35,36]. Using topGO's classic algorithm, and based on *p*-values generated using Fisher's exact method, differentially expressed genes were grouped based on their ontologies. Enrichment percentage was calculated as the ratio of the number of times particular genes in the pathway were differentially expressed compared to the expected number by chance.

2.4 Results

2.4.1 Whole Genome Sequencing of CHIKV

The chikungunya virus isolate 06113879 was used to infect *Aedes albopictus* mosquitoes. Although a 559 bp portion of the E1 gene has been published (GenBank ID: EU404186.1), full genome sequencing of this isolate has not been performed, which can inform us about the genotype of this virus as well as be used as a reference for removing the virus reads that are detected during the RNASeq analysis.

Whole genome sequencing performed on the CHIKV isolate, after single Vero passaging, using the Illumina MiniSeq, resulted in about 8.5 million quality-trimmed, paired-end reads. The assembly resulted in an 11,929 bp long consensus sequence (MH229986), which perfectly matched the previously published 559 bp portion of the E1 gene from this isolate.

The viral consensus sequence was most similar (Identity: 11,705/11,985 (97.7%), Similarity: 11,705/11,985 (97.7%), Gaps: 245/11,985 (2.0%)) to the CHIKV strain LR2006_OPY1 (GenBank: KT449801.1) and had the E1-A226V mutation, indicating that this isolate also belongs to the same lineage as the CHIKV that caused the La Reunion outbreak in the Indian ocean in 2006.

2.4.2 RNASeq

To determine differentially expressed genes, five pools of midguts (six mosquitoes per pool) collected at 2 dpi from infected mosquitoes were created. For controls, three pools of midguts were used. Initially, to determine the infection status of these tissues, qRT-PCR was performed using CHIKV-specific primers. Based on these results and qualitative and quantitative requirements of the Nugen Ovation universal RNAseq kit, two control and three infected midgut pools were used to prepare sequencing libraries.

The sequencing of five libraries on a single lane of HiSeq-2500 resulted in 37 million to 170 million reads each. After quality trimming, reads mapping to the chicken genome were discarded to remove those originating from undigested chicken blood. The remaining reads were aligned to the *Aedes albopictus* reference genome with an average alignment of 62.25%. The read alignment to the CHIKV reference sequence (MH229986) also confirmed that all the three infected libraries contained viral reads, while the two control libraries did not, as shown in Table 2.1.

Table 2.1 RNASeq next-generation sequencing (NGS) data summary.

	Total Reads (millions)	% Mapped to RefSeq Genome	% of CHIKV Reads
Infected MG 1	170.65	60.83%	0.01%
Infected MG 2	37.13	60.46%	0.02%
Infected MG 3	38.02	65.28%	0.10%
Control MG1	44.77	61.53%	0.00%
Control MG2	44.72	63.15%	0.00%

The total number of obtained reads, the reads' alignment percentage to the reference genome and the percentage of reads aligned to the chikungunya virus genome.

2.4.3 Differential Expression and TopGO Analysis

Differentially expressed genes were identified using DESeq2 (for reads aligned to the RefSeq genome) and edgeR (for the de novo transcriptome built with aligned reads) and were plotted as Volcano plots (Figure 2.1). The results showed 25 genes to be differentially expressed as detected by DESeq2 (Up: 14 and Down: 11). edgeR did not show statistically significant (False Discovery Rate <0.05) differential expression of genes due to a sub-optimal number of control libraries. However, targets from this dataset were chosen based on raw p-values for validation. The complete list of genes and transcripts that were differentially expressed with p-values of less than 0.05 is provided in supplementary information S2. The fasta files that were obtained as output for the custom transcriptome assembly are provided in supplementary information S3.

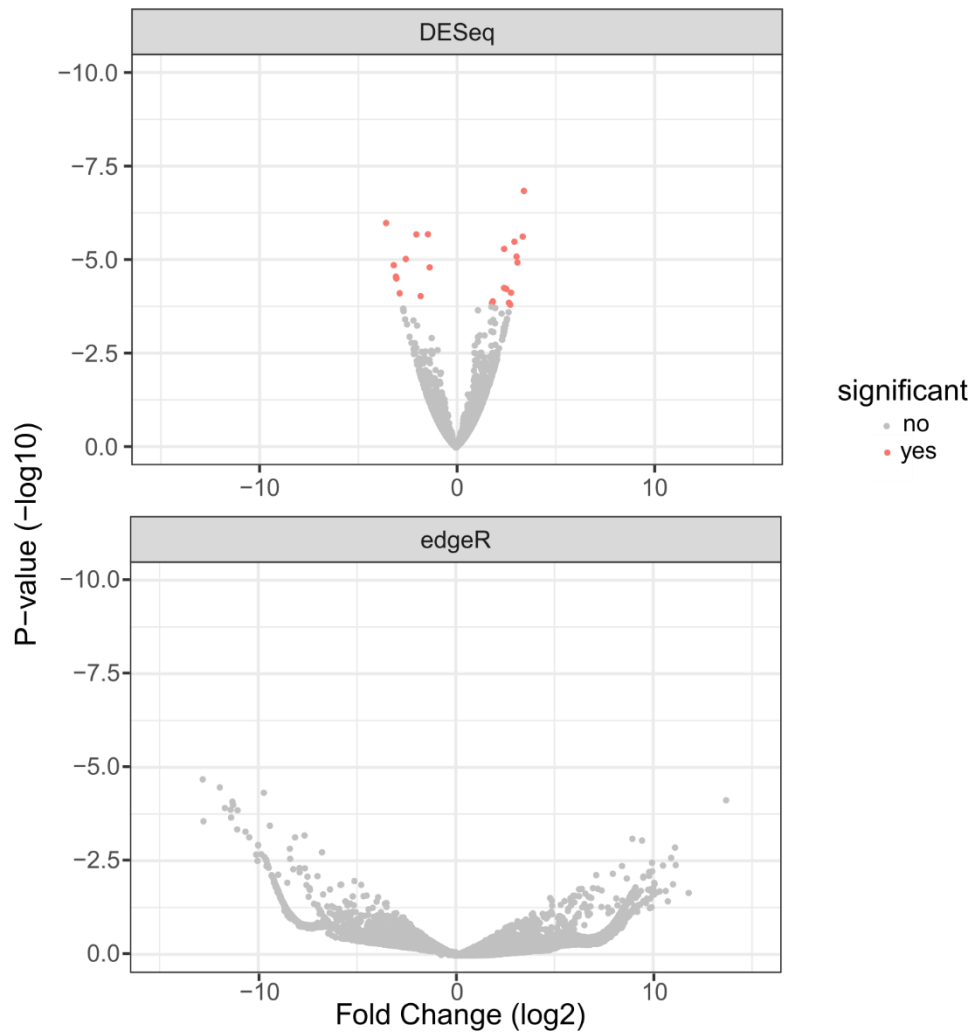


Figure 2.1 Volcano plots from DESeq2 and edgeR for 2 dpi differential gene expression; Volcano plots from DESeq2 (top panel) and edgeR (bottom panel) of differentially expressed genes from 2 dpi. DESeq2 was performed by aligning reads to the Aedes albopictus reference genome. edgeR analysis was done on reads that did not align to the reference genome and were aligned to the custom transcriptome.

To determine the biological processes and molecular functions of the differentially expressed genes, gene set enrichment analysis and ontology was performed using topGO (Figure 2.2). As expected, several biological and molecular processes were significantly affected during CHIKV infection.

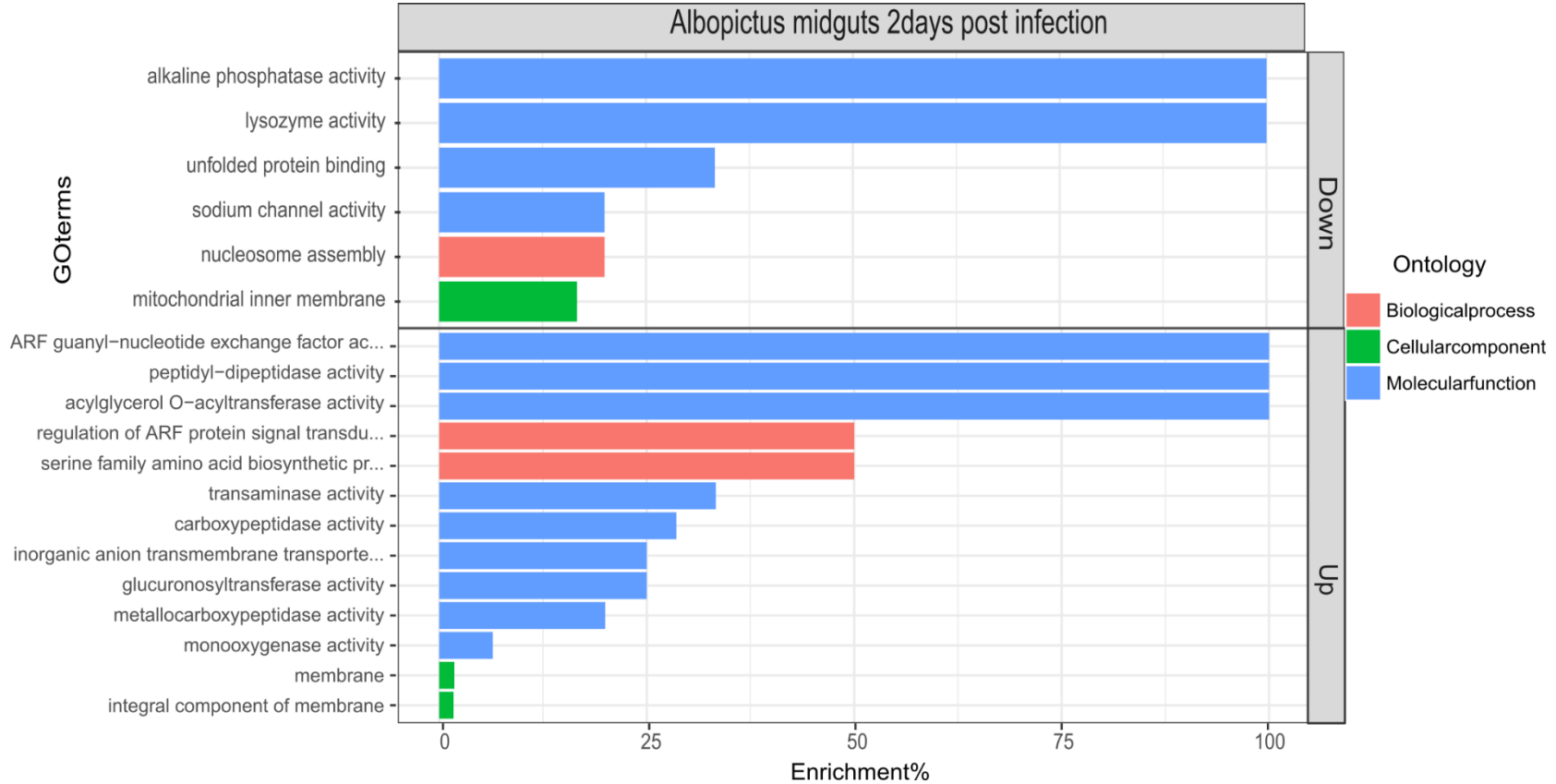


Figure 2.2 topGo enrichment comparison in differentially expressed genes. Enrichment analysis of down- and upregulated genes in the midguts of Aedes albopictus mosquitoes in response to Chikungunya virus (CHIKV) at 2 dpi. Enrichment % is calculated as the ratio of 'significant' (Number of times the gene ontology number is observed as differentially expressed) to 'expected' (Number of times the gene ontology number is expected based on observation in control samples) gene numbers

The differentially regulated biological processes were metabolic (p -value = 0.012) and the serine family amino acid biosynthetic process (p -value = 0.026). The differentially regulated molecular functions, likely of interest from an innate immune response point of view, were lysozyme activity (downregulated, p -value = 0.028), alkaline phosphatase (downregulated, p -value = 0.033) and carboxypeptidase activity (upregulated, p -value = 0.042).

Apart from protein-coding genes, five long non-coding RNA (lnc RNA) were also detected to be differentially expressed. These were >200 bp long sequences with no apparent reading frames and, when searched using Blast against the published *Aedes albopictus* genomes on NCBI, showed high similarity to sequences annotated as long non-coding RNAs.

2.4.4 RNASeq Data Validation on qRT-PCR

Based on previously known immune involvement, we selected eight genes (one aligned to the reference genome and seven from the custom transcriptome) and five long non-coding RNA (from the custom transcriptome) for validation by qRT-PCR (Table 2.2). For this, midguts were dissected from five individual CHIKV-infected adult *Aedes albopictus* female mosquitoes (2 dpi). Midguts from uninfected mosquitoes were used as controls.

Table 2.2 List of genes validated by qRT-PCR and comparison of expression fold changes.

Genes	<i>Aedes albopictus</i>		<i>Aedes aegypti</i>
	LogFC (RNAseq)	Expression Fold Change (qRT-PCR)	Expression Fold Change (qRT-PCR)
<i>ARF GTPase-activating protein GIT2</i>	-8.7	0.76(↓)	39.74(↑)
<i>NPC2 homolog</i>	6.29	5.35(↑)	11.63(↑)
<i>Mucin-22/FLO-11-like</i>	-8.61	0.16(↓)	7.34(↑)
<i>Translocon-associated protein subunit delta</i>	8.82	1.88(↑)	40.18(↑)
<i>ATP-dependent RNA helicase dbp2</i>	-9.07	6.53(↑)	26.22(↑)
<i>Uncharacterized gene coding for Sina and RING_Ubox domains containing protein</i>	8.84	1.51(↑)	41.07(↑)
<i>E3 ubiquitin-protein ligase MARCH6</i>	-9.04	1.03(↑)	28.65(↑)
<i>Ankyrin repeat domain-containing protein 44</i>	-5.56	0.5(↓)	No homologue/Not tested
<i>PREDICTED: Aedes albopictus uncharacterized LOC109424229 (LOC109424229), ncRNA</i>	-11.22	2.14(↑)	No homologue/Not tested
<i>PREDICTED: Aedes albopictus uncharacterized LOC109622934 (LOC109622934), ncRNA</i>	-7.13	0.06(↓)	No homologue/Not tested
<i>PREDICTED: Aedes albopictus uncharacterized LOC109423409 (LOC109423409), ncRNA</i>	-9.07	0.73(↓)	No homologue/Not tested
<i>PREDICTED: Aedes albopictus uncharacterized LOC109414360 (LOC109414360), ncRNA</i>	-9.53	1.02(↑)	No homologue/Not tested
<i>PREDICTED: Aedes albopictus uncharacterized LOC109424229 (LOC109424229), ncRNA</i>	-8.98	0.04(↓)	No homologue/Not tested

As the results showed, for *Aedes albopictus* mosquitoes, among the eight protein coding transcripts chosen for validation, the expression pattern for six targets was concordant, and the expression pattern for two targets was discordant, between RNASeq and qRT-PCR. Among the five tested long non-coding RNAs, two were concordant. All seven identified homologue targets, tested in *Aedes aegypti* midguts at 2 dpi, were upregulated

as compared to uninfected controls. In *Aedes albopictus*, only five of these targets were upregulated as per qRT-PCR.

2.5 Discussion

Chikungunya virus is a re-emerging alphavirus causing a high morbidity with long-term arthralgia in infected patients. Previous studies have taken approaches to understand the interaction between chikungunya virus and the *Aedes aegypti* vector, although these focused only on certain known genes and pathways [37]. However, considering the switch in vector preference towards *Aedes albopictus* by the Indian Ocean strains and invasive nature of this mosquito species, it is paramount to characterise the interaction between CHIKV and the new vector.

Previous studies with whole transcriptome analysis in mosquito vectors have used either whole mosquitoes or a cell culture [19,21–23,38]. Our objective here was to study the vector–virus interaction specifically at the midgut, which is the first barrier site to understand the factors that play a critical role in determining mosquito vector competence.

In the current study, unbiased transcriptional analysis was performed on midgut tissues collected from lab-reared adult female *Aedes albopictus* mosquitoes post CHIKV infection. The gene expression patterns, when compared to uninfected samples, revealed the transcriptional changes that are likely to be in response to the viral infection. Our analysis revealed that at 2 dpi in the midgut, most of the transcriptional changes were related to metabolism. An analysis of molecular functions revealed that while lysozyme activity and alkaline phosphatase were downregulated, carboxypeptidase activity was upregulated. Indeed, lysozymal and carboxypeptidase pathways have previously been implicated in innate immune responses [39–43].

One of the genes that was identified to be upregulated, and later validated by qRT-PCR, was a homolog of the Neimann Pick 2 (*NPC2*) gene, which in humans encodes for an intracellular cholesterol transporter. Loss of function mutations in the *NPC2* gene lead to a lysosomal disorder known as Niemann–Pick disease type C, which causes an increased accumulation of lipids in cellular compartments and leads to cell death [44,45]. In many viral infections, replication and assembly of the viral particles occur at the lysosomal and other intracellular membrane-bound organelles, including DENV infection in its vector *Aedes aegypti* [46]. *NPC2* has previously been shown to be involved in the replication and transport of several viruses, such as ebolavirus, vesicular stomatitis virus and influenza A virus, into and out of cells [47–49]. Interestingly, we detected a significant upregulation of the *NPC2* homolog both in *Aedes albopictus* as well as *Aedes aegypti* midguts 2 days post infection with CHIKV. Recent studies have shown that Imipramine-based inhibition of the *NPC2* protein results in severely diminished CHIKV replication in human fibroblast skin cells [50]. The fact that the *NPC2* gene is significant and essential for CHIKV replication in humans and is significantly upregulated in the mosquito midgut after infection implies that an evolutionarily conserved mechanism may be at play and presents possible therapeutic opportunities in clinical treatment.

Multiple prior publications have also shown that the RNAi pathway is one of the major pathways involved in antiviral responses in insects [16,51–53]. We did not detect differential expression of the traditional innate-immune response pathways, such as JAK/STAT, IMD and Toll, consistent with previous studies with CHIKV infection of *Aedes aegypti* [37]. It is possible that the regulation of this pathway either does not occur at the transcriptional level or the proteins involved are ubiquitously expressed and not differentially regulated. It is also possible that the time point we selected did not coincide with RNAi activation.

Long non-coding RNAs are RNA molecules that are over 200 bp long and do not contain an open reading frame. They are produced by RNA Polymerase II and are processed like mRNAs by the cellular mechanism, including polyadenylation. lncRNAs have been implicated with involvement in multiple viral infections, including dengue and Influenza [39,54,55]. The mechanism of their involvement is complex, with pro or anti-viral activity [56–61]. Our understanding of lncRNA involvement in host viral interactions is still limited. Our results showed an increase in the number of lncRNAs in *Aedes albopictus* midguts after CHIKV challenge, suggesting a role during the infection. The functional significance of this differential regulation remains to be seen.

While the DESeq2 analysis identified statistically significant differential gene expression, edgeR, performed on the custom transcriptome that was assembled using reads that did not align to the published *Aedes albopictus* reference genome, was not able to find significantly altered genes with the set FDR < 0.05. This may be due to the small sample size.

To address this issue, we performed RT-qPCR-based validation of transcripts that appeared to be differentially expressed based on raw *p*-values, on a fresh set of individual mosquito midguts (five controls vs. five infected). RT-qPCR showed significant differential expression among all the transcripts tested, including in the targets from the edgeR dataset. These genes also showed differential expression when tested in CHIKV-infected *Aedes aegypti*, further validating their significance during infection.

The targets from the edgeR dataset, chosen for qPCR-based validation, were selected based on evidence from previously published data regarding their involvement in innate immune pathways. Seven out of eight protein coding targets and all of the five lncRNAs validated on RT-qPCR were from the edgeR dataset, and most showed varying levels of

differential expression. Functional characterisation of the identified genes may help us to decipher the results and understand their role in mosquito–virus interactions.

Our results showed differences in gene expression pattern between *Aedes aegypti* and *Aedes albopictus*. While all of the seven tested genes in *Aedes aegypti* were upregulated, only five were upregulated in *Aedes albopictus* with the remaining two being downregulated. This may indicate differences in host–pathogen interactions between the two species of mosquitoes when infected with CHIKV.

Overall, our results showed significant changes in the transcriptome of *Aedes albopictus* mosquitoes after CHIKV infection, with the identified genes being involved in multiple cellular processes. This study examined differential gene expression at the midgut (the first critical barrier site) in infected *Aedes albopictus* mosquitoes. This study can be utilised in determining potential pro-viral and antiviral host factors and, in turn, will be helpful in reducing the high impact of CHIKV infections by targeting the vector *Aedes albopictus*.

Supplementary Materials: The following are available online at <https://www.mdpi.com/1999-4915/11/6/513/s1>, Table S1: List of primers, S2: List of differentially expressed genes, S3: Custom transcriptome output.

Author Contributions: R.V., P.G., J.B.D., and P.N.P. conceived and designed the experiments. R.V., M.K., and J.B.D. performed the mosquito experiments. R.V. performed the RNASeq library prep. R.V. and M.N. performed the data analysis for RNAseq. R.V. and M.T. performed the whole genome sequencing of the virus. R.V. performed the qRT-PCR-based validations. R.V. and P.N.P performed the overall data analysis. R.V. wrote the manuscript and prepared the figures. All authors reviewed and approved the final manuscript.

Funding: This research received no external funding.

Acknowledgments: The chikungunya virus isolate was obtained from the Victorian Infectious disease reference laboratory, Melbourne. Thanks to Kim Blasdell for helping with the CLC Genomics workbench and to Chris Freebairn for collection of *Aedes albopictus* eggs from Torres Strait islands. Thanks to Dr Omar Akbari of the University of California, San Diego for providing the *Aedes aegypti* Liverpool strain. Thanks to Adam Foord from CSIRO (AAHL) for discussions about optimisation of qRT-PCR and Dr Maria Doyle from the Peter MacCallum Cancer centre for guidance with the RNASeq data analysis.

Conflicts of Interest: The authors declare no conflicts of interest.

2.6 References

1. Bhatt, S.; Gething, P.W.; Brady, O.J.; Messina, J.P.; Farlow, A.W.; Moyes, C.L.; Drake, J.M.; Brownstein, J.S.; Hoen, A.G.; Sankoh, O.; et al. The global distribution and burden of dengue. *Nature* 2013, 496, 504, doi:10.1038/nature12060.
2. Lumsden, W.H. An epidemic of virus disease in Southern Province, Tanganyika Territory, in 1952-53. II. General description and epidemiology. *Trans. R. Soc. Trop. Med. Hyg.* 1955, 49, 33–57.
3. Robinson, M.C. An epidemic of virus disease in Southern Province, Tanganyika Territory, in 1952-53. I. Clinical features. *Trans. R. Soc. Trop. Med. Hyg.* 1955, 49, 28–32.
4. Kamath, S.; Das, A.K.; Parikh, F.S. Chikungunya. *J. Assoc. Physicians India* 2006, 54, 725-726.
5. Higgs, S.; Vanlandingham, D. Chikungunya virus and its mosquito vectors. *Vector Borne Zoonotic Dis.* 2015, 15, 231–240, doi:10.1089/vbz.2014.1745.
6. Simon, F.; Javelle, E.; Oliver, M.; Leparc-Goffart, I.; Marimoutou, C. Chikungunya Virus Infection. *Curr. Infect. Dis. Rep.* 2011, 13, 218–228, doi:10.1007/s11908-011-0180-1.

7. Reiter, P.; Fontenille, D.; Paupy, C. *Aedes albopictus* as an epidemic vector of chikungunya virus: Another emerging problem? *Lancet Infect. Dis.* 2006, 6, 463–464, doi:10.1016/s1473-3099(06)70531-x.
8. Tsetsarkin, K.A.; Chen, R.; Weaver, S.C. Interspecies transmission and chikungunya virus emergence. *Curr. Opin. Virol.* 2016, 16, 143–150, doi:10.1016/j.coviro.2016.02.007.
9. Waldock, J.; Chandra, N.L.; Lelieveld, J.; Proestos, Y.; Michael, E.; Christophides, G.; Parham, P.E. The role of environmental variables on *Aedes albopictus* biology and chikungunya epidemiology. *Pathog. Glob. Health* 2013, 107, 224–241, doi:10.1179/2047773213Y.0000000100.
10. Rezza, G.; Nicoletti, L.; Angelini, R.; Romi, R.; Finarelli, A.C.; Panning, M.; Cordioli, P.; Fortuna, C.; Boros, S.; Magurano, F.; et al. Infection with chikungunya virus in Italy: An outbreak in a temperate region. *Lancet* 2007, 370, 1840–1846, doi:10.1016/s0140-6736(07)61779-6.
11. Enserink, M. Chikungunya: No Longer a Third World Disease. *Science* 2007, 318, 1860.
12. Jupatanakul, N.; Sim, S.; Dimopoulos, G. The insect microbiome modulates vector competence for arboviruses. *Viruses* 2014, 6, 4294–4313, doi:10.3390/v6114294.
13. Arias-Goeta, C.; Mousson, L.; Rougeon, F.; Failloux, A.-B. Dissemination and Transmission of the E1-226V Variant of Chikungunya Virus in *Aedes albopictus* Are Controlled at the Midgut Barrier Level. *PLoS ONE* 2013, 8, e57548, doi:10.1371/journal.pone.0057548.
14. Dong, S.; Kantor, A.M.; Lin, J.; Passarelli, A.L.; Clem, R.J.; Franz, A.W.E. Infection pattern and transmission potential of chikungunya virus in two New World laboratory-adapted *Aedes aegypti* strains. *Sci. Rep.* 2016, 6, 24729, doi:10.1038/srep24729.
15. Dubrulle, M.; Mousson, L.; Moutailler, S.; Vazeille, M.; Failloux, A.-B. Chikungunya Virus and *Aedes* Mosquitoes: Saliva Is Infectious as soon as Two Days after Oral Infection. *PLoS ONE* 2009, 4, e5895, doi:10.1371/journal.pone.0005895.
16. Franz, A.W.E.; Kantor, A.M.; Passarelli, A.L.; Clem, R.J. Tissue Barriers to Arbovirus Infection in Mosquitoes. *Viruses* 2015, 7, 3741–3767, doi:10.3390/v7072795.
17. Kuno, G.; Chang, G.-J.J. Biological Transmission of Arboviruses: Reexamination of and New Insights into Components, Mechanisms, and Unique Traits as Well as

- Their Evolutionary Trends. *Clin. Microbiol. Rev.* 2005, 18, 608–637, doi:10.1128/CMR.18.4.608-637.2005.
18. Chompoonsri, J.; Thavara, U.; Tawatsin, A.; Boonserm, R.; Phumee, A.; Sangkitporn, S.; Siriyasatien, P. Vertical transmission of Indian Ocean Lineage of chikungunya virus in *Aedes aegypti* and *Aedes albopictus* mosquitoes. *Parasites Vectors* 2016, 9, 227.
 19. Dong, S.; Behura, S.K.; Franz, A.W.E. The midgut transcriptome of *Aedes aegypti* fed with saline or protein meals containing chikungunya virus reveals genes potentially involved in viral midgut escape. *BMC Genom.* 2017, 18, 382, doi:10.1186/s12864-017-3775-6.
 20. Etebari, K.; Hegde, S.; Saldaña, M.A.; Widen, S.G.; Wood, T.G.; Asgari, S.; Hughes, G.L. Global Transcriptome Analysis of *Aedes aegypti* Mosquitoes in Response to Zika Virus Infection. *mSphere* 2017, 2, e00456-00417, doi:10.1128/mSphere.00456-17.
 21. Shrinet, J.; Srivastava, P.; Sunil, S. Transcriptome analysis of *Aedes aegypti* in response to mono-infections and co-infections of dengue virus-2 and chikungunya virus. *Biochem. Biophys. Res. Commun.* 2017, 492, 617–623, doi:10.1016/j.bbrc.2017.01.162.
 22. Bonizzoni, M.; Dunn, W.A.; Campbell, C.L.; Olson, K.E.; Marinotti, O.; James, A.A. Complex Modulation of the *Aedes aegypti* Transcriptome in Response to Dengue Virus Infection. *PLoS ONE* 2012, 7, e50512, doi:10.1371/journal.pone.0050512.
 23. Fragkoudis, R.; Chi, Y.; Siu, R.W.; Barry, G.; Attarzadeh-Yazdi, G.; Merits, A.; Nash, A.A.; Fazakerley, J.K.; Kohl, A. Semliki Forest virus strongly reduces mosquito host defence signaling. *Insect Mol. Biol.* 2008, 17, 647–656, doi:10.1111/j.1365-2583.2008.00834.x.
 24. Liu, Y.; Zhou, Y.; Wu, J.; Zheng, P.; Li, Y.; Zheng, X.; Puthiyakunnon, S.; Tu, Z.; Chen, X.G. The expression profile of *Aedes albopictus* miRNAs is altered by dengue virus serotype-2 infection. *Cell Biosci.* 2015, 5, 16, doi:10.1186/s13578-015-0009-y.
 25. Pyke, A.T. Partial E1 gene Sequence of Mauritius 2006 isolate 06113879. Unpublished work, 2008.
 26. Kim, D.; Langmead, B.; Salzberg, S.L. HISAT: A fast spliced aligner with low memory requirements. *Nat. Methods* 2015, 12, 357, doi:10.1038/nmeth.3317.
 27. Lawson, D.; Arensburger, P.; Atkinson, P.; Besansky, N.J.; Bruggner, R.V.; Butler, R.; Campbell, K.S.; Christophides, G.K.; Christley, S.; Dialynas, E.; et al. VectorBase:

- A data resource for invertebrate vector genomics. *Nucleic Acids Res.* 2009, 37, D583–D587, doi:10.1093/nar/gkn857.
28. Li, H.; Handsaker, B.; Wysoker, A.; Fennell, T.; Ruan, J.; Homer, N.; Marth, G.; Abecasis, G.; Durbin, R. The Sequence Alignment/Map format and SAMtools. *Bioinformatics* 2009, 25, 2078–2079, doi:10.1093/bioinformatics/btp352.
 29. Afgan, E.; Sloggett, C.; Goonasekera, N.; Makunin, I.; Benson, D.; Crowe, M.; Gladman, S.; Kowsar, Y.; Pheasant, M.; Horst, R.; et al. Genomics Virtual Laboratory: A Practical Bioinformatics Workbench for the Cloud. *PLoS ONE* 2015, 10, e0140829, doi:10.1371/journal.pone.0140829.
 30. Love, M.I.; Huber, W.; Anders, S. Moderated estimation of fold change and dispersion for RNA-seq data with DESeq2. *Genome Biol.* 2014, 15, 550, doi:10.1186/s13059-014-0550-8.
 31. Grabherr, M.G.; Haas, B.J.; Yassour, M.; Levin, J.Z.; Thompson, D.A.; Amit, I.; Adiconis, X.; Fan, L.; Raychowdhury, R.; Zeng, Q.; et al. Full-length transcriptome assembly from RNA-Seq data without a reference genome. *Nat. Biotechnol.* 2011, 29, 644, doi:10.1038/nbt.1883.
 32. Haas, B.J.; Papanicolaou, A.; Yassour, M.; Grabherr, M.; Blood, P.D.; Bowden, J.; Couger, M.B.; Eccles, D.; Li, B.; Lieber, M.; et al. De novo transcript sequence reconstruction from RNA-Seq: Reference generation and analysis with Trinity. *Nat. Protoc.* 2013, 8, 10.1038/nprot.2013.1084, doi:10.1038/nprot.2013.084.
 33. Camacho, C.; Coulouris, G.; Avagyan, V.; Ma, N.; Papadopoulos, J.; Bealer, K.; Madden, T.L. BLAST+: Architecture and applications. *BMC Bioinform.* 2009, 10, 421–421, doi:10.1186/1471-2105-10-421.
 34. Boratyn, G.M.; Schäffer, A.A.; Agarwala, R.; Altschul, S.F.; Lipman, D.J.; Madden, T.L. Domain enhanced lookup time accelerated BLAST. *Biol. Direct* 2012, 7, 12–12, doi:10.1186/1745-6150-7-12.
 35. Alexa, A.; Rahnenfuhrer, J. topGO: Enrichment Analysis for Gene Ontology; R package Version 2.33.0; 2016. <https://bioconductor.org/packages/release/bioc/html/topGO.html> (accessed on 05-06-2018).
 36. Smedley, D.; Haider, S.; Durinck, S.; Pandini, L.; Provero, P.; Allen, J.; Arnaiz, O.; Awedh, M.H.; Baldock, R.; Barbiera, G.; et al. The BioMart community portal: An

- innovative alternative to large, centralized data repositories. *Nucleic Acids Res.* 2015, 43, W589–W598, doi:10.1093/nar/gkv350.
37. McFarlane, M.; Arias-Goeta, C.; Martin, E.; O'Hara, Z.; Lulla, A.; Mousson, L.; Rainey, S.M.; Misbah, S.; Schnettler, E.; Donald, C.L.; et al. Characterization of *Aedes aegypti* innate-immune pathways that limit Chikungunya virus replication. *PLoS Negl. Trop. Dis.* 2014, 8, e2994, doi:10.1371/journal.pntd.0002994.
 38. Colpitts, T.M.; Cox, J.; Vanlandingham, D.L.; Feitosa, F.M.; Cheng, G.; Kurscheid, S.; Wang, P.; Krishnan, M.N.; Higgs, S.; Fikrig, E. Alterations in the *Aedes aegypti* Transcriptome during Infection with West Nile, Dengue and Yellow Fever Viruses. *PLoS Pathog.* 2011, 7, e1002189, doi:10.1371/journal.ppat.1002189.
 39. Hasan, M.; Koch, J.; Rakheja, D.; Pattnaik, A.K.; Brugarolas, J.; Dozmorov, I.; Levine, B.; Wakeland, E.K.; Lee-Kirsch, M.A.; Yan, N. Trex1 regulates lysosomal biogenesis and interferon-independent activation of antiviral genes. *Nat. Immunol.* 2013, 14, 61–71.
 40. Isoe, J.; Zamora, J.; Miesfeld, R.L. Molecular Analysis of the *Aedes aegypti* Carboxypeptidase Gene Family. *Insect Biochem. Mol. Biol.* 2009, 39, 68–73, doi:10.1016/j.ibmb.2008.09.006.
 41. Johnston, C.; Jiang, W.; Chu, T.; Levine, B. Identification of Genes Involved in the Host Response to Neurovirulent Alphavirus Infection. *J. Virol.* 2001, 75, 10431–10445, doi:10.1128/JVI.75.21.10431-10445.2001.
 42. Merklings, S.H.; van Rij, R.P. Beyond RNAi: Antiviral defense strategies in *Drosophila* and mosquito. *J. Insect Physiol.* 2013, 59, 159–170, doi:10.1016/j.jinsphys.2012.07.004.
 43. Swevers, L.; Liu, J.; Smagghe, G. Defense Mechanisms against Viral Infection in *Drosophila*: RNAi and Non-RNAi. *Viruses* 2018, 10, 230, doi:10.3390/v10050230.
 44. Vance, J.E.; Karten, B. Niemann-Pick C disease and mobilization of lysosomal cholesterol by cyclodextrin. *J. Lipid Res.* 2014, 55, 1609–1621, doi:10.1194/jlr.R047837.
 45. Wang, Y.H.; Twu, Y.C.; Wang, C.K.; Lin, F.Z.; Lee, C.Y.; Liao, Y.J. Niemann-Pick Type C2 Protein Regulates Free Cholesterol Accumulation and Influences Hepatic Stellate Cell Proliferation and Mitochondrial Respiration Function. *Int. J. Mol. Sci.* 2018, 19, 1678, doi:10.3390/ijms19061678.

46. Jupatanakul, N.; Sim, S.; Dimopoulos, G. *Aedes aegypti* ML and Niemann-Pick type C family members are agonists of dengue virus infection. *Dev. Comp. Immunol.* 2014, 43, 1–9, doi:10.1016/j.dci.2013.10.002.
47. Herbert, A.S.; Davidson, C.; Kuehne, A.I.; Bakken, R.; Braigen, S.Z.; Gunn, K.E.; Whelan, S.P.; Brummelkamp, T.R.; Twenhafel, N.A.; Chandran, K.; et al. Niemann-pick C1 is essential for ebolavirus replication and pathogenesis in vivo. *mBio* 2015, 6, e00565-00515, doi:10.1128/mBio.00565-15.
48. Infante, R.E.; Wang, M.L.; Radhakrishnan, A.; Kwon, H.J.; Brown, M.S.; Goldstein, J.L. NPC2 facilitates bidirectional transfer of cholesterol between NPC1 and lipid bilayers, a step in cholesterol egress from lysosomes. *Proc. Natl. Acad. Sci.* 2008, 105, 15287–15292, doi:10.1073/pnas.0807328105.
49. Amini-Bavil-Olyae, S.; Choi, Y.J.; Lee, J.H.; Shi, M.; Huang, I.C.; Farzan, M.; Jung, J.U. The antiviral effector IFITM3 disrupts intracellular cholesterol homeostasis to block viral entry. *Cell Host Microbe* 2013, 13, 452–464, doi:10.1016/j.chom.2013.03.006.
50. Wichit, S.; Hamel, R.; Bernard, E.; Talignani, L.; Diop, F.; Ferraris, P.; Liegeois, F.; Ekchariyawat, P.; Luplertlop, N.; Surasombatpattana, P.; et al. Imipramine Inhibits Chikungunya Virus Replication in Human Skin Fibroblasts through Interference with Intracellular Cholesterol Trafficking. *Sci. Rep.* 2017, 7, 3145–3145, doi:10.1038/s41598-017-03316-5.
51. Cirimotich, C.M.; Scott, J.C.; Phillips, A.T.; Geiss, B.J.; Olson, K.E. Suppression of RNA interference increases alphavirus replication and virus-associated mortality in *Aedes aegypti* mosquitoes. *BMC Microbiol.* 2009, 9, 49–49, doi:10.1186/1471-2180-9-49.
52. Saleh, M.C.; Tassetto, M.; van Rij, R.P.; Goic, B.; Gausson, V.; Berry, B.; Jacquier, C.; Antoniewski, C.; Andino, R. Antiviral immunity in *Drosophila* requires systemic RNA interference spread. *Nature* 2009, 458, 346–350, doi:10.1038/nature07712.
53. Wang, J.; Wang, Y.; Zhou, R.; Zhao, J.; Zhang, Y.; Yi, D.; Li, Q.; Zhou, J.; Guo, F.; Liang, C.; et al. Host Long Noncoding RNA lncRNA-PAAN Regulates the Replication of Influenza A Virus. *Viruses* 2018, 10, 330.
54. Etebari, K.; Asad, S.; Zhang, G.; Asgari, S. Identification of *Aedes aegypti* Long Intergenic Non-coding RNAs and Their Association with Wolbachia and Dengue

- Virus Infection. PLoS Negl. Trop. Dis. 2016, 10, e0005069, doi:10.1371/journal.pntd.0005069.
55. Wang, X.J.; Jiang, S.C.; Wei, H.X.; Deng, S.Q.; He, C.; Peng, H.J. The Differential Expression and Possible Function of Long Noncoding RNAs in Liver Cells Infected by Dengue Virus. *Am. J. Trop. Med. Hyg.* 2017, 97, 1904–1912.
 56. Liu, W.; Ding, C. Roles of LncRNAs in Viral Infections. *Front. Cell. Infect. Microbiol.* 2017, 7, 205, doi:10.3389/fcimb.2017.00205.
 57. Qiu, L.; Wang, T.; Tang, Q.; Li, G.; Wu, P.; Chen, K. Long Non-coding RNAs: Regulators of Viral Infection and the Interferon Antiviral Response. *Front. Microbiol.* 2018, 9, 1621.
 58. Du, M.; Yuan, L.; Tan, X.; Huang, D.; Wang, X.; Zheng, Z.; Mao, X.; Li, X.; Yang, L.; Huang, K.; et al. The LPS-inducible lncRNA Mirt2 is a negative regulator of inflammation. *Nat. Commun.* 2017, 8, 2049, doi:10.1038/s41467-017-02229-1.
 59. Nikhil, S.; Singh, S. Implications of non-coding RNAs in viral infections. *Rev. Med. Virol.* 2016, 26, 356–368, doi:10.1002/rmv.1893.
 60. Valadkhan, S.; Gunawardane, L.S. lncRNA-mediated regulation of the interferon response. *Virus Res.* 2016, 212, 127–136, doi:10.1016/j.virusres.2015.09.023.

Chapter-3

Whole transcriptome analysis of *Aedes albopictus* mosquito head & thorax post-chikungunya virus infection

Vedururu RK, Neave MJ, Sundaramoorthy V, Green D, Harper JA, Gorry PR, Duchemin J-B, Paradkar PN. Whole Transcriptome Analysis of *Aedes albopictus* Mosquito Head and Thorax Post-Chikungunya Virus Infection. *Pathogens*. 2019;8(3):132. Published 2019 Aug 27. doi:10.3390/pathogens8030132

Chapter 3: Whole transcriptome analysis of *Aedes albopictus* mosquito head & thorax post-chikungunya virus infection

Ravi kiran Vedururu ^{1,2}, Matthew J. Neave ³, Vinod Sundaramoorthy ³, Diane Green ³, Jennifer A Harper³, Paul R. Gorry ⁴, Jean-Bernard Duchemin ^{1#}, Prasad N. Paradkar ^{1*}

¹ CSIRO Health & Biosecurity, Australian Animal Health Laboratory, Geelong, Australia

² School of Sciences, RMIT University, Bundoora, Australia

³ CSIRO, Australian Animal Health Laboratory, Geelong, 3220, Australia

⁴ School of Health and Biomedical Science, RMIT University, Bundoora, Australia

Current Address: Institut Pasteur de la Guyane, Cayenne, French Guiana

* Corresponding author: Prasad.Paradkar@csiro.au

Received: 24 July 2019; Accepted: 23 August 2019; Published: 27 August 2019

3.1 Abstract

Chikungunya virus (CHIKV) is an alphavirus transmitted by *Aedes* mosquitoes and causes prolonged arthralgia in patients. After crossing the mosquito midgut barrier, virus disseminates to secondary tissues including the head and salivary glands. To better understand the interaction between *Aedes albopictus* and CHIKV, we performed RNASeq analysis on pools of mosquito head and thorax 8 days post-infection. The results identified 159 differentially expressed transcripts. After validation by RT-qPCR of 14 of the identified transcripts, Inhibitor of Bruton's Tyrosine Kinase (*BTKi*), which has previously shown to be anti-inflammatory in mammals after viral infection, was further evaluated for its functional significance. Knockdown of *BTKi* using dsRNA in a mosquito cell line showed no significant difference in viral RNA or infectivity titer as measured by RT-qPCR or TCID₅₀, respectively. However, *BTKi* gene knocked-down cells showed

increased apoptosis 24 hpi compared with control cells, suggesting involvement of *BTKi* in the mosquito response to viral infection. Since BTK in mammals promotes inflammatory response and has been shown to be involved in osteoclastogenesis, a hallmark of CHIKV pathogenesis, our results suggest a possible conserved mechanism at play between mosquitoes and mammals. Taken together, these results will add to our understanding of *Aedes Albopictus* interactions with CHIKV.

Keywords: Chikungunya; *Aedes albopictus*; RNASeq; Host–pathogen interactions

3.2 Introduction

Chikungunya virus (CHIKV) is an enveloped, positive sense RNA virus belonging to the Alphavirus genus in *Togaviridae* family [1,2]. The virus causes a disease characterised by a high febrile illness and debilitating and protracted arthralgia [3-5].

Since the 2004-2005 outbreak in Reunion island, east of Africa, *Aedes albopictus* has played a significant role in expansion of CHIKV outbreaks around the world. A single mutation in the E1 viral gene has been shown to confer increased vector competence to this mosquito [6]. In the mosquito after blood-feeding, the virus needs to cross 2 critical barrier tissues, the midgut and salivary glands. The virus must infect and cross the epithelial cells before digestion of the blood meal and then overcome the midgut escape barriers to disseminate into the haemocoel, from where it reaches and infects other mosquito tissues including the salivary glands [7]. The mosquito is considered to be infective, once the virus is detected in the saliva [8,9].

Previous research has identified a number of genes involved in early stages of *Aedes albopictus* infection with CHIKV [10]. However, to understand the interactions between the virus and mosquito at the transcriptomic level after dissemination of the virus, we

performed RNASeq analysis of the head and anterior 1/3rd part of mosquitoes (containing the salivary glands), collected 8 days post CHIKV infection. The results identified multiple differentially expressed genes, involved in various biological and molecular cellular functions. Our results identified *BTKi* to be functionally significant in the mosquito response to CHIKV infection.

3.3 Results

3.3.1 RNASeq and DGE analysis

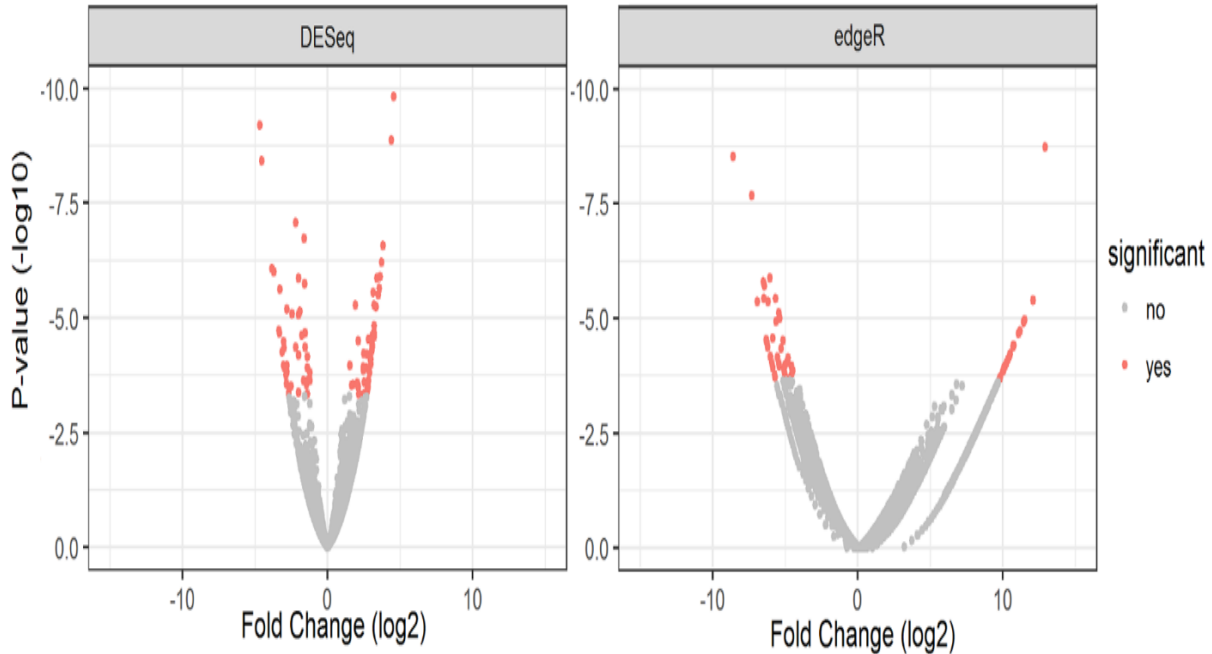
To determine differentially expressed genes, two pools of head/thorax (six per pool) collected at 8 dpi from infected mosquitoes were created. For controls, one pool of head/thorax from uninfected mosquitoes was used. The three libraries yielded between 40.6 million and 47.15 million reads. After quality trimming and removing the reads mapping to the chicken genome, the remaining reads were aligned to the *Aedes albopictus* reference genome [Foshan strain genome sequence (AaloF1) from Vectorbase]. The reads that did not map to the genome were then used to build a custom de novo transcriptome. The results confirmed the infection status of the two pools, and the control library contained no CHIKV reads as expected (Reference sequence: MH229986) (Table 3.1).

Table 3.1 RNASeq NGS data summary.

	Total reads (millions)	% mapped to Refseq genome	% of CHIKV reads
Infected HT1	47.15	63.28%	1.12
Infected HT2	40.60	60.35%	2.09
Control HT	42.10	62.91%	0.00

Total reads obtained, their alignment percentage to the reference Aedes albopictus genome and the percentage of reads aligned to the chikungunya virus genome.

Several differentially expressed genes were identified using both DESeq2 (for reads aligned to the RefSeq genome) and edgeR (for the *de novo* transcriptome built with unaligned reads) (Table 3.2) and the data is visualised as Volcano plots (Figure 3.1). The full list of genes and transcripts differentially expressed with *p-values* (and FDR) of less than 0.05 is provided in supplementary file S2 (Total: 159, Up: 74 & Down: 85). The fasta file obtained as output for the custom transcriptome assembly is provided in supplementary information S3.



Figure

Figure 3.1 Volcano plots from DESeq2 and edgeR

Volcano plots from DESeq2 and edgeR of differentially expressed genes in CHIKV infected mosquito head/thorax compared to control. DESeq2 was performed by aligning reads to the reference Aedes albopictus genome; while edgeR analysis was done on reads that did not align to the reference genome and were aligned to the custom transcriptome.

Table 3.2 Differential Gene Expression analysis.

No of Differentially expressed genes			
	Total	Up	Down
DESe	96	51	45
q2			
edgeR	63	23	40

Number of genes found to be differentially expressed in mosquito head/thorax 8 dpi using DeSeq2 (p-value: <0.05) and edgeR (FDR: <0.05) analysis.

3.3.2 Ontology analysis

Gene set enrichment analysis and ontology performed using TopGO revealed that several biological and molecular processes were significantly modified during CHIKV infection (Figure 3.2). The complete output of TopGO analysis is provided in supplementary data (S4).

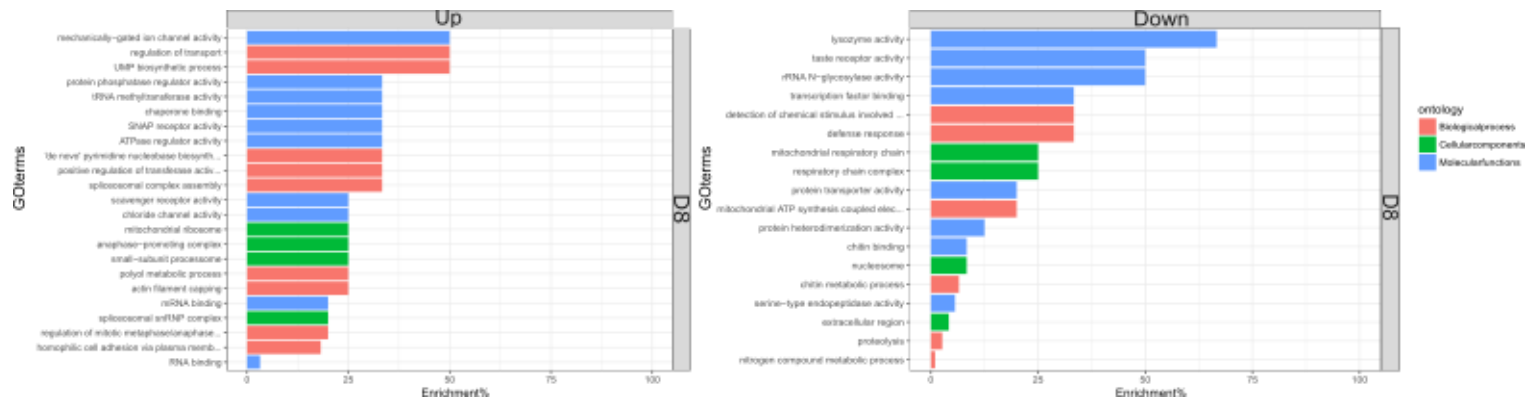


Figure 3.2 topGo enrichment comparison in differentially expressed genes

Enrichment analysis of up and down regulated genes in the heads and thorax of *Aedes albopictus* mosquitoes in response to CHIKV at 8 dpi. Enrichment % is calculated as the ratio of 'significant' (Number of times the gene ontology number is observed as differentially expressed) to 'expected' (Number of times the gene ontology number is expected based on observation in control samples) gene numbers.

In the head/thorax of *Aedes albopictus*, upregulated molecular functions were RNA (*p-value*: 0.046) and mRNA binding (*p-value*: 0.049) and molecular functions down regulated were lysozyme activity (*p-value*: 0.0038), serine-type endopeptidase activity (*p-value*: 0.0058), protein heterodimerisation (*p-value*: 0.00181) and chitin binding (*p-value*: 0.00532). Biological processes down regulated were defence response (*p-value*: 9.70E-05), proteolysis (*p-value*: 0.0075) and chitin metabolic process (*p-value*: 0.0106). Up regulated biological processes were homophilic cell adhesion via plasma membrane (*p-value*: 0.0056), UMP biosynthetic process (*p-value*: 0.0245), regulation of transport (*p-value*: 0.0245), spliceosomal complex assembly (*p-value*: 0.0342).

3.3.3 RT-qPCR based Validation of RNASeq data

Fourteen differentially expressed genes were selected, based on previously described involvement in the immune response, for validation by RT-qPCR (11 aligned to reference genome and 3 from custom transcriptome) (see Table 3.3 for details). For this, head/thorax were dissected from five individual CHIKV-infected adult *Aedes albopictus* female mosquitoes (8 dpi). Head/thorax from uninfected mosquitoes were used as controls.

Table 3.3 List of genes validated by qRT-PCR.

	GeneID	Gene Annotation
1	AALF011899	Quaking protein A
2	AALF004300	PREDICTED: PDZ and LIM domain protein 7-like isoform X1
3	AALF008354	Putative ecdysteroid-regulated 16 kDa protein [Source:UniProtKB/TrEMBL;Acc:A0A023EHE1]
4	AALF012634	PREDICTED: fat-like cadherin-related tumor suppressor homolog [<i>Aedes albopictus</i>]
5	AALF023547	Peptidylprolyl isomerase [Source:UniProtKB/TrEMBL;Acc:A0A023EQ01]
6	AALF021910	PREDICTED: fasciclin-2-like isoform X1 [<i>Aedes albopictus</i>]
7	AALF012324	glycine rich RNA binding protein, putative
8	AALF016505	leucine-rich immune protein (Long)
9	AALF025245	PREDICTED: inhibitor of Bruton tyrosine kinase [<i>Aedes albopictus</i>]
10	AALF016704	phosrestin i (arrestin b) (arrestin 2) [Source:Projected from <i>Aedes aegypti</i> (AAEL003116) VB Community Annotation]
11	AALF026574	Putative uncharacterised protein containing CCHC zinc finger domain
12	TRINITY_DN12 9476_c0_g1_i1	PREDICTED: protein no-on-transient A isoform X2 [<i>Aedes albopictus</i>]
13	TRINITY_DN13 1737_c0_g1_i2	PREDICTED: ficolin-3-like [<i>Aedes albopictus</i>]
14	TRINITY_DN13 1885_c0_g2_i2	PREDICTED: PDZ and LIM domain protein Zasp-like isoform X5 [<i>Aedes albopictus</i>]

List of genes selected for validation by qRT-PCR and their annotation based on BlastX and BlastN.

The qRT-PCR results, using gene-specific primers, compared with the RNAseq data (Table 3.4) showed that 7 out of 14 target genes were concordant.

Table 3.4 Comparison of expression fold changes in chosen targets between qRT-PCR and RNASeq.

Target ID	Expression fold change (RT-qPCR)	LogFC (RNASeq)
AALF011899	0.8(↓)	2.54
AALF004300	0.43(↓)	1.53
AALF008354	0.96(↓)	2.07
AALF012634	0.01(↓)	3.51
AALF023547	0.75(↓)	2.24
TRINITY_DN129476_c0_g1_i1	0.01(↓)	-5.08
TRINITY_DN131737_c0_g1_i2	0.07(↓)	-6.42
TRINITY_DN131885_c0_g2_i2	2.9(↑)	10
AALF021910	2.97(↑)	3.55
AALF012324	0(↓)	2.96
AALF016505	3.65(↑)	-1.65
AALF025245	17.54(↑)	2.49
AALF016704	1149.59(↑)	1.51
AALF026574	0.09(↓)	-3.12

Results of RT-qPCR on the 14 gene targets selected from RNAseq DGE analysis. Expression fold change for RT-qPCR is calculated as $2^{-\Delta\Delta Ct}$ and the up or down regulation compared to controls is indicated by arrows, while LogFC (from RNA-Seq data) was calculated by DESeq2 and edgeR

3.3.4 Functional significance of BTKi in CHIKV infected RML12 cells

Inhibitor of Bruton's tyrosine kinase (*BTKi*) was identified to be one of the significantly upregulated transcripts, both in RT-qPCR and RNASeq. To assess the functional significance of *BTKi*, *Aedes albopictus* larval cell line (RML12) was transfected with anti-*BTKi* dsRNA. Twenty-four hours post transfection, the cells were infected with CHIKV

(MOI: 1). Twenty-four hours post infection, successful knockdown of BTKi was confirmed with RT-qPCR returning a $\Delta\Delta C_t$ value of 2.39 (Expression fold change: 0.1913, Decrease in expression of *BTKi*: 80.87%). However, there were no significant changes in the viral RNA ($\Delta\Delta C_t$: -0.022, Expression fold change: 1.015) as well as TCID₅₀ (Figure 3.3). Indicating, inhibition of *BTKi*, while detrimental to host cells, may not have a direct impact on viral replication.

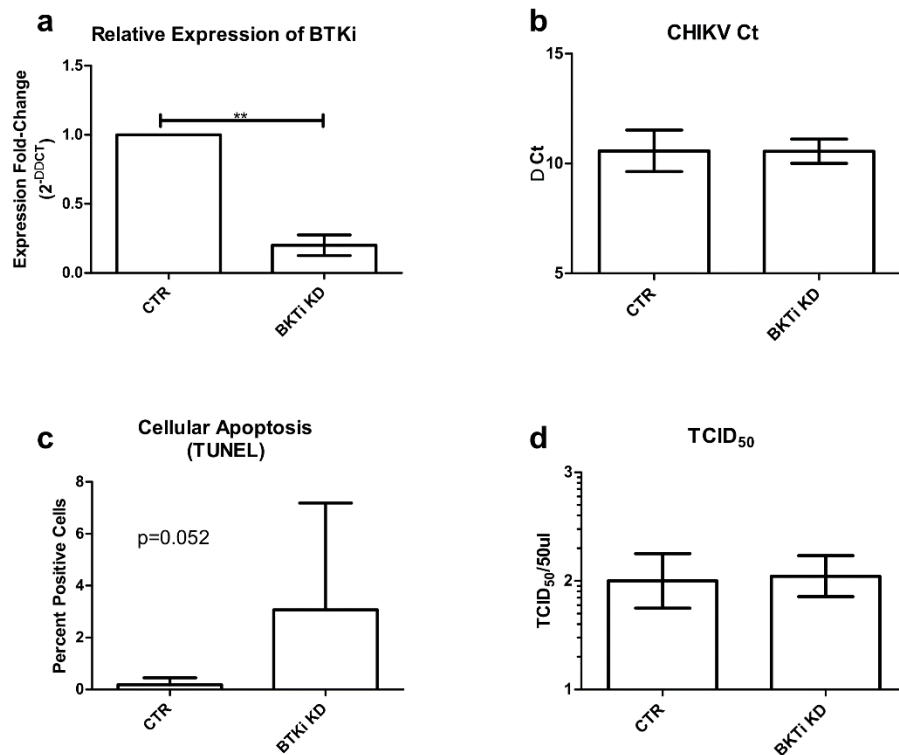


Figure 3.3 A: Comparison of BTKi expression between BTKi-KD and GFP-KD RML12 cells; B: Comparison of intracellular CHIKV RNA via RT-qPCR in BTKi and GFP knockdown RML12 cells; C: Comparison of % of apoptosis detected in BTKi-KD and GFP-KD RML12 cells; D: Comparison of TCID₅₀ of extracellular CHIKV between BTKi and GFP knockdown RML12 cells

BTK has previously shown to be involved in inducing apoptosis. To determine whether similar pathways are involved in CHIKV-infected mosquito cells, anti-BTKi dsRNA transfected and CHIKV infected RML12 cells were grown on glass cover slips and 24 hpi

TUNEL staining was performed to quantify apoptosis. RML12 cells transfected with anti-GFP dsRNA and infected with CHIKV were used as controls. Cell nuclei were stained using DAPI and apoptosis was measured as number of cells showing terminal deoxynucleotidyl transferase dUTP nick end labelling. Percentage of apoptosis was measured as ratio of apoptotic cells to DAPI stained cells (i.e. nuclei) (Figure 3.4). Significant apoptosis was detected in BTKi-KD cells compared to control cells (plot c), 3.07% in BTKi-KD RML12 cells vs 0.186% in control RML12 cells (t: 2.0965, df: 16 & p: 0.0261) (Figure 3.3).

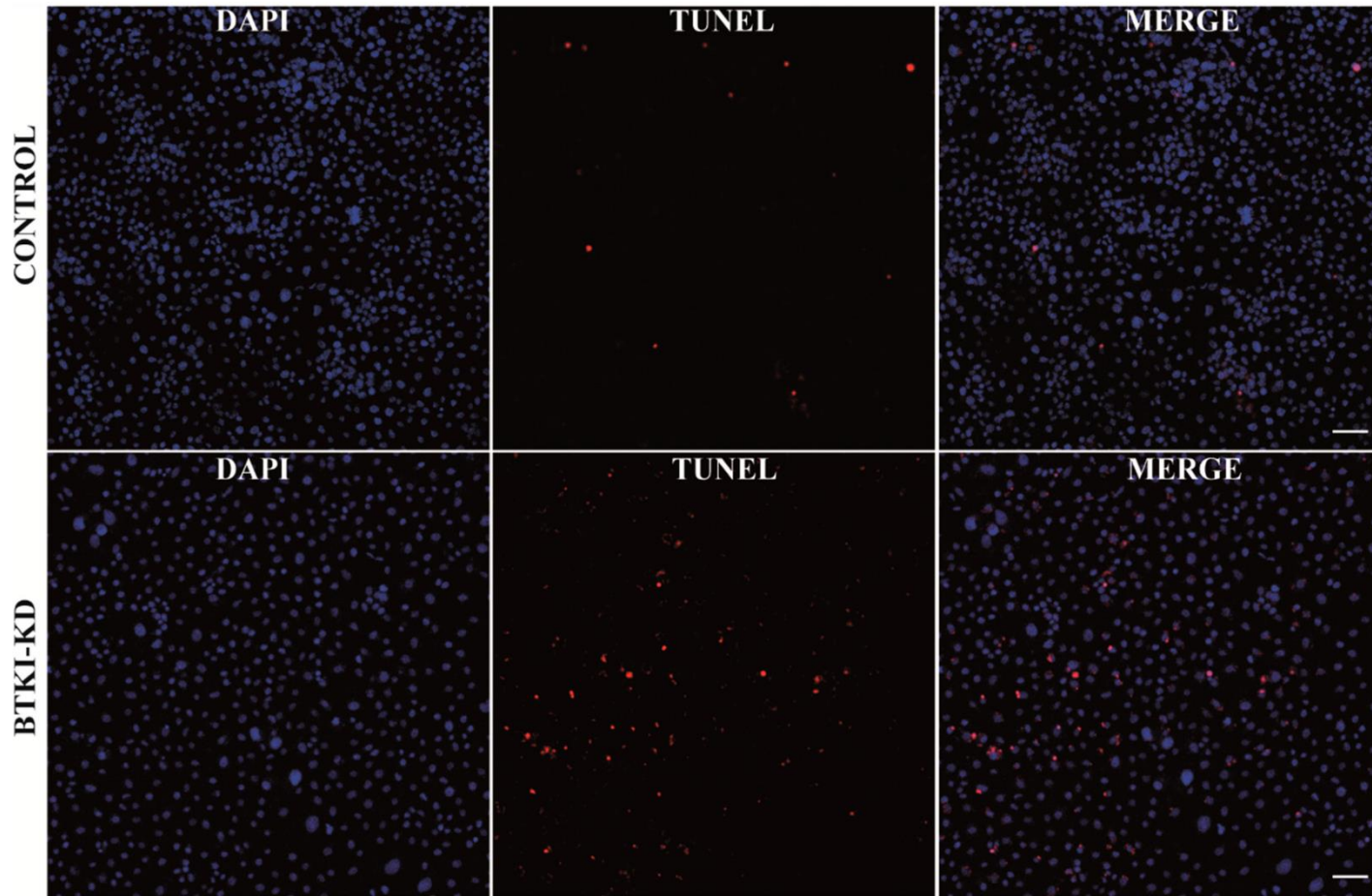


Figure 3.4 TUNEL staining of BTkI knocked down RML-12 cells post infection with CHIKV showing increased apoptosis compared to control RML12 cells (Scale bar: 50 μ M).

3.4 Discussion

Multiple previous studies have been performed to understand the interactions between chikungunya virus and *Aedes aegypti*, the traditional vector [11-13]. Previously, RNASeq was performed on *Aedes albopictus* midguts 2 days post CHIKV infection which identified a number of differentially expressed genes[10]. These results helped in understanding the host-pathogen interaction at the first critical barrier site, the midgut. Yet, our understanding of transcriptome level interactions in *Aedes albopictus*, after viral dissemination is preliminary. We attempted to study the virus-vector interaction in the head/thorax region 8 dpi, as a proxy for dissemination site. This site is important as successful infection of salivary glands (included in the thorax) ensures the presence of virus in the saliva of the mosquito and in turn enables successful transmission.

Our results show differential regulation of biological processes including RNA and mRNA binding, lysosomal and serpin pathways and down regulation of defensin genes. These could be due to either mosquito immune responses to CHIKV or viral modulation of immunity. Processes such as the regulation of transport and homophilic cell adhesion via plasma membrane could be involved in viral assembly and export [14-17]. Functional studies to determine whether these genes are pro or anti-viral are needed and could explain the role of these genes in the infection process.

Interestingly, two odorant binding proteins (OBPs) were found to be differentially expressed. While Obp25 (AALF018602) was upregulated, D7 protein (AALF024478) was down regulated. In *Aedes aegypti*, salivary glands infected with dengue virus also showed differential expression of odorant binding proteins [18] and it was shown that down regulation of OBPs reduced the chemosensory abilities of the mosquitoes and hence

reduced exposure to virus via feeding and thus hindered transmission capabilities. Our results suggest that similar mechanisms may be in play here as well, although that remains to be verified with functional studies.

The RNAi pathway is one of the major pathways involved in antiviral responses in insects [19-21]. Consistent with our previous study on *Aedes albopictus* midguts post CHIKV infection, our data does not show statistically significant changes in expression of genes involved in RNAi pathways in head and thorax. This is consistent with a previous study involving chikungunya virus and *Aedes aegypti*, where genes from JAK/STAT, IMD and Toll pathways were not found to be differentially regulated [11]. While it is possible that regulation of this pathway does not occur at the transcriptional level or RNAi proteins are not differentially regulated but ubiquitously expressed, more focused validation may provide a clearer conclusion to this observation. Expression levels at different time points post infections may also need to be assessed before reaching this conclusion.

Our results showed that the concordance between our RNASeq and RT-qPCR data was low (50%). This was possibly because there were not enough biological replicates for RNA-Seq analysis. Higher concordance can be achieved by increasing the number of infected and control samples. For functional analysis, further research was focused on *BTKi*, which was validated through RT-qPCR.

BTKi is an inhibitor of Bruton's tyrosine kinase (Btk) [22]. Btk is heavily involved in innate-immune responses [23]. In higher level organisms, inactivating mutations in Btk results in a condition known as X-Linked agammaglobulinemia (XLA), characterised by inability to produce mature B-cells and gamma globulins (including antibodies). Increased susceptibility to apoptotic death on exposure to pathogen associated inflammatory signals is observed in BTK-deficient macrophages. BTK is involved in NK

cell activation via upregulated NF- κ B pathway [24]. Btk along with Tec kinases are heavily involved in osteoclast differentiation and regulation. Severe osteopetrosis is observed in mice with non-functional Btk gene. Reduced osteoclastic bone resorption was observed in osteoporosis and inflammation-induced bone destruction on inhibition of Tec kinases. Btk and Tec kinases, among Tec Kinases are selectively expressed in osteoclasts and not in osteoblasts. Increased bone mass in mouse without Btk is due to defective osteoclastic bone resorption because of defective osteoclast differentiation [25]. CHIKV is known to infect osteoblasts and upregulate IL-6 and RANKL generation and decrease OPG production. An altered RANKL/OPG ratio gives rise to arthralgia, a characteristic morbidity of chikungunya fever [26]. Literature also presents evidence of benefit of Btk inhibition in viral inflammatory disease. Specifically, BTK inhibition with ibrutinib has shown major protective effect in lung tissue of mice during influenza viral infection by ameliorating excessive inflammatory response [27].

Our data suggests that BTKi is significantly up-regulated in the head & thorax tissue of *Aedes albopictus* mosquito after chikungunya virus infection. While knock-down of *BTKi* in RML12 cells did not result in significant differences in viral titers or RNA levels, there was increased apoptosis in cells. These observations are consistent with a recently published study that show that inhibition of BTK is protective in host tissue during a viral infection [27]. In the context of CHIKV induced arthritis in patients, it is interesting to note that BTK is involved in osteoclastogenesis and inhibition of BTK on bone resorption is protective. Our data suggests a possible conserved mechanism at play for BTK and associated Tec kinases in the context of chikungunya infections in both mosquitoes and mammals.

Overall, our results showed significant changes in the transcriptome of *Aedes albopictus* mosquitoes after CHIKV dissemination. This study, for the first time, examined

differential gene expression in the head and thorax (dissemination site containing salivary glands) of infected mosquitoes. Our results can be utilized in determining potential pro-viral and antiviral host factors and in turn, will be helpful in reducing the high impact of CHIKV infections by targeting the vector, *Aedes albopictus*.

3.5 Materials and Methods

Aedes albopictus mosquitoes were grown in BSL-3 insectary at the Australian Animal Health Labs with the following conditions, 27.5 °C and 70% in relative humidity with a 12 h light and dark cycle. Five to eight-day old female mosquitoes were infected with CHIKV (1:100 dilution of stock, TCID₅₀ 1.5 × 10⁹/mL) spiked in chicken blood, through membrane feeding for one hour. Post feeding, blood fed mosquitoes were separated and maintained in 200 mL cardboard containers at 27.5 °C, 70% humidity and a 14:10 day:night photoperiod for 8 days with 10% sugar solution *ad libitum*. For controls, chicken blood mixed with media supernatant from uninfected Vero cell culture was fed to female mosquitoes. Eight days post infection, the heads and anterior 1/3rd of the thorax of the mosquitoes were dissected and tissue from 6 mosquitoes each were pooled into tubes, each with 50µL of Qiagen RLTplus buffer along with 5–10 silica beads (1 mm) and stored at -80 °C.

Tissue homogenisation was performed on MP Biomedicals FastPrep -24™ homogeniser (3 cycles, speed: 6.5 m/s, 45s/cycle) via bead beating. RNA was then extracted using the RNeasy™ kit (Qiagen, Chadstone, Victoria, Australia). Complementary DNA was generated by using random hexamers and Superscript-III reverse transcriptase (Thermo Fisher Scientific Inc. Scoresby, Victoria, Australia) following the manufacturer's protocols. cDNA generated from the RNA was tested for CHIKV RNA using an in-house-designed qRT-PCR, using E1 gene specific primers (Table S1). For RNASeq data

validation, adult *Aedes albopictus* female mosquitoes were infected with CHIKV as described above. RNA was extracted from the HTs of 5 infected mosquitoes 8 dpi, and cDNA was generated individually by previously described protocols. cDNA from the head/thorax of 5 uninfected mosquitoes was used as controls.

RNASeq libraries were prepared using Nugen's Ovation Universal RNASeq kit, following manufacturer's specification with a minor modification in the HL-dsDNase treatment. HL-dsDNase from Thermo Fisher Scientific was used in our library preparation, along with the 10x buffer supplied that their protocol used. The libraries were pooled and sequenced on a single lane of Hiseq-2500 (Macrogen Inc., Seoul, South Korea) to generate 2×100 bp reads. The fastq files were deposited in NCBI's (National Center for Biotechnology Information) Sequence Read Archive (SRA Accession ID: SRP140387).

Gene-specific primers were designed for the 14 targets to be validated and using 18s rRNA as internal control, qPCR based validation was performed on an Applied Biosystems QuantStudio™ 6 using the SYBR Green Master Mix: SYBR Premix Ex Taq II (Tli RNase H Plus) (Takara- Scientifix Pty Ltd., Clayton, Victoria, Australia) (Cycling conditions: 30 s at 95 °C, 40 cycles of 5 s at 95 °C and 30 s at 60 °C and a melt curve). Thresh-hold cycle values were automatically calculated on the QuantStudio™ Software (Thermo Fisher Scientific Inc. Scoresby, Victoria, Australia). $\Delta\Delta C_t$ values were calculated using the average ΔC_t value of controls and 18s rRNA as a reference. All primer sequences are provided in supplementary table S1.

Trimmomatic v0.36 was used for quality trimming of raw sequences [28]. Using Hisat2 v2.0.5, the reads were aligned to CHIKV reference sequence (GenBank ID: MH229986) to assess infection status [29]. The reads were then aligned to the *Aedes albopictus* Foshan

strain genome sequence (AaloF1) from Vectorbase using Hisat2 [30]. The sorted Bam files were uploaded into Galaxy virtual lab v1.4.6.p5 and aligned transcripts were quantified using featureCounts [31]. Using default parameters, DESeq2 v2.11.38 was used to obtain differentially expressed genes [32].

A Custom *de novo* transcriptome was generated using Trinity v2.3.2, by combining the unaligned reads [33]. edgeR was used to align the reads, measure the transcript counts and quantify the differentially expressed genes using the custom transcriptome. Blastx and BlastN were used to annotate the genes [34,35].

Using topGO and based on p-values (Fisher's exact method) differentially expressed genes were grouped based on their ontologies [36]. Enrichment percentage was calculated as the ratio of the number of times genes in the pathway were differentially expressed compared to the expected number by chance.

Anti-BTKi dsRNA was generated by using a 422bp (Including the T7 promoter tag) long segment of the coding sequence as a template via the Invitrogen™ MEGAscript™ RNAi Kit by following manufacturer's protocol (Reaction incubation time: 4 hours) (Primer details in supplementary table S1). RML12 cells were grown in modified Leibovitz's L-15 Medium (For 400mL of L15 medium, 65mL of FCS, 40mL of TPB, 1.25mL of Pen-strep and 5mL of glutamine were added). Cells were maintained at 27°C with 1% CO₂.

RML12 cells, grown in 24 well plates, were transfected with anti-BTKI dsRNA using Cellfectin® II (Thermo Fisher Scientific, Australia) by following manufacturer's protocol. Briefly, cells were incubated for 5 hours with a mixture of 800ng of purified dsRNA, 8µL of Cellfectin® II reagent and 240µL of transfection media (L15 medium with TPB and Glutamine but no FCS and antibiotics) per well. The mixture was replaced with normal

L15 growth medium at the end of incubation. For controls, RML12 cells were transfected with anti-GFP dsRNA.

Twenty-four hours post transfection with dsRNA, the cells were infected with CHIKV (MOI: 1, Stock TCID₅₀: 1.5x10⁷/mL). Briefly, each well (in a 24 well plate) of RML12 cells were incubated for one hour with 250µl of infection medium (L15 medium with TPB and glutamine but no antibiotics and 2% FCS) and CHIKV. At the end of incubation, the infection media was replaced with regular L15 growth media.

Twenty-four hours post infection, cell culture supernatant was collected and TCID₅₀ performed on Vero cells. RNA was extracted by lysing the monolayer of RML12 cells with 350µL of RLT Plus buffer. RNA extraction and cDNA generation were performed as described before. qPCR was performed to assess knock down of BTKI and change in viral RNA.

For detection of apoptosis, RML12 cells were grown on glass cover slips (13mm diameter) compatible with 24 well plates. The cells were transfected with anti-BTKI dsRNA or anti-GFP dsRNA (for controls) followed by CHIKV infection as described before. BD Cytotfix/Cytoperm™ (BD Biosciences, Australia) was used to fix the cells for one hour and stored in PBS at 4°C.

TUNEL (Terminal deoxynucleotidyl transferase dUTP nick end labelling) staining was performed using *in situ* cell death detection kit, TMR red (Sigma, Cat # 12156792910), as per manufacturer's protocol and the nuclei was stained with 4',6-Diamidine-2'-phenylindole dihydrochloride (DAPI) (Sigma-aldrich). The cells were then imaged in Zeiss LSM 800 confocal system using 10x objective covering at least 500 cells per image. Percentage of TUNEL positive apoptotic cells against the total number of cells (DAPI stained nuclei) was quantified using ImageJ (particle analyser plugin) from each image.

Supplementary Materials: The following are available online at <https://www.mdpi.com/2076-0817/8/3/132/s1>, S1: List of primers, S2: List of differentially expressed genes, S3: Custom transcriptome, S4 TopGo output.

Author Contributions:

R.k.V., P.R.G., J.B.D., and P.N.P. conceived and designed the experiments. R.k.V and J.B.D. performed the mosquito experiments. R.k.V. performed the RNASeq library prep. R.k.V. and M.N. performed the data analysis for RNAseq. R.k.V. performed the cell culture and functional studies. V.S., J.H. and D.G performed staining and microscopy. R.k.V. and P.N.P performed the overall data analysis. R.k.V. wrote the manuscript and prepared the figures. All authors reviewed and approved the final manuscript.

Funding: This research received no external funding

Acknowledgments: The chikungunya virus isolate was obtained from the Victorian Infectious disease reference laboratory, Melbourne. Thanks to Chris Freebairn for collection of *Aedes albopictus* eggs from Torres Strait islands. Thanks to Adam Foord from CSIRO (AAHL) for discussions about optimisation of qRT-PCR and Dr Maria Doyle from the Peter MacCallum Cancer Centre for guidance with the RNASeq data analysis. We thank the Australian Microscopy & Microanalysis Research Facility (AMMRF) for supporting confocal imaging capability at AAHL, utilised in this study.

Conflicts of Interest: The authors declare no conflict of interest.

3.6 References

1. Lumsden, W.H. An epidemic of virus disease in Southern Province, Tanganyika Territory, in 1952-53. II. General description and epidemiology. *Transactions of the Royal Society of Tropical Medicine and Hygiene* 1955, 49, 33-57.
2. Robinson, M.C. An epidemic of virus disease in Southern Province, Tanganyika Territory, in 1952-53. I. Clinical features. *Transactions of the Royal Society of Tropical Medicine and Hygiene* 1955, 49, 28-32.
3. Kamath, S.; Das, A.K.; Parikh, F.S. Chikungunya. *J Assoc Physicians India* 2006, 54.
4. Higgs, S.; Vanlandingham, D. Chikungunya virus and its mosquito vectors. *Vector Borne Zoonotic Dis* 2015, 15, 231-240, doi:10.1089/vbz.2014.1745.
5. Simon, F.; Javelle, E.; Oliver, M.; Leparc-Goffart, I.; Marimoutou, C. Chikungunya Virus Infection. *Current Infectious Disease Reports* 2011, 13, 218-228, doi:10.1007/s11908-011-0180-1.
6. Tsetsarkin, K.A.; Vanlandingham, D.L.; McGee, C.E.; Higgs, S. A single mutation in chikungunya virus affects vector specificity and epidemic potential. *PLoS pathogens* 2007, 3, e201, doi:10.1371/journal.ppat.0030201.
7. Franz, A.W.E.; Kantor, A.M.; Passarelli, A.L.; Clem, R.J. Tissue Barriers to Arbovirus Infection in Mosquitoes. *Viruses* 2015, 7, 3741-3767, doi:10.3390/v7072795.
8. Kuno, G.; Chang, G.-J.J. Biological Transmission of Arboviruses: Reexamination of and New Insights into Components, Mechanisms, and Unique Traits as Well as Their Evolutionary Trends. *Clinical Microbiology Reviews* 2005, 18, 608-637, doi:10.1128/CMR.18.4.608-637.2005.
9. Chomposri, J.; Thavara, U.; Tawatsin, A.; Boonserm, R.; Phumee, A.; Sangkitporn, S.; Siriyasatien, P. Vertical transmission of Indian Ocean Lineage of chikungunya virus in *Aedes aegypti* and *Aedes albopictus* mosquitoes. [Parasite Vectors](#) 2016, 9,227.
10. Vedururu, R.k.; Neave, M.J.; Tachedjian, M.; Klein, M.J.; Gorry, P.R.; Duchemin, J.-B.; Paradkar, P.N. RNASeq Analysis of *Aedes albopictus* Mosquito Midguts after Chikungunya Virus Infection. *Viruses* 2019, 11, 513.
11. McFarlane, M.; Arias-Goeta, C.; Martin, E.; O'Hara, Z.; Lulla, A.; Mousson, L.; Rainey, S.M.; Misbah, S.; Schnettler, E.; Donald, C.L., et al. Characterization of *Aedes aegypti* innate-immune pathways that limit Chikungunya virus replication. *PLoS neglected tropical diseases* 2014, 8, e2994, doi:10.1371/journal.pntd.0002994.

12. Dong, S.; Behura, S.K.; Franz, A.W.E. The midgut transcriptome of *Aedes aegypti* fed with saline or protein meals containing chikungunya virus reveals genes potentially involved in viral midgut escape. *BMC Genomics* 2017, 18, 382, doi:10.1186/s12864-017-3775-6.
13. Shrinet, J.; Srivastava, P.; Sunil, S. Transcriptome analysis of *Aedes aegypti* in response to mono-infections and co-infections of dengue virus-2 and chikungunya virus. *Biochemical and Biophysical Research Communications* 2017, 492, 617-623, doi:https://doi.org/10.1016/j.bbrc.2017.01.162.
14. Mateo, M.; Generous, A.; Sinn, P.L.; Cattaneo, R. Connections matter – how viruses use cell–cell adhesion components. *Journal of Cell Science* 2015, 128, 431-439, doi:10.1242/jcs.159400.
15. Bhella, D. The role of cellular adhesion molecules in virus attachment and entry. *Philosophical Transactions of the Royal Society B: Biological Sciences* 2015, 370, 20140035, doi:10.1098/rstb.2014.0035.
16. Chisenhall, D.M.; Christofferson, R.C.; McCracken, M.K.; Johnson, A.-M.F.; Londono-Renteria, B.; Mores, C.N. Infection with dengue-2 virus alters proteins in naturally expectorated saliva of *Aedes aegypti* mosquitoes. *Parasites & vectors* 2014, 7, 252, doi:10.1186/1756-3305-7-252.
17. Gulley, M.M.; Zhang, X.; Michel, K. The roles of serpins in mosquito immunology and physiology. *Journal of Insect Physiology* 2013, 59, 138-147, doi:https://doi.org/10.1016/j.jinsphys.2012.08.015.
18. Sim, S.; Ramirez, J.L.; Dimopoulos, G. Dengue Virus Infection of the *Aedes aegypti* Salivary Gland and Chemosensory Apparatus Induces Genes that Modulate Infection and Blood-Feeding Behavior. *PLoS pathogens* 2012, 8, e1002631, doi:10.1371/journal.ppat.1002631.
19. Campbell, C.L.; Keene, K.M.; Brackney, D.E.; Olson, K.E.; Blair, C.D.; Wilusz, J.; Foy, B.D. *Aedes aegypti* uses RNA interference in defense against Sindbis virus infection. *BMC Microbiology* 2008, 8, 47, doi:10.1186/1471-2180-8-47.
20. Cirimotich, C.M.; Scott, J.C.; Phillips, A.T.; Geiss, B.J.; Olson, K.E. Suppression of RNA interference increases alphavirus replication and virus-associated mortality in *Aedes aegypti* mosquitoes. *BMC Microbiology* 2009, 9, 49-49, doi:10.1186/1471-2180-9-49.

21. McFarlane, M.; Arias-Goeta, C.; Martin, E.; O'Hara, Z.; Lulla, A.; Mousson, L.; Rainey, S.M.; Misbah, S.; Schnettler, E.; Donald, C.L., et al. Characterization of *Aedes aegypti* Innate-Immune Pathways that Limit Chikungunya Virus Replication. *PLoS neglected tropical diseases* 2014, 8, e2994, doi:10.1371/journal.pntd.0002994.
22. Liu, W.; Quinto, I.; Chen, X.; Palmieri, C.; Rabin, R.L.; Schwartz, O.M.; Nelson, D.L.; Scala, G. Direct inhibition of Bruton's tyrosine kinase by IBtk, a Btk-binding protein. *Nature Immunology* 2001, 2, 939, doi:10.1038/ni1001-939
23. <https://www.nature.com/articles/ni1001-939#supplementary-information>.
24. Lopez-Herrera, G.; Vargas-Hernandez, A.; Gonzalez-Serrano, M.E.; Berron-Ruiz, L.; Rodriguez-Alba, J.C.; Espinosa-Rosales, F.; Santos-Argumedo, L. Bruton's tyrosine kinase--an integral protein of B cell development that also has an essential role in the innate immune system. *Journal of Leukocyte Biology* 2014, 95, 243-250, doi:10.1189/jlb.0513307.
25. Bao, Y.; Zheng, J.; Han, C.; Jin, J.; Han, H.; Liu, Y.; Lau, Y.L.; Tu, W.; Cao, X. Tyrosine kinase Btk is required for NK cell activation. *The Journal of biological chemistry* 2012, 287, 23769-23778, doi:10.1074/jbc.M112.372425.
26. Shinohara, M.; Koga, T.; Okamoto, K.; Sakaguchi, S.; Arai, K.; Yasuda, H.; Takai, T.; Kodama, T.; Morio, T.; Geha, R.S., et al. Tyrosine kinases Btk and Tec regulate osteoclast differentiation by linking RANK and ITAM signals. *Cell* 2008, 132, 794-806, doi:10.1016/j.cell.2007.12.037.
27. Amdekar, S.; Parashar, D.; Alagarasu, K. Chikungunya Virus-Induced Arthritis: Role of Host and Viral Factors in the Pathogenesis. *Viral Immunology* 2017, 30, 691-702, doi:10.1089/vim.2017.0052.
28. Florence, J.M.; Krupa, A.; Booshehri, L.M.; Davis, S.A.; Matthay, M.A.; Kurdowska, A.K. Inhibiting Bruton's tyrosine kinase rescues mice from lethal influenza-induced acute lung injury. *American journal of physiology. Lung Cellular and Molecular Physiology* 2018, 315, L52-L58, doi:10.1152/ajplung.00047.2018.
29. Bolger, A.M.; Lohse, M.; Usadel, B. Trimmomatic: a flexible trimmer for Illumina sequence data. *Bioinformatics* 2014, 30, 2114-2120, doi:10.1093/bioinformatics/btu170.
30. Kim, D.; Langmead, B.; Salzberg, S.L. HISAT: a fast spliced aligner with low memory requirements. *Nature Methods* 2015, 12, 357, doi:10.1038/nmeth.3317

31. Giraldo-Calderon, G.I.; Emrich, S.J.; MacCallum, R.M.; Maslen, G.; Dialynas, E.; Topalis, P.; Ho, N.; Gesing, S.; Madey, G.; Collins, F.H., et al. VectorBase: an updated bioinformatics resource for invertebrate vectors and other organisms related with human diseases. *Nucleic Acids Research* 2015, 43, D707-713, doi:10.1093/nar/gku1117.
32. Afgan, E.; Sloggett, C.; Goonasekera, N.; Makunin, I.; Benson, D.; Crowe, M.; Gladman, S.; Kowsar, Y.; Pheasant, M.; Horst, R., et al. Genomics Virtual Laboratory: A Practical Bioinformatics Workbench for the Cloud. *PLoS One* 2015, 10, e0140829, doi:10.1371/journal.pone.0140829.
33. Love, M.I.; Huber, W.; Anders, S. Moderated estimation of fold change and dispersion for RNA-seq data with DESeq2. *Genome biology* 2014, 15, 550, doi:10.1186/s13059-014-0550-8.
34. Haas, B.J.; Papanicolaou, A.; Yassour, M.; Grabherr, M.; Blood, P.D.; Bowden, J.; Couger, M.B.; Eccles, D.; Li, B.; Lieber, M., et al. De novo transcript sequence reconstruction from RNA-Seq: reference generation and analysis with Trinity. *Nature Protocols* 2013, 8, 10.1038/nprot.2013.1084, doi:10.1038/nprot.2013.084.
35. Boratyn, G.M.; Schäffer, A.A.; Agarwala, R.; Altschul, S.F.; Lipman, D.J.; Madden, T.L. Domain enhanced lookup time accelerated BLAST. *Biology Direct* 2012, 7, 12-12, doi:10.1186/1745-6150-7-12.
36. Camacho, C.; Coulouris, G.; Avagyan, V.; Ma, N.; Papadopoulos, J.; Bealer, K.; Madden, T.L. BLAST+: architecture and applications. *BMC Bioinformatics* 2009, 10, 421-421, doi:10.1186/1471-2105-10-421.
37. Adrian Alexa, J.R. topGO: Enrichment Analysis for Gene Ontology. R package version 2.32.0 2016.

Chapter-4

Chikungunya virus undergoes genomic bottleneck during
Aedes albopictus infection

Chapter 4: Chikungunya virus undergoes genomic bottleneck during *Aedes albopictus* infection

Ravikiran Vedururu^{1, 2}, Matthew J. Neave¹, Mary Tachedjian¹, Paul R. Gorry³, Jean-Bernard Duchemin^{1#}, Prasad N. Paradkar^{1*}

1. CSIRO Health & Biosecurity, Australian Animal Health Laboratory, Geelong, 3220, VIC, Australia

2. School of Applied Sciences, RMIT University, Bundoora, 3083, VIC, Australia

3. School of Health and Biomedical Science, RMIT University, Bundoora, 3083, VIC, Australia

#Current Address: Medical Entomology Lab., Institut Pasteur de la Guyane, Cayenne 97306, French Guiana.

*Corresponding author: Prasad.Paradkar@csiro.au

4.1 Abstract

Objective: Although RNA viruses have a very high mutation rate, arboviruses are constrained genetically due to fitness trade-off, when adapting simultaneously for infection and replication in mosquitoes as well as mammals. Previous studies have identified genomic bottleneck events during mosquito infection, when virus crosses the midgut barrier before its replication in the body. Here, adult female *Aedes albopictus* mosquitoes were infected with chikungunya virus (CHIKV) by blood-feeding. RNASeq libraries prepared from pooled midguts (2 days post infection) and heads and the anterior 1/3rd of the thorax (8 days post infection) were sequenced on an Illumina HiSeq-2500. Variant calling was performed on viral reads after alignment to a Vero cell-derived (input) consensus sequence (MH229986).

Results: Compared to mammalian Vero cell derived CHIKV sequence, there was a significant increase in the number of mutations in the viral genome in the midgut, followed by a substantial reduction in mutations in the viral genome from the head and thorax. These results indicate possible genomic bottleneck events during viral adaptation to the mosquito host system from a mammalian host system.

Keywords: Chikungunya; *Aedes albopictus*; RNA-Seq; Host–pathogen interactions, Genomic diversity

4.2 Introduction & Methods

Traditionally transmitted by *Aedes* genus mosquitoes, chikungunya virus (CHIKV) has caused a massive outbreak starting 2005 and has now become endemic in tropical and Indian Ocean regions, infecting millions and causing high morbidity with long-term arthritis (1, 2). RNA viruses, such as CHIKV, have an inherent ability to rapidly mutate and generate variants for adaptation in novel environments through an error-prone polymerase. Viral diversification during mosquito infection is thought to be driven by the host immune system leading to evolution of new genotypes (3). Previous study has shown that West Nile virus exhibits stochastic reductions in genetic diversity, which was recovered during intra-tissue population expansions (4). Here, we studied the chikungunya viral genome as the virus infects and disseminates in the mosquito to reach the salivary glands from a mammalian host (Vero cells).

Whole genomic sequencing of the chikungunya virus (Isolate 06113879), isolated from a viremic traveller who returned to Australia from Mauritius and passaged in Vero cells (4 passages), once in C6/36 cells and once more in Vero cells was performed previously and the annotated consensus sequence deposited in GenBank (ID: MH229986) (5). *Ae. albopictus* mosquitoes were challenged with CHIKV (1 in 100 dilution of stock virus,

TCID₅₀ 1.5 × 10⁹/mL). RNA-Seq libraries were prepared from RNA extracted at 2- and 8-days post infection from *Ae. albopictus* midguts and heads and thoraces respectively. Sequencing was performed on a single lane of Illumina HiSeq-2500. Quality trimming of the sequence reads was performed using Trimmomatic. SAMtools was used to extract CHIKV reads, from the 2-dpi midgut and 8-dpi head/thorax RNA-Seq libraries. These reads were mapped to the reference sequence generated from the whole genome sequencing of the original Vero cell culture isolate of the virus. The RNA-Seq libraries contained varying number of reads. To account for this, reads were subsampled randomly to the library with lowest number of viral reads (4064 reads). Variant calling (SNPs and INDELs >5%) was performed using VarScan2 v2.3.9 on sub-sampled individual libraries as well as all midgut libraries merged together and all head/thorax libraries merged together (6, 7).

The current data is a result of an extended analysis of our RNA-Seq data to assess transcriptional changes in *Ae. albopictus* midguts and head and thorax in response to CHIKV infection. Detailed methods are described in our previous publications (8, 9).

4.3 Results & Discussion

Earlier studies have shown that significant viral genetic bottleneck events occur during arbovirus infection in mosquito vectors (10, 11). Each bottleneck event may result in significant reduction in viral variant diversity and thus affects the viral variant ultimately transmitted via mosquito saliva to a susceptible mammal. To determine the CHIKV variant diversity in midgut and head/thorax samples, we used a previously sequenced CHIKV isolate 06113879 (5). Briefly, after passaging in Vero cells, whole genome sequencing was performed using the Illumina MiniSeq, resulting in about 8.5 million quality trimmed paired end reads. The assembly resulted in an 11,929bp long consensus

sequence, which perfectly matched a 559bp portion of the E1 gene from this isolate already in the database (GenBank ID: EU404186.1).

Reads from the Vero isolate, as well as from midgut and head/thorax, were compared with the consensus sequence to determine the number of mutations in each sample (Figure 4.1). The number of mutations in the coding region of the midgut samples (50; SNPs: 43 and Indels: 7) were substantially higher compared with Vero (16; SNPs: 9 and Indels: 7), while the number of mutations in head/thorax were lower compared with other samples (7; SNPs: 4 and Indels: 3). The A226V variant in the E1 gene of the virus was identified and maintained from the mammalian host all the way to the viral reads extracted from the head and thorax of the mosquito indicating this virus's fitness for *Ae. albopictus* mosquito (12) and its potential origin from the Indian Ocean region. Two variants appear in D8 samples that were not detected in either the midgut samples or the Vero cell samples. They may have existed in low level, below the limit of detection in the previous two samples and only appears when the other variants disappeared. They could also be novel variants that occurred in the viral genome during the replication in the mosquito tissue. A definitive conclusion cannot be drawn without additional work.

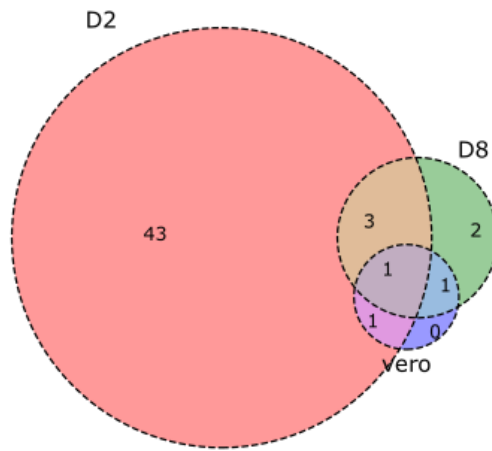


Figure 4.1 Total number of unique variants (coding and non-Coding) from CHIKV from Vero cells (Vero), Ae. albopictus midguts (D2) and head and thoraces (D8). Size of the circle is proportional to the number of variants as denoted.

The location of the SNPs and Indels with respect to their location in the CHIKV genome are presented in Figure 4.2.



Figure 4.2 Variants detected in Vero cell culture isolate, midgut and head/thorax independent libraries plotted as per their location on the CHIKV genome

SNPs (red circles) and indels (blue circles) detected in the viral extract from Vero cell culture, three midgut pools and two head/thorax pools are plotted with reference to their position on the viral genome. The variants were called using Varscan2 and the figure was generated using R-Studio and annotated in Inkscape v0.91.

Arbovirus evolution is constrained by the requirement for alternating replication in vertebrate host and mosquito vectors. Here we found mutations in both the midgut and head/thorax and possible genomic bottleneck events that might indicate adaptation of the virus to the mammalian and mosquito cellular environments. Vero cells (derived from African green monkey kidney), are known to be type-1 interferon response deficient (13). Without any antibody-type and interferon response, there may be limited incentive for viral genome adaptation. The low amount of CHIKV viral diversity from Vero cell culture isolate is also consistent with previous literature (14). While it is also possible that a sub-population of CHIKV is selected resulting in low genomic divergence, more research is needed in this area. Our results suggest that this diversity increases significantly in the mosquito midgut samples at 2-dpi. We hypothesise that this increased genomic diversity represents CHIKV adapting and replicating in the mosquito midgut milieu. Interestingly, the number of CHIKV viral variants decreased considerably in head/thorax by 8-dpi, possibly indicating a genetic bottleneck and adaptation of virus after dissemination. These results are consistent with previous literature that show an increase in CHIKV fitness and its adaptability during host switch (15). The 3'-UTR of the CHIKV genome showed high variation in all our samples. This region enhances viral replication in mosquitoes by interacting with mosquito cell-specific factors (14). It contains highly conserved sequence elements for viral replication, binding sites for cellular miRNAs that determine cell tropism, host range, and pathogenesis, and conserved binding regions for a cellular protein that influences viral RNA stability (16). Although significant, it is possible that this may be due to sequencing errors at this AT-rich region. It is also interesting to note that the number of variants common between different tissue samples was very low, which is consistent with previous report (4). While the results are

consistent with previous literature (17), they are indicative of a bottleneck and our results add to existing knowledge in the subject of viral genomic diversity changes in mosquito vector during infection.

List of abbreviations: CHIKV- Chikungunya virus, dpi- Days post infection, MG- Midgut, HT- Head & Thorax

4.4 Declarations

Ethics approval and consent to participate: Not applicable

Consent for publication: All authors consent for publication

Availability of data and material: The fastq files generated from RNASeq are available in the NCBI's (National Center for Biotechnology Information) Sequence Read Archive (SRA Accession ID: SRP140387). The Viral consensus sequence has been annotated and available in the NCBI's Genbank <https://www.ncbi.nlm.nih.gov/nucore/MH229986.1/>. The VCF files, python script to subsample reads and R-scripts to summarise and plot the variants are provided in the supplementary files and through the data access portal of CSIRO <https://data.csiro.au/dap/landingpage?pid=csiro:42337>.

Competing interests: The authors declare no competing or conflicts of interest.

Funding: This research received no external funding.

Authors' contributions: RV, PNP, PG, and JBD conceived and designed experiments. RV and JBD performed the experiments. MT sequenced and assembled the CHIKV Vero isolate. RV and MN performed the data analysis for RNASeq. RV and PNP performed

overall data analysis. RV wrote the manuscript and prepared figures. All authors reviewed and approved the final manuscript.

Acknowledgements: The chikungunya virus isolate was obtained from the Victorian Infectious disease reference laboratory, Melbourne. Thanks to Chris Freebairn for collection of *Aedes albopictus* eggs from Torres Strait islands.

4.5 References

1. Hua C, Combe B. Chikungunya Virus-Associated Disease. *Current rheumatology reports*. 2017;19(11):69.
2. Petersen LR, Powers AM. Chikungunya: epidemiology. *F1000Research*. 2016;5:F1000 Faculty Rev-82.
3. Forrester NL, Coffey LL, Weaver SC. Arboviral bottlenecks and challenges to maintaining diversity and fitness during mosquito transmission. *Viruses*. 2014;6(10):3991-4004.
4. Grubaugh ND, Weger-Lucarelli J, Murrieta RA, Fauver JR, Garcia-Luna SM, Prasad AN, et al. Genetic Drift during Systemic Arbovirus Infection of Mosquito Vectors Leads to Decreased Relative Fitness during Host Switching. *Cell host & microbe*. 2016;19(4):481-92.
5. Vedururu R, Neave M, Duchemin J.-B., Tachedjian M, Gorry P, and Paradkar P.N. RNA-SEQ analysis identifies differentially expressed genes at critical barrier sites in Chikungunya virus infected *Aedes albopictus* mosquitoes NCBI: National Center for Biotechnology Information, U.S. National Library of Medicine; 2018 [Available from: <https://www.ncbi.nlm.nih.gov/nuccore/1518058344>].
6. Koboldt DC, Zhang Q, Larson DE, Shen D, McLellan MD, Lin L, et al. VarScan 2: somatic mutation and copy number alteration discovery in cancer by exome sequencing. *Genome Research*. 2012;22(3):568-76.
7. Koboldt DC, Zhang Q, Larson DE, Shen D, McLellan MD, Lin L, et al. VarScan 2: Somatic mutation and copy number alteration discovery in cancer by exome sequencing. *Genome Research*. 2012;22(3):568-76.

8. Vedururu Rk, Neave MJ, Tachedjian M, Klein MJ, Gorry PR, Duchemin J-B, et al. RNASeq Analysis of *Aedes albopictus* Mosquito Midguts after Chikungunya Virus Infection. *Viruses*. 2019;11(6):513.
9. Vedururu Rk, Neave MJ, Sundaramoorthy V, Green D, Harper JA, Gorry PR, et al. Whole Transcriptome Analysis of *Aedes albopictus* Mosquito Head and Thorax Post-Chikungunya Virus Infection. *Pathogens*. 2019;8(3):132.
10. Mudiganti U, Hernandez R, Brown DT. Insect response to alphavirus infection--establishment of alphavirus persistence in insect cells involves inhibition of viral polyprotein cleavage. *Virus Research*. 2010;150(1-2):73-84.
11. Pyke AT. Partial E1 gene sequence of Mauritius 2006 isolate 06113879. Unpublished. 2008.
12. Arias-Goeta C, Mousson L, Rougeon F, Failloux A-B. Dissemination and Transmission of the E1-226V Variant of Chikungunya Virus in *Aedes albopictus* Are Controlled at the Midgut Barrier Level. *PLoS One*. 2013;8(2):e57548.
13. Desmyter J, Melnick JL, Rawls WE. Defectiveness of Interferon Production and of Rubella Virus Interference in a Line of African Green Monkey Kidney Cells (Vero). *Journal of Virology*. 1968;2(10):955-61.
14. Stapleford KA, Moratorio G, Henningson R, Chen R, Matheus S, Enfissi A, et al. Whole-Genome Sequencing Analysis from the Chikungunya Virus Caribbean Outbreak Reveals Novel Evolutionary Genomic Elements. *PLoS Neglected Tropical Diseases*. 2016;10(1):e0004402.
15. Coffey LL, Vignuzzi M. Host Alternation of Chikungunya Virus Increases Fitness while Restricting Population Diversity and Adaptability to Novel Selective Pressures. *Journal of Virology*. 2011;85(2):1025-35.
16. Hyde JL, Chen R, Trobaugh DW, Diamond MS, Weaver SC, Klimstra WB, et al. The 5' and 3' ends of alphavirus RNAs – non-coding is not non-functional. *Virus Research*. 2015;206:99-107.
17. Stapleford KA, Coffey LL, Lay S, Borderia AV, Duong V, Isakov O, et al. Emergence and transmission of arbovirus evolutionary intermediates with epidemic potential. *Cell Host Microbe*. 2014;15(6):706-16.

Chapter-5

Evaluating Functional Significance of NPC2 Gene Homologue in *Aedes albopictus* during Chikungunya Virus Infection

Chapter 5: Evaluating Functional Significance of Niemann-Pick 2 Gene Homologue in *Aedes albopictus* during Chikungunya Virus Infection

Ravi kiran Vedururu ^{1,2}, Vinod Sundaramoorthy³, Diane Green³, Paul R. Gorry⁴ and Prasad N. Paradkar ^{1,*}

1CSIRO Health & Biosecurity, Australian Animal Health Laboratory, Geelong, 3220, Australia;

2School of Applied Sciences, RMIT University, Bundoora, 3083, Australia

3CSIRO, Australian Animal Health Laboratory, Geelong, 3220, Australia

4School of Health and Biomedical Science, RMIT University, Bundoora, 3083, Australia.

* Correspondence: Prasad N. Paradkar Prasad.Paradkar@csiro.au

Keywords: *Aedes albopictus*, Chikungunya virus, NPC2, RNASeq, Host-Pathogen Interaction

5.1 Abstract

Chikungunya virus (CHIKV) is an alphavirus belonging to *Togaviridae* family. Following a single nucleotide mutation in the E1 gene of the virus, *Aedes albopictus* has improved vector competence for CHIKV. Previously we performed RNASeq analysis of *Aedes albopictus* midguts, 2 days post infection with CHIKV. Differential gene expression analysis showed an upregulation of Niemann-Pick 2 (*NPC2*) gene homologue (LogFC: 6.29), which was confirmed via RT-qPCR in independent samples (Expression fold change: 5.35). Our results also showed that *NPC2* gene is also upregulated significantly (Expression fold change: 11.63) in *Aedes aegypti* mosquitoes infected with CHIKV. *NPC2* gene, which encodes for an intracellular cholesterol transporter protein was previously

shown to be essential for CHIKV replication in human fibroblasts and when inhibited, severely diminished viral replication. To verify the functional significance in mosquito infection, we overexpressed *NPC2* gene in an *Ae. albopictus* cell line followed by infection with CHIKV. Twenty-four hours post-infection, while there were no significant differences in extracellular (as measured by TCID₅₀) and intracellular CHIKV (as measured by Δ Ct), confocal imaging showed partial co-localisation NPC2 protein (V5 tag) and virus particles (pan-Alphavirus antibody) around membrane bound organelles. Our results indicate that while NPC2 may be implicated in CHIKV infection of *Ae. albopictus* mosquitoes, its actual role during infection remains to be characterized.

5.2 Introduction

Chikungunya virus is a re-emerging arbovirus from the *Alphavirus* genus in *Togaviridae* family. Single nucleotide change in the E1 gene of the virus has led to its increased vector competence in the *Aedes albopictus* mosquitoes (1). This change in the virus sequence has caused the last major outbreak since around 2005 in the East African Reunion island and has since spread to majority of the land mass in the Indian ocean region where seasonal outbreaks are now normal (2). The traditional vector for CHIKV is *Ae. aegypti*, a mosquito well adapted to living in close proximity to human settlements in tropical regions with well understood dawn-dusk feeding cycle (3). The new vector, *Ae. albopictus*, is an invasive pest with greater tolerance to cold and temperate weather zones and aggressive feeding patterns (4). These attributes have conferred advantages to CHIKV and chikungunya fever outbreaks have been noted in regions where arboviral disease outbreaks are uncommon, including temperate Europe (Italy) and northern United states (5, 6). CHIKV causes a severe febrile illness with prolonged arthralgia (7, 8). Treatment is symptomatic and no proven vaccine exists (9). While rate of mortality is low, the

economic impact on a region due to hospitalisations of patients and loss of productive man hours is significant (10, 11).

In our previous publication, we showed that a *Neiman Pick-2* (NPC2) gene homologue is significantly upregulated in the midguts of both *Ae. albopictus* and *Ae. aegypti* mosquitoes, 2 days post-infection with CHIKV (12). Literature suggested NPC2 protein to be essential for successful replication of CHIKV in human fibroblast cells (13). To further understand the functional significance of NPC2 gene during CHIKV infection in *Ae. albopictus*, we overexpressed the gene by transfecting C6/36 cells with a plasmid containing the NPC2 coding sequence before CHIKV infection. The results showed that overexpression did not have an impact on CHIKV titers.

5.3 Materials and Methods

Chikungunya virus isolate 06113879, originally isolated from a viremic traveller from Mauritius was obtained from the Victorian Infectious Diseases Reference Laboratory (VIDRL), Melbourne. The virus isolate also contained the E246V mutation and was most similar to the Indian Ocean region isolate that had also caused the Reunion island outbreak. All experiments were performed under biosafety level 3 (BSL-3) conditions at the Australian Animal Health Laboratory, CSIRO.

The coding sequence of NPC2 gene homologue was amplified from cDNA, prepared from complete RNA extracted from a CHIKV infected *Aedes albopictus*, using the gene specific primers (details provided in the supplementary data) and cloned into the pIZ/V5-His (Thermo Scientific) plasmid after restriction digestion with HindIII & XbaI (NEB) and ligation with T4 ligation enzyme (NEB). Electrocompetent DH5 α *Escherichia Coli* were transformed with PiZ plasmid with NPC2 insert using a Bio-Rad Gene Pulser Xcell™ Electroporation Systems and grown on Zeocin infused (35 μ l per 100ml) low salt

LB agar plates. Successful integration of the sequence in the cloning site in-frame with the V5 tag was confirmed via Sanger sequencing post extraction of plasmid using Qiagen MiniPrep kit. The bacterial plug containing the clone with right insert was grown overnight in 500ml of low salt LB broth with Zeocin (35µl per 100ml) with shaking and the cloned plasmid extracted using the Qiagen MidiPrep kit to obtain endotoxin free plasmid. All procedures were followed as per the respective manufacturer's recommendations without modifications.

C6/36 cells, which are a continuous cell line derived from *Ae. albopictus* larvae (14), were grown in Leibovitz's L-15 Medium (For 400 ml of L15 medium, 65ml of FCS, 40ml of TPB, 1.25ml of Pen-strep and 5ml of Glutamine were added) and maintained at 27°C. Transfection of cells were performed using FlyFectin™ Transfection Reagent (OZ Biosciences, San Diego, CA) at 1.5µg plasmid DNA to 6µL reagent per well of 70% confluent cells, mixed with 250µl of transfection L15 medium (L15 medium with TPB and Glutamine but no FCS and antibiotics) incubated for 5 hours. After five hours of incubation, the mixture was replaced with L15 growth medium. For controls, C6/36 cells were transfected with GFP expressing pIZ plasmid.

Twenty-four hours post-transfection, the cells were infected with CHIKV (MOI: 1). Briefly, the growth medium on the cells grown in 24-well plates, was replaced with 250µl of infection medium (L15 medium with TPB and Glutamine but no antibiotics and 2% FCS) and CHIKV per well. The cells were incubated for one hour after which the infection medium was replaced with regular L15 growth medium.

Twenty-four hours post-infection, the supernatant from three wells was collected for TCID₅₀. The cell monolayer was lysed using 350µl of RLT+ buffer. RNA was extracted from the same three wells and cDNA prepared using methods previously described (12).

Quantitative PCR (qPCR) was performed on technical triplicates using NPC2 and CHIKV sequence specific primers. 18s rRNA specific primers were used as internal controls to calculate ΔC_t values. qPCR was performed on an Applied Biosystems QuantStudio™ 6 using the Takara-Clontech SYBR Green Master Mix: SYBR Premix Ex Taq II (Tli RNase H Plus). The following cycling conditions were used with a melt curve analysis at the end. Cycling conditions were: 30 seconds at 95°C, 40 cycles of 5 seconds at 95°C and 30 seconds at 60°C followed by a melt curve. The baseline and C_t values were calculated automatically using the supplied QuantStudio™ Software.

TCID₅₀ assay was performed on Vero cells, using the supernatant from the three NPC2-pIZ or GFP-pIZ transfected C6/36 cells. Wells of cells showing cytopathic effects were counted 4 days post infection and infectivity titer measurements were calculated using the Spearman & Kärber algorithm (15).

For Confocal microscopy, C6/36 cells were grown on glass cover slips (13mm diameter) compatible with 24-well plates as described before in chapter 3. The cells were transfected using NPC2-pIZ and GFP-pIZ plasmids (1.5µg/well). Twenty-four hours post-transfection, they were infected with CHIKV (MOI: 1). The cells were then fixed using BD Cytofix/Cytoperm™ (BD Biosciences, Australia) for one hour and stored in PBS at 4°C. The cells were stained with an Anti-V5 tag antibody (ab9116, 1:100) (abcam, USA) and an alphavirus antibody (3581, sc-58088, 1:50) (Santa Cruz Biotechnology, Dallas, Texas, U.S.A) and 4',6-Diamidino-2'-phenylindole dihydrochloride (DAPI) (Sigma-Aldrich). Briefly, cells were permeabilized in 0.1% Triton X-100 in PBS for 5 mins, blocked for 30 mins with 0.5% BSA in PBS and incubated with primary antibodies for 16 h at 4 °C. AlexaFluor-594 or 647 conjugated anti-mouse or anti-Rabbit secondary antibodies (1:200; ThermoFisher Scientific) were incubated for 1 h at room temperature, cells were then stained with DAPI and mounted on slides using Vectashield mounting medium (Vector

Laboratories). The cells were imaged on Zeiss LSM 800 confocal microscope and image analysis was performed on Zen lite software (v2.6).

5.4 Results

Initial experiments were performed to check whether overexpression of mosquito NPC2 homologue has any effect on CHIKV titers in mosquito cells. C6/36 cells were transfected with plasmid containing *Ae. albopictus* NPC2 gene homologue. As a control, cells were transfected with GFP plasmid. Cells were infected with CHIKV 24 hours post-transfection and samples were collected 24 hpi. While there was successful overexpression of NPC2 gene homologue (Expression fold change: 1473.012) as measured by realtime RT-qPCR, there was no significant difference in intracellular CHIKV RNA between NPC2 and GFP overexpressing C6/36 cells (Expression fold change: 1.04) (Figure 5.1a). TCID₅₀ was performed on cell culture supernatant from the two conditions 24 hpi and the results did not show significant difference (Figure 5.1b).

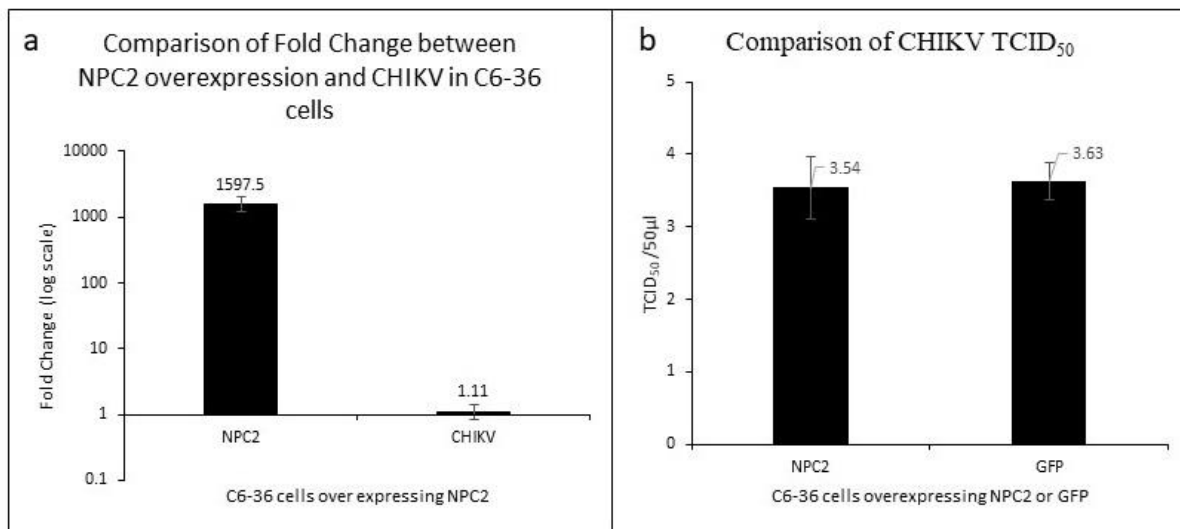


Figure 5.1 Comparison of fold change NPC2 and CHIKV & CHIKV TCID₅₀ between GFP/NPC2 overexpressing C6/36 cells

In mammals, NPC2 has previously been identified as an intracellular cholesterol transporter, involved in egress of cholesterol from the late endosomal/ lysosomal compartment (16). NPC2 has been implicated in CHIKV replication in human fibroblasts. To determine whether NPC2 co-localises with CHIKV in mosquito cells, confocal microscopy was performed on C6/36 cells overexpressing NPC2 and infected with CHIKV. Cells that showed both NPC2 over expression (visualised through staining with anti-V5 antibody) and CHIKV infection (Visualised through staining with pan-alphavirus antibody) were manually scanned for localisation patterns. Confocal imaging showed vesicular and membrane bound localization of overexpressed NPC2 protein. Viral particles partially co-localised with NPC2 at the cell membranes (Fig 5.2a) or vesicles (Fig 5.2b). Cells that showed the two patterns, i.e. cytoplasmic and vesicular localisations were imaged. Up to 10-20 Airyscan images of the selected cells were taken in total. No special treatment was applied to visualise the vesicular localisation.

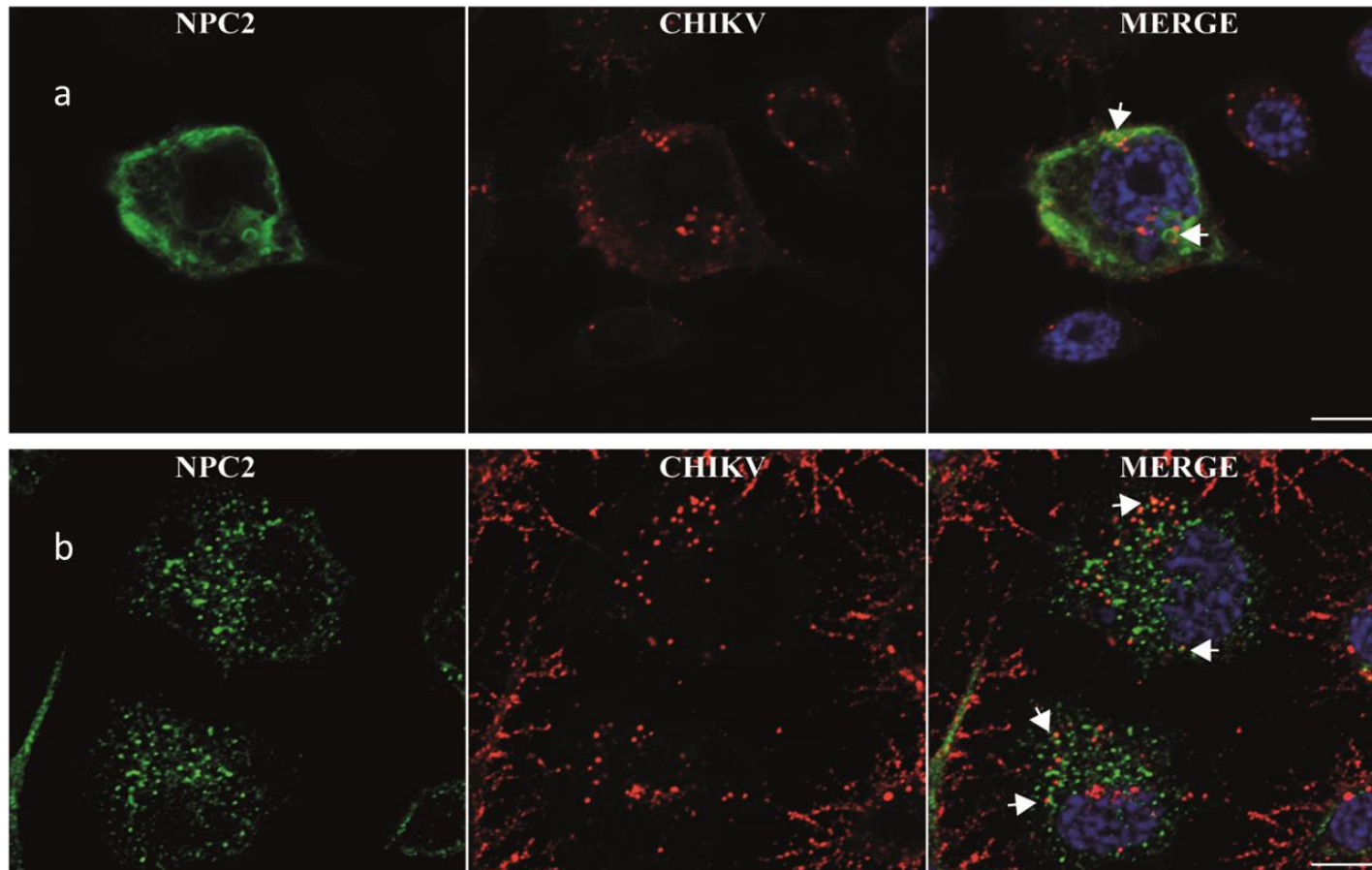


Figure 5.2C6/36 cells over expressing NPC2 protein, infected with CHIKV.

NPC2 protein (Green) is localised to membranes (a) and vesicles (b) and confocal imaging shows partial co-localisation of CHIKV (Red) particles to the same areas. Nucleus is stained with DAPI (Blue) (Scale bar: 50 μ M).

5.5 Discussion

Our previous study identified NPC2 homologue to be significantly upregulated in the midguts of *Ae. aegypti* and *Ae. albopictus* after CHIKV infection (12). Primarily existing in lysosomes and late endosomes, NPC2 is a small soluble lipid transporter that mediates movement of cholesterol molecules in conjunction with NPC1 in cells (17). In humans, *NPC2* gene is located on the X-chromosome and loss of function mutations causes pathological accumulation of lipid particles in cells causing a condition called Niemann-Pick disease. Characterised by build-up of cholesterol within cells, the condition manifests into several impairments including but not limited to neurological, lung and liver problems. Abnormal accumulation of lipids in cells eventually result in cell death and tissue injury (17-19).

NPC family proteins were shown to be involved in multiple viral replication and cell entry-exit mechanisms including ebolavirus (20-23) and HIV1 (24). Apart from these, multiple viruses including Influenza A (25) and vesicular stomatitis virus (26) use lipid membrane rafts which are also associated with NPC family proteins.

Interestingly, CHIKV replication is completely restricted when NPC proteins were inhibited using Imipramine in human fibroblast cells. Flaviviruses including dengue and Zika viruses also exhibited diminished replication on inhibition of NPC proteins using Imipramine (13). The fact that the same family of proteins are involved in viral infections in multiple vectors (evident from upregulation in both *Ae. aegypti* and *Ae. albopictus* midguts) and higher order animals including humans indicates their highly conserved involvement.

Our results showed that there was no significant change in the infectivity titers and viral RNA quantities in cells that over-expressed NPC2, possibly indicating the relationship is not rate-limiting in nature, i.e. more NPC2 protein may not lead to more virus replication or production. Although, we were not able to establish direct implications of NPC2 during CHIKV infection, more research needs to be performed to confirm this. Previous research has also indicated that the E1-226 mutant CHIKV strain may not be cholesterol dependent (27), which may be relevant in this research. However, on confocal imaging, we could see viral clustering around membranes and vesicles stained by NPC2 proteins. This observation is consistent with previous literature that suggest NPC protein involvement in lipid transport and multiple viruses depending on the lipid transport mechanisms for entry/exit into cells and movement of different viral particles inside cells between endosomal and lysosomal systems, indicating the significance of NPC proteins in viral infections (13, 21, 22, 24). Our findings indicate that although NPC2 did not play a role in mosquito viral replication at the conditions tested, its exact role remains to be identified.

Conflict of Interest: *The authors declare that the research was conducted in the absence of any commercial or financial relationships that could be construed as a potential conflict of interest.*

Author Contributions: RV, PG and PNP conceived and designed experiments. RV performed the experiments. VS and DG performed staining and Confocal imaging. RV and PNP performed overall data analysis. RV wrote the manuscript and prepared figures. All authors reviewed and approved the final manuscript.

Funding: This research received no external funding.

Acknowledgments: The chikungunya virus isolate was obtained from the Victorian Infectious disease reference laboratory, Melbourne. We thank the Australian Microscopy

& Microanalysis Research Facility (AMMRF) for supporting confocal imaging capability at AAHL, utilised in this study.

5.6 References

1. Tsetsarkin KA, Vanlandingham DL, McGee CE, Higgs S. A single mutation in chikungunya virus affects vector specificity and epidemic potential. *PLoS Pathogens*. 2007;3(12):e201.
2. Petersen LR, Powers AM. Chikungunya: epidemiology. *F1000Research*. 2016;5:F1000 Faculty Rev-82.
3. Higgs S, Vanlandingham D. Chikungunya virus and its mosquito vectors. *Vector Borne Zoonotic Diseases*. 2015;15(4):231-40.
4. Waldock J, Chandra NL, Lelieveld J, Proestos Y, Michael E, Christophides G, *et al*. The role of environmental variables on *Aedes albopictus* biology and chikungunya epidemiology. *Pathogens and Global Health*. 2013;107(5):224-41.
5. Rezza G, Nicoletti L, Angelini R, Romi R, Finarelli AC, Panning M, *et al*. Infection with chikungunya virus in Italy: an outbreak in a temperate region. *Lancet*. 2007;370(9602):1840-6.
6. Enserink M. Chikungunya: No Longer a Third World Disease. *Science*. 2007;318(5858):1860.
7. Hua C, Combe B. Chikungunya Virus-Associated Disease. *Current Rheumatology Reports*. 2017;19(11):69.
8. Amdekar S, Parashar D, Alagarasu K. Chikungunya Virus-Induced Arthritis: Role of Host and Viral Factors in the Pathogenesis. *Viral Immunology*. 2017;30(10):691-702.
9. Rezza G, Weaver SC. Chikungunya as a paradigm for emerging viral diseases: Evaluating disease impact and hurdles to vaccine development. *PLoS Neglected Tropical Diseases*. 2019;13(1):e0006919.
10. Alvis-Zakzuk NJ, Díaz-Jiménez D, Castillo-Rodríguez L, Castañeda-Orjuela C, Paternina-Caicedo Á, Pinzón-Redondo H, *et al*. Economic Costs of Chikungunya Virus in Colombia. *Value in Health Regional Issues*. 2018;17:32-7.

11. Paixão ES, Teixeira MG, Rodrigues LC. Zika, chikungunya and dengue: the causes and threats of new and re-emerging arboviral diseases. *BMJ Global Health*. 2018;3(Suppl 1):e000530.
12. Vedururu Rk, Neave MJ, Tachedjian M, Klein MJ, Gorry PR, Duchemin J-B, et al. RNASeq Analysis of *Aedes albopictus* Mosquito Midguts after Chikungunya Virus Infection. *Viruses*. 2019;11(6):513.
13. Wichit S, Hamel R, Bernard E, Talignani L, Diop F, Ferraris P, et al. Imipramine Inhibits Chikungunya Virus Replication in Human Skin Fibroblasts through Interference with Intracellular Cholesterol Trafficking. *Scientific reports*. 2017;7(1):3145-.
14. Singh Krp. Cell Cultures Derived from Larvae of *Aedes Albopictus* (Skuse) and *Aedes Aegypti* (L.). *Current Science*. 1967;36(19):506-8.
15. Hamilton MA, Russo RC, Thurston RV. Trimmed Spearman-Kärber method for estimating median lethal concentrations in toxicity bioassays. *Environmental Science & Technology*. 1977;11(7):714-9.
16. Storch J, Xu Z. Niemann-Pick C2 (NPC2) and intracellular cholesterol trafficking. *Biochim Biophys Acta*. 2009;1791(7):671-8.
17. Infante RE, Wang ML, Radhakrishnan A, Kwon HJ, Brown MS, Goldstein JL. NPC2 facilitates bidirectional transfer of cholesterol between NPC1 and lipid bilayers, a step in cholesterol egress from lysosomes. *Proceedings of the National Academy of Sciences*. 2008;105(40):15287-92.
18. Wang YH, Twu YC, Wang CK, Lin FZ, Lee CY, Liao YJ. Niemann-Pick Type C2 Protein Regulates Free Cholesterol Accumulation and Influences Hepatic Stellate Cell Proliferation and Mitochondrial Respiration Function. *International Journal of Molecular Sciences*. 2018;19(6).
19. Vance JE, Karten B. Niemann-Pick C disease and mobilization of lysosomal cholesterol by cyclodextrin. *Journal of lipid research*. 2014;55(8):1609-21.
20. Herbert AS, Davidson C, Kuehne AI, Bakken R, Braigen SZ, Gunn KE, et al. Niemann-pick C1 is essential for ebolavirus replication and pathogenesis in vivo. *mBio*. 2015;6(3):e00565-15.
21. Jupatanakul N, Sim S, Dimopoulos G. *Aedes aegypti* ML and Niemann-Pick type C family members are agonists of dengue virus infection. *Developmental & Comparative Immunology*. 2014;43(1):1-9.

22. Carette JE, Raaben M, Wong AC, Herbert AS, Obernosterer G, Mulherkar N, et al. Ebola virus entry requires the cholesterol transporter Niemann-Pick C1. *Nature*. 2011;477(7364):340-3.
23. Krishnan A, Miller EH, Herbert AS, Ng M, Ndungo E, Whelan SP, et al. Niemann-Pick C1 (NPC1)/NPC1-like1 Chimeras Define Sequences Critical for NPC1's Function as a Filovirus Entry Receptor. *Viruses*. 2012;4(11):2471-84.
24. Tang Y, Leao IC, Coleman EM, Broughton RS, Hildreth JE. Deficiency of niemann-pick type C-1 protein impairs release of human immunodeficiency virus type 1 and results in Gag accumulation in late endosomal/lysosomal compartments. *Journal of Virology*. 2009;83(16):7982-95.
25. Veit M, Thaa B. Association of influenza virus proteins with membrane rafts. *Advances in Virology*. 2011;2011:370606-.
26. Carneiro FA, Bianconi ML, Weissmüller G, Stauffer F, Da Poian AT. Membrane Recognition by Vesicular Stomatitis Virus Involves Enthalpy-Driven Protein-Lipid Interactions. *Journal of Virology*. 2002;76(8):3756.
27. Schuffenecker I, Itean I, Michault A, Murri S, Frangeul L, Vaney M-C, et al. Genome Microevolution of Chikungunya Viruses Causing the Indian Ocean Outbreak. *PLoS Medicine*. 2006;3(7):e263.

Chapter-6

Discussion

Chapter 6: Discussion

CHIKV is a re-emerging alphavirus causing a high morbidity with long term arthralgia. Previous studies have taken approaches to understand the interaction between CHIKV and the *Ae. aegypti* vector (1). However, considering the switch in vector preference towards *Ae. albopictus* by Indian Ocean isolates (due to a single amino acid change) and invasive nature of this mosquito species, it is paramount to characterize the interaction between CHIKV and the new vector.

One study has explored the interaction between CHIKV and *Ae. Aegypti* in the mosquito midgut (2). Previous studies with whole transcriptome analysis in mosquito vectors have used either whole mosquitoes or cell culture (3-7). Our objective here was to study the vector-virus interaction specifically at midgut, the first barrier site, and head/thorax, the second barrier site, which denote the dissemination sites and include salivary glands, to understand the factors that play a critical role in determining mosquito vector competence.

Here we performed an unbiased transcriptional analysis on tissues collected from lab reared adult female *Ae. albopictus* mosquitoes at two different time points after exposure to CHIKV infection. The gene expression patterns at these tissue sites compared to uninfected samples revealed the transcriptional changes that are likely to be in response to the viral infection.

The analysis revealed that 25 transcripts were differentially regulated at 2 dpi in midgut, with most of the transcriptional changes related to metabolism. Analysis of molecular functions revealed that while lysozyme activity and alkaline phosphatase were down regulated, carboxypeptidase activity was upregulated. Indeed, lysozymal and

carboxypeptidase pathways have previously been implicated in innate immune responses against multiple arboviral infections (8-11).

At 8dpi in head/thorax, differential expression of 159 transcripts and differential regulation of biological processes including RNA and mRNA binding, lysosomal and serpin pathways and down regulation of defensin genes were observed. These could be due to either mosquito immune responses to CHIKV or viral modulation of immunity. Processes such as the regulation of transport and homophilic cell adhesion via plasma membrane could be involved in viral assembly and export (12-15). Functional studies to determine whether these genes are pro or anti-viral are needed and could explain the role of these genes in the infection process.

Multiple prior publications have also shown that the RNAi pathway is one of the major pathways involved in anti-viral responses in insects (16-18). In this study, we did not find any statistically significant changes in expression of genes involved in the RNAi pathways. It is possible that the regulation of this pathway either does not occur at the transcriptional level or the proteins involved are ubiquitously expressed and not differentially regulated. It is also possible that the time points we selected did not coincide with RNAi activation.

Twenty-two protein coding targets (8 from midguts/2dpi dataset and 14 from Head&Thorax/8dpi dataset) and 5 lncRNAs (all from midguts/2dpi dataset) were selected for validation by qRT-PCR, based on their possible involvement in mosquito immunity. The concordance was lower in the 8dpi genes compared to 2 dpi genes. This could be due to the lower number of replicates in 8 dpi samples in the RNA-Seq analysis.

Seven targets from midguts/2dpi dataset were chosen for assessment of their differential expression status post infection with CHIKV in *Ae. aegypti*, the tradition vector. While the

seven chosen targets were differentially expressed in *Ae. albopictus* midguts 2dpi with CHIKV with varied regulation, all the seven targets tested were significantly upregulated in *Ae. aegypti* midguts. These results may indicate that although both *Ae. albopictus* and *Ae. aegypti* are from the same *Aedes* genus, there are significant differences between them when it comes to transcriptomic changes post CHIKV infection. This also indicates that the response of the mosquitoes to the virus could also be significantly different and may account for different vector competence, enough to warrant further study.

List of all the primers used for this project are presented in Appendix-I. Appendix-II to V list the differentially expressed genes from edgeR and DESeq2 from midguts and head and thorax of *Ae. albopictus*, 2dpi and 8dpi with CHIKV.

The incomplete and poorly annotated reference genome of *Ae. albopictus* was a hindrance in performing data analysis and robust pathway analysis. We also used heads and anterior 1/3rd of the thorax, which included salivary glands at 8 dpi. The results from these samples represent data from heterogeneous tissue, and care needs to be taken before any broad conclusions are drawn. Functional characterisation of the identified genes may help in deciphering the results and understanding their role in mosquito-virus interactions.

RNA viruses, such as CHIKV, have an inherent ability to rapidly mutate and generate variants for adaptation in novel environments through an error-prone polymerase (19). Viral diversification is thought to be driven by the mosquito immune system leading to evolution of new genotypes (20). A study has shown that West Nile virus exhibits stochastic reductions in genetic diversity, which was recovered during intra-tissue population expansions (21). Here, utilising the high-throughput viral sequencing data, we showed that the mutations that arose in midgut and head/thorax samples compared

to the original Vero cell culture isolate indicate possible changes in the viral sequence as it adapts from a mammalian host to different mosquito tissues. Vero cells, derived from African green monkey kidney, are known to be type-1 interferon response deficient (22), which may result in a high amount of CHIKV viral diversity as seen by high number of viral variants. Our results suggest that this diversity increases significantly in the mosquito midgut samples at 2dpi. We hypothesise that this increased genomic diversity represents CHIKV adapting and replicating in the mosquito midgut milieu. Interestingly, the number of CHIKV viral variants decreased considerably in head/thorax by 8 dpi, possibly indicating a genetic bottleneck at this stage. These results are consistent with previous literature that show increase in CHIKV fitness and its adaptability during host switch (23). Additional research focussed on this observation may provide conclusive answers as to the nature of the changes observed in the viral genome. The CHIKV 3'-UTR enhances viral replication in mosquitoes by interacting with mosquito cell-specific factors. This region contains highly conserved sequence elements for viral replication, binding sites for cellular miRNAs that determine cell tropism, host range, and pathogenesis, and conserved binding regions for a cellular protein that influences viral RNA stability (24). The 3'-UTR of the CHIKV genome showed the most variation in all our samples. Although significant, this may also be due sequencing errors at this AT-rich region.

A *Neiman Pick-2* (NPC2) homologue transcript was found to be significantly upregulated in the midgut of *Ae. albopictus* mosquito 2 dpi with CHIKV both by RNA-Seq and RT-qPCR. The same gene was also upregulated in the midgut of *Ae. aegypti* mosquito 2 dpi with CHIKV (25). Known to be a lipid transporter that localises to lysosomes and late endosomes, NPC family of proteins have previously been implicated in multiple viral infections and intra-cellular viral replication. NPC1 has been shown to be essential for

Ebola virus entry into cells, replication and pathogenesis (26, 27). In *Ae. aegypti*, NPC family members were shown to be agonists of dengue viral infection (28). NPC1 deficiency is shown to impair the release of mature HIV1 particles (29). Most importantly, inhibition of NPC proteins by using Imipramine has been shown to successfully block replication of chikungunya virus in a rate limiting manner. This mechanism was also shown to be effective in blocking replication of flaviviruses including dengue and Zika viruses (30). Considering the significance of NPC proteins in viral infections, we attempted to assess the functional significance of the NPC2 upregulation in our dataset. NPC2 was over expressed in *Ae. albopictus* cell line, C6/36. Supernatant and RNA was collected from C6/36 cells, over-expressing NPC2 protein, 24 hours post infection with CHIKV. Compared to controls, C6/36 cells transfected with NPC2 expressing pIZ plasmid had significantly higher levels of NPC2 expression. However, there was no significant differences in extra-cellular infective mature viral particles as measured TCID₅₀. Significant difference was also not detected in intra-cellular viral RNA levels as measured by RT-qPCR. On confocal microscopy, C6/36 being a mixed cell line, there were at least two different patterns of NPC2 distribution across the cells. In one pattern, NPC2 was localised to various intra-cellular membranes while in the second pattern, NPC2 formed cytoplasmic vesicles. In both patterns, CHIKV and NPC2 are observed to be co-localising. This observation is consistent with previous publications (referenced above) in that NPC2 proteins play a part in viral entry/exit of cells and participate in replication of viruses. While NPC2 over expression did not result in changes to quantity of viral particle or RNA, co-localisation of CHIKV particles and NPC2 protein suggest functional significance of NPC2 during viral pathogenesis in insect cells.

A transcript that was significantly upregulated at 8 dpi in head/thorax, was *Inhibitor of Bruton's tyrosine kinase* (BTKi). Bruton's tyrosine kinase (BTK) is a non-receptor, cytosolic,

Tec kinase. BTK has been linked to multiple innate and adaptive immune system functions. In mammals, loss of function mutations in BTK gene is pathogenic and results in X-Linked agammaglobulinemia (XLA), a condition characterised by inability to produce mature B-cells and gamma globulins (including antibodies) (31). BTK-deficient macrophages show increased susceptibility to apoptosis when exposed to pathogen associated inflammatory signals. BTK is known to upregulate the NF- κ B pathway and lead to NK cell activation (32).

A classical symptom of CHIKV pathogenesis is severe arthralgia where patients experience prolonged muscle and joint pains (33). CHIKV is known to infect osteoblasts, the bone forming cells and upregulate Interleukin-6 (IL-6) and Receptor activator of nuclear factor kappa-B ligand (RANKL) generation and decrease Osteoprotegerin (OPG) production. An altered RANKL/OPG ratio gives rise to arthralgia, a characteristic morbidity of chikungunya fever (34).

Btk along with other Tec family kinases are heavily involved in osteoclast, the cells involved in bone resorption, differentiation and regulation. Severe osteopetrosis is observed in mice with non-functional Btk gene. Reduced osteoclastic bone resorption was observed in osteoporosis and inflammation-induced bone destruction on inhibition of Tec kinases. Btk and Tec kinases, among Tec Kinases are selectively expressed in osteoclasts and not in osteoblasts. Increased bone mass in mouse without Btk is due to defective osteoclastic bone resorption because of defective osteoclast differentiation (35). Literature also presents evidence of benefit of Btk inhibition in viral inflammatory disease. Specifically, BTK inhibition with ibrutinib has shown major protective effect in lung tissue of mice during influenza viral infection by ameliorating excessive inflammatory response (36).

Taking all published literature into account, inhibition of BTK appears to be protective to host cells as a method of limiting tissue damage due to inflammatory response. Particularly during CHIKV infection, inhibition of BTK may result in reduced bone loss. It is interesting to observe the significant upregulation of BTKi in the *Aedes albopictus* at a later stage of CHIKV infection in the site of dissemination. While definitive conclusions can not be drawn as to possible role of BTK or BTKi in humans and the effect of BTK inhibition during CHIKV, evidence to a highly conserved mechanism at play from insect vector to end point-host is highly suggestive and warrants further study.

Overall, the results showed significant changes in the transcriptome of *Aedes albopictus* mosquitoes after CHIKV infection, with identified genes involved in multiple cellular processes. This study, for the first time, examines differential gene expression at the midgut (the first critical barrier site) and head and thorax (dissemination site containing salivary glands) in infected mosquitoes. The outcomes can be utilized in determining potential pro-viral and antiviral host factors and in turn, will be helpful in reducing the high impact of CHIKV infections by targeting the vector, *Ae. albopictus*.

6.1 References

1. McFarlane M, Arias-Goeta C, Martin E, O'Hara Z, Lulla A, Mousson L, et al. Characterization of *Aedes aegypti* innate-immune pathways that limit Chikungunya virus replication. PLoS Neglected Tropical Diseases. 2014;8(7):e2994.
2. Dong S, Behura SK, Franz AWE. The midgut transcriptome of *Aedes aegypti* fed with saline or protein meals containing chikungunya virus reveals genes potentially involved in viral midgut escape. BMC Genomics. 2017;18(1):382.
3. Etebari K, Hegde S, Saldaña MA, Widen SG, Wood TG, Asgari S, et al. Global Transcriptome Analysis of *Aedes aegypti* Mosquitoes in Response to Zika Virus Infection. mSphere. 2017;2(6):e00456-17.

4. Shrinet J, Srivastava P, Sunil S. Transcriptome analysis of *Aedes aegypti* in response to mono-infections and co-infections of dengue virus-2 and chikungunya virus. *Biochemical and Biophysical Research Communications*. 2017;492(4):617-23.
5. Bonizzoni M, Dunn WA, Campbell CL, Olson KE, Marinotti O, James AA. Complex Modulation of the *Aedes aegypti* Transcriptome in Response to Dengue Virus Infection. *PLoS One*. 2012;7(11):e50512.
6. Fragkoudis R, Chi Y, Siu RW, Barry G, Attarzadeh-Yazdi G, Merits A, et al. Semliki Forest virus strongly reduces mosquito host defence signaling. *Insect Molecular Biology*. 2008;17(6):647-56.
7. Colpitts TM, Cox J, Vanlandingham DL, Feitosa FM, Cheng G, Kurscheid S, et al. Alterations in the *Aedes aegypti* Transcriptome during Infection with West Nile, Dengue and Yellow Fever Viruses. *PLoS Pathogens*. 2011;7(9):e1002189.
8. Johnston C, Jiang W, Chu T, Levine B. Identification of Genes Involved in the Host Response to Neurovirulent Alphavirus Infection. *Journal of Virology*. 2001;75(21):10431-45.
9. Merklings SH, van Rij RP. Beyond RNAi: Antiviral defense strategies in *Drosophila* and mosquito. *Journal of Insect Physiology*. 2013;59(2):159-70.
10. Swevers L, Liu J, Smagghe G. Defense Mechanisms against Viral Infection in *Drosophila*: RNAi and Non-RNAi. *Viruses*. 2018;10(5).
11. Isoe J, Zamora J, Miesfeld RL. Molecular Analysis of the *Aedes aegypti* Carboxypeptidase Gene Family. *Insect Biochemistry and Molecular Biology*. 2009;39(1):68-73.
12. Mateo M, Generous A, Sinn PL, Cattaneo R. Connections matter – how viruses use cell–cell adhesion components. *Journal of Cell Science*. 2015;128(3):431-9.
13. Bhella D. The role of cellular adhesion molecules in virus attachment and entry. *Philosophical Transactions of the Royal Society B: Biological Sciences*. 2015;370(1661):20140035.
14. Chisenhall DM, Christofferson RC, McCracken MK, Johnson A-MF, Londono-Renteria B, Mores CN. Infection with dengue-2 virus alters proteins in naturally expectorated saliva of *Aedes aegypti* mosquitoes. *Parasites & Vectors*. 2014;7(1):252.
15. Gulley MM, Zhang X, Michel K. The roles of serpins in mosquito immunology and physiology. *Journal of Insect Physiology*. 2013;59(2):138-47.

16. Campbell CL, Keene KM, Brackney DE, Olson KE, Blair CD, Wilusz J, et al. *Aedes aegypti* uses RNA interference in defense against Sindbis virus infection. BMC Microbiology. 2008;8(1):47.
17. Cirimotich CM, Scott JC, Phillips AT, Geiss BJ, Olson KE. Suppression of RNA interference increases alphavirus replication and virus-associated mortality in *Aedes aegypti* mosquitoes. BMC Microbiology. 2009;9:49-.
18. McFarlane M, Arias-Goeta C, Martin E, O'Hara Z, Lulla A, Mousson L, et al. Characterization of *Aedes aegypti* Innate-Immune Pathways that Limit Chikungunya Virus Replication. PLoS Neglected Tropical Diseases. 2014;8(7):e2994.
19. Holland J, Spindler K, Horodyski F, Grabau E, Nichol S, VandePol S. Rapid evolution of RNA genomes. Science. 1982;215(4540):1577.
20. Sim S, Aw PPK, Wilm A, Teoh G, Hue KDT, Nguyen NM, et al. Tracking Dengue Virus Intra-host Genetic Diversity during Human-to-Mosquito Transmission. PLoS Neglected Tropical Diseases. 2015;9(9):e0004052.
21. Grubaugh ND, Weger-Lucarelli J, Murrieta RA, Fauver JR, Garcia-Luna SM, Prasad AN, et al. Genetic drift during systemic arbovirus infection of mosquito vectors leads to decreased relative fitness during host switching. Cell Host & Microbe. 2016;19(4):481-92.
22. Desmyter J, Melnick JL, Rawls WE. Defectiveness of Interferon Production and of Rubella Virus Interference in a Line of African Green Monkey Kidney Cells (Vero). Journal of Virology. 1968;2(10):955-61.
23. Coffey LL, Vignuzzi M. Host Alternation of Chikungunya Virus Increases Fitness while Restricting Population Diversity and Adaptability to Novel Selective Pressures. Journal of Virology. 2011;85(2):1025-35.
24. Hyde JL, Chen R, Trobaugh DW, Diamond MS, Weaver SC, Klimstra WB, et al. The 5' and 3' ends of alphavirus RNAs – non-coding is not non-functional. Virus Research. 2015;206:99-107.
25. Infante RE, Wang ML, Radhakrishnan A, Kwon HJ, Brown MS, Goldstein JL. NPC2 facilitates bidirectional transfer of cholesterol between NPC1 and lipid bilayers, a step in cholesterol egress from lysosomes. Proceedings of the National Academy of Sciences. 2008;105(40):15287-92.

26. Herbert AS, Davidson C, Kuehne AI, Bakken R, Braigen SZ, Gunn KE, *et al.* Niemann-pick C1 is essential for ebolavirus replication and pathogenesis in vivo. *mBio*. 2015;6(3):e00565-15.
27. Carette JE, Raaben M, Wong AC, Herbert AS, Obernosterer G, Mulherkar N, *et al.* Ebola virus entry requires the cholesterol transporter Niemann-Pick C1. *Nature*. 2011;477(7364):340-3.
28. Jupatanakul N, Sim S, Dimopoulos G. *Aedes aegypti* ML and Niemann-Pick type C family members are agonists of dengue virus infection. *Developmental & Comparative Immunology*. 2014;43(1):1-9.
29. Tang Y, Leao IC, Coleman EM, Broughton RS, Hildreth JEK. Deficiency of niemann-pick type C-1 protein impairs release of human immunodeficiency virus type 1 and results in Gag accumulation in late endosomal/lysosomal compartments. *Journal of Virology*. 2009;83(16):7982-95.
30. Wichit S, Hamel R, Bernard E, Talignani L, Diop F, Ferraris P, *et al.* Imipramine Inhibits Chikungunya Virus Replication in Human Skin Fibroblasts through Interference with Intracellular Cholesterol Trafficking. *Scientific reports*. 2017;7(1):3145-.
31. Lopez-Herrera G, Vargas-Hernandez A, Gonzalez-Serrano ME, Berron-Ruiz L, Rodriguez-Alba JC, Espinosa-Rosales F, *et al.* Bruton's tyrosine kinase--an integral protein of B cell development that also has an essential role in the innate immune system. *Journal of Leukocyte Biology*. 2014;95(2):243-50.
32. Bao Y, Zheng J, Han C, Jin J, Han H, Liu Y, *et al.* Tyrosine kinase Btk is required for NK cell activation. *The Journal of biological chemistry*. 2012;287(28):23769-78.
33. Assunção-Miranda I, Cruz-Oliveira C, Da Poian AT. Molecular Mechanisms Involved in the Pathogenesis of Alphavirus-Induced Arthritis. *BioMed Research International*. 2013;2013:973516.
34. Amdekar S, Parashar D, Alagarasu K. Chikungunya Virus-Induced Arthritis: Role of Host and Viral Factors in the Pathogenesis. *Viral Immunol*. 2017;30(10):691-702.
35. Shinohara M, Koga T, Okamoto K, Sakaguchi S, Arai K, Yasuda H, *et al.* Tyrosine kinases Btk and Tec regulate osteoclast differentiation by linking RANK and ITAM signals. *Cell*. 2008;132(5):794-806.
36. Florence JM, Krupa A, Booshehri LM, Davis SA, Matthay MA, Kurdowska AK. Inhibiting Bruton's tyrosine kinase rescues mice from lethal influenza-induced

acute lung injury. American journal of physiology Lung Cellular and Molecular Physiology. 2018;315(1):L52-18.

Appendices

Appendix-I: List of Primers

Primer	Sequence
CHIKV_E1_FOR	AAGAGCGATGAACTGCGCCGTAG
CHIKV_E1_REV	CTGGTACCTCGCATGACATGTC
AALF004300_D8_FOR	CACGAACCGAACGGATATG
AALF004300_D8_REV	TTCTGCTGCTGCTGTTG
AALF008354_D8_FOR	CGTGTCTTCTACCAAATCC
AALF008354_D8_REV	TCTTGCCTTCAGCTTAC
AALF011899_D8_FOR	GCTCGATGCGAGATAAGAAG
AALF011899_D8_REV	CTCGGTATCTTCAACGGTAATC
AALF012324_D8_FOR	GGCACCATCAATAGGGTAAC
AALF012324_D8_REV	CCTTCGAGCCAAACTCTATG
AALF012634_D8_FOR	CGGGAGATTTACGAGGTTTC
AALF012634_D8_REV	GCGTTCTTCCCTTCATCTC
AALF016505_D8_FOR	GGAATGTGGCAATGTGAATAC
AALF016505_D8_REV	GATCACTCGATCGGCATAAG
AALF016704_D8_FOR	ACTGACGTTCCCTTCAAAC
AALF016704_D8_REV	GCTCGATCGACTTCATCTTC
AALF021910_D8_FOR	GTGAACCTCATTCCGGATAC
AALF021910_D8_REV	CTTTCACCTCGGTCCAATC
AALF023547_D8_FOR	GAACCATCGTGGAAGAAGAG
AALF023547_D8_REV	CATCAGCTTCAGAGCCATATC
AALF025245_D8_FOR	CGGAGAAGCAGTTGGTATTC
AALF025245_D8_REV	CGATCGAGTGGAAGTCTTTG
AALF026574_D8_FOR	GAGGTGCTCGTTACATCTTG
AALF026574_D8_REV	GCAATGGGTGGTACCTTATC
DN129476_D8_FOR	GTGCTCTTCCGATCTTTCTC
DN129476_D8_REV	GAAGGTATCGTCGAGTTCAAG
DN131737_D8_FOR	GGGTCTTGAGCGAATGTATC
DN131737_D8_REV	TGCCGCATACTTGTAGTTATC

DN131885_D8_FOR	ACTCTGGTGTACCCTTATCC
DN131885_D8_REV	TTCCTAGTGGTAGTGATCGAG
AALF020406_D2_FOR	GTACGATAGGACAGCCAAAC
AALF020406_D2_REV	GTCTCCTTTCTCCCGATTTG
DN102975_D2_FOR	GAATTGTGCGTACGATTTGG
DN102975_D2_REV	GGTGCATGGTGTATGAAATTG
DN109582_D2_FOR	GGAGAAGAGCTATCCACCTATC
DN109582_D2_REV	TCCCTTGCACACTGAAAC
DN109663_D2_FOR	TCCGTTACTTCGGTTGATTG
DN109663_D2_REV	ATGCCACAGATCCTGAAAC
DN110186_D2_FOR	CATGGATCAACTCGGAGATTC
DN110186_D2_REV	ATCTCCTCTTCCCGCTTAC
DN110327_D2_FOR	ACACACGCCTCGCTGATATG
DN110327_D2_REV	AAGATCAATAGGGAAATTTCAAAGC
DN110556_D2_FOR	CATCGCCTACTACGTGATTC
DN110556_D2_REV	GCAAATGACCGTCCAAATG
DN46100_D2_FOR	CACGCGAATACGTTAAATTCC
DN46100_D2_REV	ATTTTCGCAGCACAATTTTCAG
18srRNA_Fwd	CGGCTACCACATCCAAGGAA
18srRNA_Rev	GCTGGAATTACCGCGGCT
Aegypti_D2_Mucin_qPCR_FOR	CTCAAACGGAGACCTCAAGC
Aegypti_D2_Mucin_qPCR_REV	TGGGTTCGTCTCGGTAGAATC
Aegypti_D2_NPCV2_qPCR_FOR	TAGTTCCGGTCAAGGAATGC
Aegypti_D2_NPCV2_qPCR_REV	TCGCTGACACTGAAGTCCAC
Aegypti_D2_DN110556_qPCR_FOR	CTGAAATGTCCAGGATGTGC
Aegypti_D2_DN110556_qPCR_REV	GCATTTCCGGTCAGCTTCTTC
Aegypti_D2_DN110186_qPCR_FOR	ACGGAATTCACCCTGAAGTG
Aegypti_D2_DN110186_qPCR_REV	CCAGCTGACCTGGTACTTGC
Aegypti_D2_DN102975_qPCR_FOR	TAGCGTTTGGGAGCACCTAC
Aegypti_D2_DN102975_qPCR_REV	CGACAGATTCACGTGTTTGG
Aegypti_D2_DN46100_qPCR_FOR	TGAACGATCCGGACTTTAGC
Aegypti_D2_DN46100_qPCR_REV	GCCACAGCATTAGGAGAAC
Aegypti_D2_DN110327_qPCR_FOR	ACAGGCACCTGGTGGTAAAG
Aegypti_D2_DN110327_qPCR_REV	CGAATGGCTTCTTCTGGAAC

AALF004300_D8_FOR	CACGAACCGAACGGATATG
AALF004300_D8_REV	TTCTGCTGCTGCTGTTG
AALF008354_D8_FOR	CGTGCCTTCTACCAAATCC
AALF008354_D8_REV	TCTTGCGCTTCAGCTTAC
AALF011899_D8_FOR	GCTCGATGCGAGATAAGAAG
AALF011899_D8_REV	CTCGGTATCTTCAACGGTAATC
AALF012324_D8_FOR	GGCACCATCAATAGGGTAAC
AALF012324_D8_REV	CCTTCGAGCCAAACTCTATG
AALF012634_D8_FOR	CGGGAGATTTACGAGGTTTC
AALF012634_D8_REV	GCGTTCCTCCCTTCATCTC
AALF016505_D8_FOR	GGAATGTGGCAATGTGAATAC
AALF016505_D8_REV	GATCACTCGATCGGCATAAG
AALF016704_D8_FOR	ACTGACGTTCCCTTCAAAC
AALF016704_D8_REV	GCTCGATCGACTTCATCTTC
AALF021910_D8_FOR	GTGAACCTCATTCCGGATAC
AALF021910_D8_REV	CTTTCACCTCGGTCCAATC
AALF023547_D8_FOR	GAACCATCGTGGGAAGAAGAG
AALF023547_D8_REV	CATCAGCTTCAGAGCCATATC
AALF025245_D8_FOR	CGGAGAAGCAGTTGGTATTC
AALF025245_D8_REV	CGATCGAGTGGAAGTCTTTG
AALF026574_D8_FOR	GAGGTGCTCGTTACATCTTG
AALF026574_D8_REV	GCAATGGGTGGTACCTTATC
DN129476_D8_FOR	GTGCTCTTCCGATCTTTCTC
DN129476_D8_REV	GAAGGTATCGTCGAGTTCAAG
DN131737_D8_FOR	GGGTCTTGAGCGAATGTATC
DN131737_D8_REV	TGCCGCATACTTGTAGTTATC
DN131885_D8_FOR	ACTCTGGTGTACCCTTATCC
DN131885_D8_REV	TTCCTAGTGGTAGTGATCGAG
BTKi_dsRNA_FWD	<i>GTCATAATACGACTCACTATA</i>
	<i>GGGAGATGTTACGATTTGAGCTTCG</i>
BTKi_dsRNA_REV	<i>GTCATAATACGACTCACTATA</i>
	<i>GGGAGAAGATCTGGGTAGGCATCACG</i>

Appendix-II: List of differentially expressed genes D2_DESeq2

GeneID	Base mean	log2(FC)	StdErr	Wald-Stats	P-value	P-adj
AALF020406	216.7005	-5.56282	0.685547	-8.11442	4.88E-16	3.93E-12
AALF012050	1919.848	4.968855	0.636043	7.81214	5.62E-15	2.26E-11
AALF005925	207.2692	3.431226	0.651706	5.264988	1.40E-07	0.000376
AALF016850	231.3505	-3.54486	0.725066	-4.88902	1.01E-06	0.002041
AALF015699	7062.463	-1.42751	0.300412	-4.75183	2.02E-06	0.002676
AALF029854	1722.729	-2.01367	0.423985	-4.74939	2.04E-06	0.002676
AALF027085	111.1469	3.373469	0.714286	4.722851	2.33E-06	0.002676
AALF020983	177.9063	2.950483	0.633377	4.658338	3.19E-06	0.00321
AALF025203	2013.3	2.431263	0.532464	4.566061	4.97E-06	0.004448
AALF023645	111.604	3.059275	0.68506	4.465701	7.98E-06	0.006429
AALF001554	621.3091	-2.5475	0.574526	-4.4341	9.25E-06	0.006771
AALF015302	90.97449	3.104544	0.707611	4.387361	1.15E-05	0.007702
AALF027756	87.29894	-3.15954	0.725976	-4.35212	1.35E-05	0.008355
AALF013306	11931.84	-1.33999	0.310066	-4.32162	1.55E-05	0.008913
AALF004977	74.09452	-3.04832	0.726769	-4.19435	2.74E-05	0.014697
AALF027007	104.2738	-3.02727	0.726324	-4.16794	3.07E-05	0.015476
AALF019954	824.7693	2.425737	0.601446	4.033177	5.50E-05	0.026077
AALF018103	231.8302	2.538813	0.631615	4.019556	5.83E-05	0.026096
AALF016689	108.2655	2.779222	0.701054	3.964346	7.36E-05	0.030833
AALF019776	171.4389	-2.86038	0.723238	-3.95496	7.65E-05	0.030833
AALF011874	1818.249	-1.79901	0.459684	-3.91357	9.09E-05	0.034887
AALF006972	2730.712	1.85584	0.483838	3.835662	0.000125	0.045856
AALF028549	98.38542	2.674245	0.70129	3.813325	0.000137	0.047312
AALF002386	5133.129	1.815648	0.476986	3.806499	0.000141	0.047312
AALF002948	78.91971	2.741821	0.724579	3.784018	0.000154	0.049727

Appendix-III: List of differentially expressed genes D2_edgeR

	sampleA	sampleB	logFC	logCPM	PValue	FDR
TRINITY_DN109499_c0_g1_i3	Infected	Control	-12.7616	8.430899	2.02E-05	0.190876
TRINITY_DN110715_c0_g3_i4	Infected	Control	-11.8975	7.573359	3.31E-05	0.190876
TRINITY_DN110618_c0_g4_i1	Infected	Control	-9.66854	7.9446	4.61E-05	0.190876
TRINITY_DN110359_c0_g2_i1	Infected	Control	13.73885	9.987767	7.31E-05	0.190876
TRINITY_DN110550_c0_g1_i2	Infected	Control	-11.2601	6.944009	7.98E-05	0.190876
TRINITY_DN109503_c0_g1_i4	Infected	Control	-11.2246	6.909069	9.75E-05	0.190876
TRINITY_DN110110_c1_g1_i3	Infected	Control	-11.6396	7.318323	0.000118	0.190876
TRINITY_DN109499_c0_g1_i4	Infected	Control	-11.348	7.030502	0.000131	0.190876
TRINITY_DN110262_c1_g1_i1	Infected	Control	-11.0003	6.688622	0.000136	0.190876
TRINITY_DN105366_c0_g2_i1	Infected	Control	-11.3263	7.009193	0.000212	0.268567
TRINITY_DN109947_c0_g1_i1	Infected	Control	-12.7254	8.394923	0.000267	0.307055
TRINITY_DN106892_c0_g2_i1	Infected	Control	-9.36271	9.497906	0.000351	0.370504
TRINITY_DN102795_c0_g1_i1	Infected	Control	-11.0194	10.88318	0.00044	0.42887
TRINITY_DN110978_c0_g1_i1	Infected	Control	-10.5981	6.294992	0.000506	0.458151
TRINITY_DN110618_c0_g4_i4	Infected	Control	-7.60732	10.99402	0.000638	0.535413
TRINITY_DN98669_c0_g1_i1	Infected	Control	-10.4076	6.109418	0.000716	0.535413
TRINITY_DN110626_c1_g2_i2	Infected	Control	-8.08592	13.67002	0.000719	0.535413
TRINITY_DN110668_c0_g1_i4	Infected	Control	8.991747	9.041062	0.000783	0.550719
TRINITY_DN110359_c0_g1_i1	Infected	Control	9.482928	8.968226	0.000872	0.581177
TRINITY_DN7727_c0_g1_i1	Infected	Control	-9.96207	5.678356	0.001151	0.706028
TRINITY_DN66099_c0_g1_i1	Infected	Control	-9.96078	5.677108	0.00117	0.706028
TRINITY_DN110644_c0_g2_i4	Infected	Control	11.15353	7.41591	0.001346	0.775103

TRINITY_DN109361_c0_g1_i1	Infected	Control	-8.35051	5.936438	0.001447	0.797185
TRINITY_DN110615_c1_g2_i3	Infected	Control	-6.7219	12.12704	0.001797	0.948666
TRINITY_DN70601_c0_g1_i1	Infected	Control	-9.79709	5.519885	0.002032	1
TRINITY_DN107541_c0_g3_i1	Infected	Control	-10.0542	5.767183	0.002079	1
TRINITY_DN109864_c0_g3_i4	Infected	Control	-9.63972	5.369456	0.002412	1
TRINITY_DN110340_c1_g1_i1	Infected	Control	10.95759	10.46041	0.002537	1
TRINITY_DN106892_c0_g1_i1	Infected	Control	-8.3369	8.53023	0.002691	1
TRINITY_DN109947_c1_g2_i1	Infected	Control	-9.55996	5.293497	0.00279	1
TRINITY_DN71695_c0_g2_i1	Infected	Control	-9.98845	7.427299	0.003052	1
TRINITY_DN110349_c1_g1_i1	Infected	Control	-9.53068	5.265663	0.003112	1
TRINITY_DN110698_c0_g4_i1	Infected	Control	9.989153	10.38533	0.003431	1
TRINITY_DN109913_c0_g1_i1	Infected	Control	-9.46198	5.200464	0.003942	1
TRINITY_DN109965_c0_g1_i1	Infected	Control	11.1866	10.71399	0.003953	1
TRINITY_DN110478_c1_g8_i1	Infected	Control	10.546	6.816766	0.004061	1
TRINITY_DN110734_c0_g3_i6	Infected	Control	8.469432	7.119743	0.004169	1
TRINITY_DN101711_c0_g1_i1	Infected	Control	-9.53386	5.26871	0.004228	1
TRINITY_DN110482_c0_g1_i2	Infected	Control	-9.42264	5.163213	0.004661	1
TRINITY_DN110618_c0_g5_i2	Infected	Control	-7.86449	5.368206	0.004742	1
TRINITY_DN107831_c0_g1_i1	Infected	Control	-7.59204	10.73823	0.004821	1
TRINITY_DN110961_c0_g1_i1	Infected	Control	-8.1769	5.76101	0.005107	1
TRINITY_DN110478_c1_g8_i7	Infected	Control	9.998378	6.280422	0.00581	1
TRINITY_DN110581_c0_g1_i1	Infected	Control	9.839772	6.1261	0.006083	1
TRINITY_DN110623_c0_g1_i6	Infected	Control	-7.85675	5.359162	0.006151	1
TRINITY_DN110632_c1_g1_i1	Infected	Control	8.001935	6.660377	0.006763	1
TRINITY_DN70511_c0_g1_i1	Infected	Control	-8.9438	6.400187	0.007159	1
TRINITY_DN110359_c0_g3_i2	Infected	Control	7.160582	8.688477	0.007316	1
TRINITY_DN110536_c1_g2_i1	Infected	Control	-9.27195	5.02097	0.00734	1

TRINITY_DN110294_c0_g2_i1	Infected	Control	9.83506	6.121448	0.007711	1
TRINITY_DN110096_c1_g1_i2	Infected	Control	-6.95361	11.30214	0.007838	1
TRINITY_DN110535_c0_g3_i1	Infected	Control	-9.26501	5.014488	0.007867	1
TRINITY_DN110208_c0_g2_i2	Infected	Control	9.556247	5.850988	0.00799	1
TRINITY_DN110064_c0_g3_i1	Infected	Control	-7.4586	9.790717	0.008066	1
TRINITY_DN110615_c1_g1_i1	Infected	Control	-9.22937	4.980935	0.008186	1
TRINITY_DN106957_c0_g2_i1	Infected	Control	9.548651	5.843636	0.008565	1
TRINITY_DN109371_c0_g1_i1	Infected	Control	8.71272	10.90362	0.009033	1
TRINITY_DN102757_c0_g1_i1	Infected	Control	-9.16505	4.920623	0.009716	1
TRINITY_DN109482_c0_g1_i2	Infected	Control	-5.08001	7.442615	0.010561	1
TRINITY_DN108974_c1_g1_i1	Infected	Control	-9.1188	4.877328	0.011452	1
TRINITY_DN110340_c1_g1_i4	Infected	Control	-8.4797	5.948287	0.011716	1
TRINITY_DN110698_c0_g4_i2	Infected	Control	10.09598	6.375815	0.011763	1
TRINITY_DN82039_c0_g1_i1	Infected	Control	-9.14783	4.904554	0.011865	1
TRINITY_DN107626_c1_g1_i1	Infected	Control	-9.09941	4.8592	0.012388	1
TRINITY_DN109177_c0_g1_i2	Infected	Control	10.12008	10.85761	0.012657	1
TRINITY_DN109466_c0_g1_i1	Infected	Control	11.04908	7.312752	0.012914	1
TRINITY_DN110096_c1_g1_i5	Infected	Control	-5.75002	12.12155	0.013141	1
TRINITY_DN71695_c0_g1_i1	Infected	Control	-5.79248	6.926392	0.013334	1
TRINITY_DN110447_c0_g4_i5	Infected	Control	-4.73961	10.83299	0.01335	1
TRINITY_DN110327_c1_g2_i1	Infected	Control	-9.07566	4.837083	0.013518	1
TRINITY_DN110644_c0_g1_i4	Infected	Control	-7.51061	5.029009	0.013529	1
TRINITY_DN108275_c0_g1_i2	Infected	Control	-9.04557	4.809027	0.014382	1
TRINITY_DN30821_c0_g1_i1	Infected	Control	-9.044	4.807534	0.014436	1
TRINITY_DN109837_c0_g3_i1	Infected	Control	-9.05618	4.818862	0.014529	1
TRINITY_DN110054_c0_g2_i4	Infected	Control	-9.07522	4.836597	0.014973	1
TRINITY_DN109298_c0_g2_i1	Infected	Control	-9.02046	4.785618	0.015485	1

TRINITY_DN110226_c0_g1_i1	Infected	Control	9.153406	5.463419	0.015567	1
TRINITY_DN46100_c0_g1_i1	Infected	Control	-9.0398	4.803693	0.016024	1
TRINITY_DN93544_c0_g1_i1	Infected	Control	-7.35726	4.985668	0.016188	1
TRINITY_DN107528_c0_g1_i1	Infected	Control	10.04045	6.321596	0.016215	1
TRINITY_DN110206_c0_g1_i3	Infected	Control	6.99942	6.513863	0.016342	1
TRINITY_DN34439_c0_g1_i1	Infected	Control	-8.99019	4.75749	0.016805	1
TRINITY_DN110609_c0_g2_i1	Infected	Control	7.237429	5.916179	0.016972	1
TRINITY_DN110359_c0_g3_i3	Infected	Control	6.435098	6.863692	0.017189	1
TRINITY_DN109582_c0_g2_i2	Infected	Control	6.293482	7.511639	0.01757	1
TRINITY_DN110629_c0_g1_i12	Infected	Control	-8.98053	4.748479	0.017602	1
TRINITY_DN109591_c1_g3_i1	Infected	Control	-6.31606	5.150155	0.017701	1
TRINITY_DN103661_c0_g1_i2	Infected	Control	9.095576	5.408016	0.017739	1
TRINITY_DN109587_c0_g1_i2	Infected	Control	9.869614	6.155106	0.017753	1
TRINITY_DN109503_c0_g1_i1	Infected	Control	-8.98308	4.750845	0.017767	1
TRINITY_DN105467_c0_g2_i1	Infected	Control	9.794479	6.082038	0.018058	1
TRINITY_DN107366_c0_g1_i1	Infected	Control	-8.96343	4.73262	0.018169	1
TRINITY_DN110715_c0_g1_i1	Infected	Control	-7.33712	4.980619	0.018271	1
TRINITY_DN93300_c0_g1_i1	Infected	Control	9.091768	5.404624	0.01887	1
TRINITY_DN110335_c0_g1_i1	Infected	Control	7.436466	6.964125	0.018877	1
TRINITY_DN111483_c0_g1_i1	Infected	Control	-8.94651	4.716971	0.018884	1
TRINITY_DN110048_c0_g2_i2	Infected	Control	9.893599	6.178449	0.019109	1
TRINITY_DN107799_c0_g1_i1	Infected	Control	-8.93759	4.708696	0.019409	1
TRINITY_DN108666_c0_g1_i2	Infected	Control	9.4239	9.851114	0.019411	1
TRINITY_DN110555_c0_g1_i4	Infected	Control	10.67724	6.945991	0.019511	1
TRINITY_DN110389_c3_g1_i3	Infected	Control	-8.98271	4.750472	0.019874	1
TRINITY_DN108374_c0_g1_i2	Infected	Control	10.37738	6.651305	0.019988	1
TRINITY_DN109529_c0_g1_i2	Infected	Control	-8.93732	4.708474	0.020288	1

TRINITY_DN109797_c0_g1_i1	Infected	Control	-8.97209	4.740601	0.020904	1
TRINITY_DN109479_c0_g3_i1	Infected	Control	10.24209	6.518662	0.020993	1
TRINITY_DN94065_c0_g2_i1	Infected	Control	-8.93402	4.705428	0.020995	1
TRINITY_DN18793_c0_g1_i1	Infected	Control	-8.94275	4.713392	0.021348	1
TRINITY_DN109483_c0_g1_i1	Infected	Control	8.969289	5.287781	0.02184	1
TRINITY_DN110564_c0_g3_i4	Infected	Control	11.8454	8.101679	0.022012	1
TRINITY_DN108555_c0_g1_i1	Infected	Control	-8.90675	4.680084	0.022025	1
TRINITY_DN110299_c3_g7_i2	Infected	Control	9.174141	5.483453	0.022133	1
TRINITY_DN108042_c0_g2_i1	Infected	Control	8.975135	5.293381	0.022339	1
TRINITY_DN110478_c1_g8_i4	Infected	Control	6.610936	6.654722	0.022912	1
TRINITY_DN110384_c0_g2_i4	Infected	Control	10.09482	6.374674	0.02327	1
TRINITY_DN109700_c0_g1_i2	Infected	Control	8.949018	5.268452	0.023654	1
TRINITY_DN109594_c0_g3_i1	Infected	Control	8.933362	5.25368	0.023751	1
TRINITY_DN102147_c0_g1_i1	Infected	Control	-6.66549	5.091573	0.024044	1
TRINITY_DN108353_c0_g1_i1	Infected	Control	8.974094	5.292517	0.024065	1
TRINITY_DN107988_c0_g1_i1	Infected	Control	10.09141	6.371332	0.024261	1
TRINITY_DN109115_c0_g2_i1	Infected	Control	10.03894	6.320102	0.024517	1
TRINITY_DN68277_c0_g1_i1	Infected	Control	-8.86361	4.640263	0.024552	1
TRINITY_DN110276_c0_g1_i4	Infected	Control	9.282878	5.587416	0.024955	1
TRINITY_DN107618_c0_g2_i1	Infected	Control	-8.86667	4.64304	0.025032	1
TRINITY_DN106868_c0_g1_i1	Infected	Control	-8.87202	4.64808	0.025365	1
TRINITY_DN110505_c0_g1_i1	Infected	Control	-4.46245	6.521945	0.025825	1
TRINITY_DN109849_c0_g1_i2	Infected	Control	6.006359	6.446461	0.025962	1
TRINITY_DN110141_c0_g2_i2	Infected	Control	6.081557	5.650486	0.026158	1
TRINITY_DN110368_c2_g3_i2	Infected	Control	-8.83832	4.616927	0.026426	1
TRINITY_DN109578_c1_g1_i1	Infected	Control	-4.62029	7.946849	0.026814	1
TRINITY_DN110544_c0_g1_i1	Infected	Control	6.289405	5.871812	0.026868	1

TRINITY_DN109280_c0_g1_i1	Infected	Control	-8.83861	4.617157	0.027004	1
TRINITY_DN110368_c2_g1_i3	Infected	Control	-5.16371	6.305765	0.027163	1
TRINITY_DN109743_c0_g1_i1	Infected	Control	-8.83367	4.612613	0.027252	1
TRINITY_DN107936_c1_g1_i1	Infected	Control	-8.85427	4.631719	0.02738	1
TRINITY_DN106859_c0_g2_i1	Infected	Control	-8.8287	4.608054	0.02743	1
TRINITY_DN110058_c0_g1_i3	Infected	Control	-8.83195	4.611082	0.027474	1
TRINITY_DN110673_c0_g1_i5	Infected	Control	8.938259	5.258143	0.027663	1
TRINITY_DN110431_c1_g1_i7	Infected	Control	-7.40144	5.63649	0.027811	1
TRINITY_DN110536_c1_g2_i2	Infected	Control	8.853601	5.17801	0.027847	1
TRINITY_DN110335_c0_g1_i2	Infected	Control	-8.82769	4.607171	0.027878	1
TRINITY_DN109430_c0_g2_i2	Infected	Control	6.774976	5.472487	0.028048	1
TRINITY_DN109818_c0_g3_i1	Infected	Control	6.831968	5.559898	0.028409	1
TRINITY_DN110348_c2_g1_i1	Infected	Control	-3.88229	9.090205	0.028522	1
TRINITY_DN12857_c0_g2_i1	Infected	Control	-8.83236	4.611502	0.028605	1
TRINITY_DN103631_c0_g1_i1	Infected	Control	-8.83397	4.612843	0.028989	1
TRINITY_DN108633_c1_g2_i1	Infected	Control	-8.83024	4.609549	0.029272	1
TRINITY_DN110447_c0_g4_i6	Infected	Control	9.167764	5.477299	0.029333	1
TRINITY_DN110729_c1_g4_i1	Infected	Control	-8.82128	4.601287	0.029415	1
TRINITY_DN108758_c0_g2_i1	Infected	Control	-8.82953	4.608898	0.029482	1
TRINITY_DN109657_c0_g2_i1	Infected	Control	9.159982	5.469867	0.029706	1
TRINITY_DN59519_c0_g1_i1	Infected	Control	6.909128	10.85333	0.029871	1
TRINITY_DN110632_c1_g1_i7	Infected	Control	4.829759	8.495025	0.030089	1
TRINITY_DN57758_c0_g1_i1	Infected	Control	-8.81699	4.59735	0.030476	1
TRINITY_DN110404_c0_g1_i2	Infected	Control	5.854872	6.299851	0.030532	1
TRINITY_DN110596_c0_g1_i6	Infected	Control	8.177442	10.48818	0.030781	1
TRINITY_DN93575_c0_g2_i1	Infected	Control	9.726356	6.015839	0.030961	1
TRINITY_DN95908_c0_g2_i1	Infected	Control	8.832378	5.157822	0.03099	1

TRINITY_DN103962_c0_g1_i1	Infected	Control	9.891431	6.176274	0.031209	1
TRINITY_DN110066_c0_g5_i1	Infected	Control	-8.77976	4.563049	0.03146	1
TRINITY_DN110186_c0_g1_i2	Infected	Control	8.823672	5.149679	0.031707	1
TRINITY_DN111536_c0_g1_i1	Infected	Control	-8.80454	4.585744	0.031725	1
TRINITY_DN110556_c0_g2_i1	Infected	Control	8.843942	5.168931	0.031835	1
TRINITY_DN104438_c0_g1_i1	Infected	Control	8.905135	5.226899	0.03199	1
TRINITY_DN67465_c0_g1_i1	Infected	Control	-8.77154	4.555424	0.032862	1
TRINITY_DN107477_c0_g1_i1	Infected	Control	-8.75188	4.537498	0.035011	1
TRINITY_DN110558_c6_g1_i1	Infected	Control	8.486349	7.171751	0.035082	1
TRINITY_DN110582_c0_g1_i4	Infected	Control	4.915382	8.292741	0.035569	1
TRINITY_DN110751_c0_g8_i2	Infected	Control	9.555462	5.850287	0.036044	1
TRINITY_DN110081_c0_g1_i2	Infected	Control	5.875045	5.995031	0.036213	1
TRINITY_DN110632_c1_g2_i8	Infected	Control	5.558413	7.580493	0.036329	1
TRINITY_DN106947_c0_g1_i1	Infected	Control	9.658076	5.949607	0.036584	1
TRINITY_DN110582_c0_g3_i1	Infected	Control	10.78809	7.055172	0.036659	1
TRINITY_DN110492_c2_g4_i1	Infected	Control	-8.75208	4.537523	0.036772	1
TRINITY_DN108203_c0_g2_i1	Infected	Control	-5.53849	5.406491	0.036818	1
TRINITY_DN108635_c0_g3_i1	Infected	Control	8.794653	5.12213	0.036995	1
TRINITY_DN110404_c0_g1_i5	Infected	Control	8.712048	5.044282	0.037186	1
TRINITY_DN98700_c0_g1_i1	Infected	Control	-3.95773	7.611426	0.037506	1
TRINITY_DN99324_c0_g1_i1	Infected	Control	-8.71412	4.502882	0.037591	1
TRINITY_DN110040_c0_g2_i2	Infected	Control	8.691967	5.025354	0.03804	1
TRINITY_DN110626_c1_g2_i3	Infected	Control	-5.51192	12.62003	0.038159	1
TRINITY_DN110611_c0_g1_i2	Infected	Control	8.800087	5.127212	0.03822	1
TRINITY_DN102975_c0_g1_i1	Infected	Control	-8.70164	4.491396	0.038288	1
TRINITY_DN105968_c0_g1_i1	Infected	Control	-8.71027	4.499373	0.038364	1
TRINITY_DN110427_c1_g3_i1	Infected	Control	-8.69976	4.489742	0.038862	1

TRINITY_DN110587_c0_g1_i2	Infected	Control	6.056915	5.649862	0.038974	1
TRINITY_DN110711_c2_g5_i2	Infected	Control	-8.70718	4.496559	0.039262	1
TRINITY_DN110388_c3_g1_i1	Infected	Control	8.936717	5.256943	0.039446	1
TRINITY_DN109717_c0_g2_i1	Infected	Control	-8.69185	4.482422	0.039715	1
TRINITY_DN60479_c0_g2_i1	Infected	Control	-8.68323	4.474579	0.040025	1
TRINITY_DN107374_c0_g1_i1	Infected	Control	8.672526	5.007057	0.040128	1
TRINITY_DN110714_c4_g1_i1	Infected	Control	-8.68683	4.477908	0.040308	1
TRINITY_DN17942_c0_g1_i1	Infected	Control	9.678862	5.96975	0.040893	1
TRINITY_DN110083_c0_g2_i2	Infected	Control	-3.46395	9.523147	0.040965	1
TRINITY_DN108909_c1_g5_i1	Infected	Control	8.657743	4.99312	0.042061	1
TRINITY_DN109499_c0_g1_i5	Infected	Control	-5.28902	8.883271	0.042289	1
TRINITY_DN110708_c0_g1_i6	Infected	Control	-3.53987	12.92877	0.042794	1
TRINITY_DN110461_c1_g4_i1	Infected	Control	-7.12678	4.665034	0.042935	1
TRINITY_DN109674_c0_g2_i1	Infected	Control	-8.67286	4.465022	0.043047	1
TRINITY_DN110708_c0_g1_i5	Infected	Control	6.566762	9.285918	0.043609	1
TRINITY_DN110791_c0_g1_i1	Infected	Control	-8.63585	4.431293	0.044583	1
TRINITY_DN94102_c0_g2_i1	Infected	Control	9.388931	5.689582	0.044584	1
TRINITY_DN107926_c0_g1_i1	Infected	Control	8.700916	5.033715	0.045406	1
TRINITY_DN109837_c0_g2_i1	Infected	Control	-8.62526	4.421687	0.045469	1
TRINITY_DN109985_c1_g1_i2	Infected	Control	5.365848	6.185328	0.045714	1
TRINITY_DN108118_c0_g2_i1	Infected	Control	-6.95359	4.630653	0.045839	1
TRINITY_DN109159_c0_g1_i1	Infected	Control	-8.6228	4.419462	0.045876	1
TRINITY_DN110410_c0_g2_i3	Infected	Control	8.6888	5.022249	0.045949	1
TRINITY_DN110663_c0_g2_i3	Infected	Control	9.293455	5.597688	0.046509	1
TRINITY_DN110627_c0_g2_i1	Infected	Control	8.239354	10.93808	0.047002	1
TRINITY_DN109180_c0_g1_i2	Infected	Control	-5.11271	5.601466	0.047002	1
TRINITY_DN41428_c0_g1_i1	Infected	Control	-8.60418	4.402533	0.047435	1

TRINITY_DN110369_c0_g2_i1	Infected	Control	5.884735	5.486452	0.047537	1
TRINITY_DN108287_c0_g1_i1	Infected	Control	-5.43029	5.308833	0.047609	1
TRINITY_DN102237_c0_g3_i1	Infected	Control	-8.61753	4.414754	0.047841	1
TRINITY_DN67064_c0_g1_i1	Infected	Control	-8.60881	4.406786	0.047852	1
TRINITY_DN110505_c0_g1_i5	Infected	Control	4.933306	6.566355	0.048208	1
TRINITY_DN93199_c0_g1_i1	Infected	Control	-8.60453	4.40278	0.048501	1
TRINITY_DN108621_c1_g1_i2	Infected	Control	-8.60466	4.403037	0.048702	1
TRINITY_DN101006_c0_g2_i1	Infected	Control	-8.63807	4.433502	0.048889	1
TRINITY_DN107887_c0_g1_i1	Infected	Control	9.187912	5.496523	0.04911	1
TRINITY_DN14104_c0_g1_i1	Infected	Control	-8.59036	4.389956	0.049153	1
TRINITY_DN109663_c0_g2_i1	Infected	Control	-8.61033	4.408028	0.049355	1
TRINITY_DN66460_c0_g1_i1	Infected	Control	8.590316	4.929804	0.049468	1
TRINITY_DN95571_c0_g1_i1	Infected	Control	-6.94967	4.627481	0.049522	1
TRINITY_DN110576_c0_g1_i6	Infected	Control	-6.22733	4.61703	0.049842	1

Appendix-IV: List of differentially expressed genes D8_DESeq2

GeneID	Base mean	log2(FC)	StdErr	Wald-Stats	P-value	P-adj
AALF003125	309.0048	-6.66141	0.67967	-9.80093	1.12E-22	1.08E-18
AALF029552	8380.408	-2.35	0.33893	-6.93356	4.10E-12	1.99E-08
AALF025212	3667.483	-2.39687	0.35417	-6.76755	1.31E-11	4.23E-08
AALF016811	209.9323	4.56912	0.71365	6.402476	1.53E-10	3.70E-07
AALF008821	123.3598	-4.65933	0.75399	-6.17957	6.43E-10	1.24E-06
AALF010140	254.9795	4.38865	0.72404	6.061328	1.35E-09	2.18E-06
AALF005487	112.1111	-4.5298	0.76903	-5.89025	3.86E-09	5.33E-06
AALF008822	2089.474	-2.19608	0.40992	-5.35738	8.44E-08	0.0001
AALF029926	49567.17	-1.60162	0.30735	-5.21106	1.88E-07	0.0002
AALF022468	148.3781	3.81626	0.74179	5.144653	2.68E-07	0.00026
AALF026213	142.0296	3.71553	0.74532	4.985161	6.19E-07	0.00055
AALF019949	82.3505	-3.82794	0.7777	-4.92214	8.56E-07	0.00069
AALF020653	105.2114	-3.71868	0.75987	-4.89383	9.89E-07	0.00074
AALF022699	1523.225	-2.00222	0.4146	-4.82931	1.37E-06	0.00085
AALF012050	208.9281	3.41336	0.70741	4.825147	1.40E-06	0.00085
AALF013568	224.4647	3.63772	0.75091	4.844416	1.27E-06	0.00085
AALF028390	16105.77	-1.5781	0.33046	-4.7755	1.79E-06	0.00102
AALF021910	140.6905	3.54935	0.75137	4.723817	2.31E-06	0.00121
AALF020193	196.0018	-3.27061	0.69316	-4.7184	2.38E-06	0.00121
AALF018314	241.1632	3.13224	0.66827	4.687073	2.77E-06	0.00134
AALF012634	142.7464	3.50692	0.75295	4.657567	3.20E-06	0.00148
AALF012608	1312.558	1.92944	0.42386	4.55211	5.31E-06	0.00227
AALF000424	189.7795	3.22009	0.70795	4.548497	5.40E-06	0.00227

AALF006357	141.1417	3.35025	0.73877	4.534891	5.76E-06	0.00233
AALF013462	281.9295	-2.8146	0.6245	-4.50696	6.58E-06	0.00255
AALF001478	1468.268	-1.9102	0.42606	-4.48346	7.34E-06	0.00274
AALF000044	1946.213	-2.00581	0.45053	-4.45216	8.50E-06	0.00294
AALF023808	504.7657	-2.45833	0.55124	-4.45964	8.21E-06	0.00294
AALF004653	133.4889	3.22406	0.74435	4.331375	1.48E-05	0.00495
AALF026733	84.07934	-3.33885	0.78091	-4.2756	1.91E-05	0.00615
AALF022003	66.79487	-3.31525	0.78043	-4.24801	2.16E-05	0.00633
AALF009184	126.5829	3.20588	0.75393	4.252206	2.12E-05	0.00633
AALF029294	12557.35	-1.53858	0.36216	-4.24834	2.15E-05	0.00633
AALF005682	119.5524	3.19284	0.75368	4.236351	2.27E-05	0.00647
AALF019283	142.6499	3.09315	0.73407	4.213692	2.51E-05	0.00657
AALF029751	1675.971	-1.77416	0.42046	-4.21958	2.45E-05	0.00657
AALF027705	112.9815	3.20909	0.76156	4.213869	2.51E-05	0.00657
AALF013811	116.7863	3.20266	0.76191	4.20348	2.63E-05	0.0067
AALF013936	218.1549	2.81212	0.67384	4.173302	3.00E-05	0.00745
AALF009808	733.2235	2.12522	0.51141	4.15564	3.24E-05	0.00783
AALF010472	136.42	-3.02563	0.72894	-4.15074	3.31E-05	0.00783
AALF007409	129.3108	3.08945	0.75066	4.115619	3.86E-05	0.0089
AALF030003	18609.42	-1.55019	0.379	-4.09021	4.31E-05	0.00908
AALF004949	115.1153	3.09592	0.75721	4.088606	4.34E-05	0.00908
AALF006290	225.9239	-2.98518	0.73163	-4.08016	4.50E-05	0.00908
AALF018602	119.851	3.09499	0.75777	4.084361	4.42E-05	0.00908
AALF006216	534.9484	-2.20591	0.5401	-4.08427	4.42E-05	0.00908
AALF004409	16064.4	-1.56286	0.38227	-4.08836	4.34E-05	0.00908
AALF009483	121.1436	3.04588	0.75142	4.053519	5.05E-05	0.00997
AALF026574	57.60346	-3.12196	0.77441	-4.03139	5.54E-05	0.01074

AALF026375	293.7806	2.50352	0.62393	4.01249	6.01E-05	0.01141
AALF018616	207.0673	2.72475	0.68046	4.004284	6.22E-05	0.01158
AALF017763	1563.739	-1.99175	0.49839	-3.99641	6.43E-05	0.01175
AALF016614	137.5492	2.95747	0.74218	3.984852	6.75E-05	0.01211
AALF029473	5904.79	-1.38429	0.34854	-3.97168	7.14E-05	0.01256
AALF004741	131.5144	2.98495	0.75606	3.948065	7.88E-05	0.01362
AALF012324	115.5417	2.96348	0.7545	3.927756	8.57E-05	0.01456
AALF007640	102.035	2.98632	0.7677	3.889961	0.0001	0.01674
AALF011696	63.36724	-3.0151	0.77867	-3.87213	0.00011	0.01741
AALF002033	166.8618	-2.81255	0.72615	-3.87325	0.00011	0.01741
AALF004300	1909.116	1.52921	0.39539	3.86758	0.00011	0.01745
AALF010879	270.3014	2.45869	0.63808	3.85328	0.00012	0.0182
AALF018416	203.4816	2.67494	0.69614	3.842541	0.00012	0.01861
AALF029707	9303.243	-1.3865	0.36106	-3.84003	0.00012	0.01861
AALF010650	53.90038	-2.9568	0.77095	-3.8353	0.00013	0.01868
AALF022562	265.6455	2.47012	0.64851	3.808907	0.00014	0.02048
AALF005662	135.9857	-2.7931	0.73739	-3.78785	0.00015	0.02196
AALF020726	103.364	2.8865	0.764	3.778131	0.00016	0.02218
AALF029966	79819.57	-1.21791	0.32236	-3.77807	0.00016	0.02218
AALF018742	52.25456	-2.88133	0.76907	-3.7465	0.00018	0.0248
AALF016505	1204.019	-1.64991	0.44845	-3.67915	0.00023	0.03075
AALF018116	101.1572	2.8398	0.77145	3.68113	0.00023	0.03075
AALF024478	2947.581	-1.3565	0.36841	-3.68206	0.00023	0.03075
AALF028389	8508.116	-1.24092	0.33739	-3.67807	0.00024	0.03075
AALF011899	185.0763	2.54016	0.69409	3.659686	0.00025	0.0326
AALF008354	457.72	2.06779	0.56669	3.648908	0.00026	0.03355
AALF002627	77.51303	-2.83372	0.77946	-3.63548	0.00028	0.03424

AALF003865	138.9563	2.76608	0.76061	3.636676	0.00028	0.03424
AALF010018	770.8866	1.75411	0.4831	3.630927	0.00028	0.03424
AALF029391	11838.58	-1.45831	0.40169	-3.63044	0.00028	0.03424
AALF027402	1241.659	1.67924	0.46433	3.616523	0.0003	0.03569
AALF012277	169.9871	-2.51851	0.69861	-3.60502	0.00031	0.03685
AALF006068	106.1849	2.78284	0.77289	3.600578	0.00032	0.03697
AALF012023	511.8153	2.11554	0.58798	3.597957	0.00032	0.03697
AALF008589	95.82241	2.754	0.76785	3.586646	0.00034	0.03815
AALF024589	118.8952	2.71411	0.75983	3.572004	0.00035	0.03988
AALF015598	92.00105	2.74768	0.77336	3.552932	0.00038	0.0424
AALF024585	93.7284	2.73652	0.77364	3.537185	0.0004	0.0445
AALF006531	438.0126	-2.00926	0.56948	-3.52825	0.00042	0.045
AALF014168	91.03864	2.73169	0.77369	3.530749	0.00041	0.045
AALF019406	48.14003	-2.68713	0.76334	-3.52025	0.00043	0.04587
AALF024475	47.72858	-2.66729	0.76267	-3.4973	0.00047	0.0479
AALF000340	313.2052	2.14223	0.61207	3.499952	0.00047	0.0479
AALF013313	144.1811	2.54665	0.72773	3.499426	0.00047	0.0479
AALF029874	2598.481	-1.37886	0.39395	-3.50004	0.00047	0.0479
AALF024243	188.1177	2.41145	0.69181	3.485717	0.00049	0.0495

Appendix-V: List of differentially expressed genes D8_edgeR

	sampleA	sampleB	logFC	logCPM	PValue	FDR
TRINITY_DN132509_c0_g1_i1	Infected	Control	12.9347	17.3283	1.87E-09	2.22E-05
TRINITY_DN130280_c0_g1_i3	Infected	Control	-8.59884	7.66879	3.00E-09	2.22E-05
TRINITY_DN132452_c0_g1_i1	Infected	Control	-7.2922	8.54038	2.05E-08	0.0001
TRINITY_DN132014_c0_g1_i7	Infected	Control	-6.05734	7.3497	1.29E-06	0.00471
TRINITY_DN131809_c1_g2_i5	Infected	Control	-6.49685	6.16019	1.59E-06	0.00471
TRINITY_DN131737_c0_g1_i2	Infected	Control	-6.42244	6.09072	1.99E-06	0.00492
TRINITY_DN121041_c0_g2_i1	Infected	Control	-6.47659	5.64515	3.67E-06	0.00588
TRINITY_DN132229_c2_g4_i1	Infected	Control	-5.66949	7.34299	3.68E-06	0.00588
TRINITY_DN119808_c0_g1_i1	Infected	Control	12.089	8.91842	3.94E-06	0.00588
TRINITY_DN117126_c0_g1_i1	Infected	Control	-6.90614	5.23935	4.35E-06	0.00588
TRINITY_DN132196_c1_g5_i2	Infected	Control	-6.17813	5.87014	4.37E-06	0.00588
TRINITY_DN130915_c0_g2_i1	Infected	Control	-5.45104	7.0423	7.59E-06	0.00937
TRINITY_DN132229_c2_g1_i2	Infected	Control	-5.38471	6.96622	9.84E-06	0.01049
TRINITY_DN132317_c0_g1_i6	Infected	Control	11.496	8.32758	1.10E-05	0.01049
TRINITY_DN132515_c1_g2_i1	Infected	Control	11.4512	8.2831	1.18E-05	0.01049
TRINITY_DN131369_c2_g1_i3	Infected	Control	-5.62186	6.00939	1.19E-05	0.01049
TRINITY_DN132103_c4_g2_i1	Infected	Control	11.4406	8.27402	1.20E-05	0.01049
TRINITY_DN132409_c0_g1_i3	Infected	Control	11.1924	8.02596	1.85E-05	0.0152
TRINITY_DN132540_c1_g1_i1	Infected	Control	11.1008	7.93602	2.16E-05	0.01685
TRINITY_DN131476_c0_g1_i1	Infected	Control	-5.86606	5.0869	2.66E-05	0.01936
TRINITY_DN132446_c0_g1_i3	Infected	Control	-6.32235	4.71887	2.87E-05	0.01936
TRINITY_DN130818_c0_g1_i1	Infected	Control	-5.13868	6.20528	3.00E-05	0.01936

TRINITY_DN82050_c0_g1_i1	Infected	Control	-6.2914	4.69561	3.14E-05	0.01936
TRINITY_DN131177_c0_g1_i2	Infected	Control	-6.2914	4.69561	3.14E-05	0.01936
TRINITY_DN132611_c3_g1_i4	Infected	Control	10.7659	7.60519	3.82E-05	0.02232
TRINITY_DN131966_c0_g5_i1	Infected	Control	10.7505	7.58745	3.93E-05	0.02232
TRINITY_DN130520_c0_g1_i1	Infected	Control	-6.2116	4.62256	4.14E-05	0.02232
TRINITY_DN132618_c0_g1_i5	Infected	Control	10.7094	7.54779	4.22E-05	0.02232
TRINITY_DN130280_c0_g1_i1	Infected	Control	-5.2948	5.43788	4.45E-05	0.02276
TRINITY_DN132103_c4_g1_i1	Infected	Control	10.5079	7.35019	5.97E-05	0.0295
TRINITY_DN132516_c0_g1_i3	Infected	Control	10.4439	7.28502	6.63E-05	0.03138
TRINITY_DN132525_c3_g1_i1	Infected	Control	-6.02365	4.46482	6.80E-05	0.03138
TRINITY_DN131481_c3_g1_i2	Infected	Control	-5.54638	4.81016	6.99E-05	0.03138
TRINITY_DN132229_c0_g1_i1	Infected	Control	-4.80446	6.18883	7.32E-05	0.03189
TRINITY_DN131949_c2_g3_i5	Infected	Control	10.3499	7.19237	7.78E-05	0.03293
TRINITY_DN132567_c0_g1_i3	Infected	Control	10.2516	7.09536	9.23E-05	0.03506
TRINITY_DN132268_c0_g2_i3	Infected	Control	-4.88654	5.5989	9.24E-05	0.03506
TRINITY_DN122618_c0_g1_i1	Infected	Control	-5.92613	4.37849	9.41E-05	0.03506
TRINITY_DN124731_c0_g1_i1	Infected	Control	-5.43817	4.72021	9.81E-05	0.03506
TRINITY_DN132011_c4_g1_i1	Infected	Control	-5.43817	4.72021	9.81E-05	0.03506
TRINITY_DN131092_c0_g4_i1	Infected	Control	-5.01627	5.1931	0.00011	0.03506
TRINITY_DN131543_c0_g2_i1	Infected	Control	-5.88658	4.34882	0.00011	0.03506
TRINITY_DN131256_c0_g1_i2	Infected	Control	10.1744	7.02123	0.00011	0.03506
TRINITY_DN131423_c1_g1_i2	Infected	Control	-5.41076	4.69675	0.00011	0.03506
TRINITY_DN129932_c0_g1_i2	Infected	Control	-4.584	6.81146	0.00011	0.03506
TRINITY_DN132054_c1_g1_i2	Infected	Control	10.1485	6.99246	0.00011	0.03506
TRINITY_DN132602_c1_g1_i4	Infected	Control	10.1041	6.95072	0.00012	0.03506
TRINITY_DN131401_c3_g2_i2	Infected	Control	-5.85422	4.31804	0.00012	0.03506
TRINITY_DN128877_c0_g1_i1	Infected	Control	-5.85422	4.31804	0.00012	0.03506

TRINITY_DN132632_c8_g1_i1	Infected	Control	-5.85018	4.31827	0.00012	0.03506
TRINITY_DN132469_c1_g3_i1	Infected	Control	10.0589	6.90559	0.00013	0.03714
TRINITY_DN130145_c0_g2_i4	Infected	Control	10.0493	6.89684	0.00013	0.03714
TRINITY_DN129476_c0_g1_i1	Infected	Control	-5.08364	4.8962	0.00013	0.03714
TRINITY_DN132014_c0_g1_i2	Infected	Control	-4.47411	7.09499	0.00014	0.03717
TRINITY_DN131885_c0_g2_i2	Infected	Control	9.99825	6.84664	0.00014	0.03826
TRINITY_DN132452_c0_g1_i4	Infected	Control	-4.55094	5.96423	0.00016	0.04136
TRINITY_DN116207_c0_g1_i1	Infected	Control	-5.01288	4.83292	0.00017	0.04348
TRINITY_DN76088_c0_g1_i1	Infected	Control	-5.7351	4.22247	0.00017	0.04348
TRINITY_DN131431_c0_g1_i1	Infected	Control	9.83462	6.68565	0.00019	0.04688
TRINITY_DN132462_c0_g1_i1	Infected	Control	-5.69461	4.18904	0.00019	0.04774
TRINITY_DN132025_c1_g1_i2	Infected	Control	9.79284	6.64384	0.0002	0.04843
TRINITY_DN128807_c0_g1_i1	Infected	Control	-4.69584	5.1937	0.00021	0.04843
TRINITY_DN92141_c0_g1_i1	Infected	Control	9.7804	6.63536	0.00021	0.04843

